LIQUID PHASE CHEMISTRY STUDY OF INDIUM AND THALLIUM FOR A FUTURE INVESTIGATION OF NIHONIUM CHEMISTRY

A Dissertation

by

MERINDA FITRI VOLIA

Submitted to the Office of Graduate and Professional Studies of
Texas A&M University
in partial fulfillment of the requirements for the degree of

DOCTOR OF PHILOSOPHY

Chair of Committee,	John W. Poston Sr.
Co-Chair of Committee,	Charles M. Folden III
Committee Members,	Sunil S. Chirayath
	Craig M. Marianno
Head of Department,	Michael Nastasi

December 2019

Major Subject: Nuclear Engineering

Copyright 2019 Merinda Fitri Volia

ABSTRACT

Nihonium is classified as a superheavy element and is only produced artificially through nuclear reaction in a particle accelerator. Its chemical properties are largely unknown and the chemical experiments involving nihonium are very challenging and require a system that is sustainably fast and reliable. The study of nihonium homologs, indium and thallium, was carried out to provide the basis for a suitable chemistry system that can potentially be used to study nihonium chemistry in the future.

This homolog study focuses on developing a novel chemical procedure to extract and separate indium and thallium metals. These elements were extracted from hydrochloric acid media into imidazolium-, pyrrolidinium-, and betainium-based ionic liquids, as well as DL-menthol-based eutectic solvents, by using a liquid-liquid extraction (LLE) technique. Generally, it was found that the aqueous phase acidity affected the extraction yield and thus, the speciation of the metals. The extraction kinetics were found to be sufficiently fast as the reaction equilibrium was reached within one minute in all the systems that were studied. Thallium, which has two oxidation states: +1 and +3, was more effectively extracted when bromine water was used as the oxidizing agent, compared to chlorine water.

Among all three metals that were studied, Tl(I) was only poorly extracted into either solvent that was tested. In(III) was best extracted into a betainium-based ionic liquid from a low HCl concentration with the presence of 15% betaine. In the case of Tl(III), the highest extraction yield was obtained in the system containing an imidazolium-based ionic liquid. The length of the alkyl chain and the anion group of this

ionic liquid affected Tl(III) extraction yield, but eventually the best extraction was obtained with an ionic liquid that has the most carbon atoms on its alkyl side.

In an attempt to understand the metal extraction mechanism in a betainium-based ionic liquid, the mutual solubility between this ionic liquid and water was studied. The influence of hydrochloric acid and zwitterionic betaine were investigated. It was found that both acid and betaine increased the mutual solubility of the aqueous and the organic phases. In addition, zwitterionic betaine was found to be partially distributed between the two phases.

DEDICATION

To my husband, Alessandro Vanni

To my son, Radja Ettore Vanni

This is for you

Thank you for being with me in this journey

ACKNOWLEDGEMENTS

I would like to express my gratitude to many people who made this Ph.D. journey possible. First, to my advisor, Prof. Cody Folden. Thank you for taking me in as your student and providing support, guidance and resources all the way from the very beginning. You've helped me set a high standard to my work and pushed me to work hard to achieve it.

To my committee members: Dr. Craig Marianno, Dr. John Poston, and Dr. Sunil Chirayath. Thank you for giving such great support during my academic journey at Texas A&M. Dr. Marianno always made me find humor in difficult times. From Dr. Poston, I learned about self-respect, wisdom and perseverance. I have never met somebody who loves his students as much as he does. For me, Dr. Poston is only comparable to Harry Potter's Dumbledore or The Lord of the Ring's Gandalf. Dr. Sunil has always been kind and supportive. I am grateful to have them all as my committee members.

Another person that I must mention here is Dr. Evgeny Tereshatov. He taught me almost everything I needed to know about my Ph.D. project (of course I read the literature myself as well!). He patiently guided me through my experiments, answered my questions, challenged my ideas, helped me with analyzing my data, and put up with me even after a series of heated discussions. You are a great mentor and friend. I am forever grateful.

I would also like to thank Dr. Maria Boltoeva from the IPHC - France. A great scientist and a mom, she is a role model I look up to. Thank you for your support, for

sharing your knowledge and giving me the opportunity to develop my research in your laboratory in Strasbourg.

To my fellow graduate student and lab mate, Kevin Glennon, who helped me prepare the samples and run many ICP-MS measurements for my experiments. Kevin was always available to help and to answer my questions about chemistry. Thanks Kevin!

To all my friends who have been my support team all through the years in graduate school: Terry, Rose, Paola, Rosanna, Charlie, Manayer, and so many more that I cannot mention one by one. Whether your names are here or not, I thank you all for being around all these times.

To my family in Indonesia, thank you for supporting me endlessly. Mama, Papa, Fera, and Ryan: I have been leaving you for years, but this dissertation means that I'll be coming home for good, something that I know you all have been waiting for. I hope I'm making you proud and I hope that your sacrifice has been worth it. To Carla and Romolo: you both are the greatest parents-in-law ever. Thank you for taking care of me and Ettore from the day that he was born until I could be independent and start working on my dissertation again. You both are just awesome!

To my beloved husband, Ale: there are not enough words to describe how grateful I am to have you. If I were Frodo of the Lord of the Ring trilogy, you were definitely my Sam. You helped me, guided me, supported me, and loved me all the way, no matter how hard I made our days sometimes. I knew you'd carry me on your back to take me to the finish line if you had to. I wouldn't have done it without your support. I love you.

To my son, Radja Ettore: I know right now you are too young to understand. But if one day you happen to read this page, I want you to know that being your mom has

been one of the greatest things that has ever happened to me. I was carrying you in my womb when I started writing this dissertation. Sometimes I had to work overnight and even until 10 AM the next morning and not a single time did you ever give me trouble. I hated it when I had to leave you at home or at the daycare when you were just weeks old so I could work and finish the dissertation. I hope I did not neglect you too much. Thank you for being so patient, whether you realized it or not. Mama loves you!

CONTRIBUTORS AND FUNDING SOURCES

Contributors

This work was supervised by a dissertation committee consisting of Dr. Charles M. Folden III [advisor] of the Department of Chemistry and Dr. John W. Poston Sr., Dr. Craig M. Marianno, and Dr. Sunil S. Chirayath of the Department of Nuclear Engineering.

The analyses depicted in Chapter 3 were conducted partially by Dr. Evgeny Tereshatov of the Cyclotron Institute at Texas A&M University, Dr. Maria Boltoeva and Valerie Mazan from the Institut Pluridisciplinaire Hubert CURIEN (IPHC) of the Centre National de la Recherche Scientifique (CNRS) and the University of Strasbourg in France and were published in 2019.

The experiments and data analyzed in Section 4.1.1 and 4.1.3 were conducted in collaboration with Dr. Evgeny Tereshatov of the Cyclotron Institute at Texas A&M University, Dr. Maria Boltoeva and Valerie Mazan from the IPHC of CNRS and the University of Strasbourg in France and were published in 2016.

All other work conducted for the dissertation was completed by the student independently.

Funding Sources

This work was made possible by U.S. Department of Energy, Office of Science, Office of Nuclear Physics under Awards No. DE-FG02-93ER40773.

This work was made possible in part by the National Center for Scientific Research (CNRS, France) through its International Program for Scientific Cooperation (PICS), specifically for the experiments described in Chapter 3.

Its contents are solely the responsibility of the authors and do not necessarily represent the official views of the U.S. Department of Energy, Office of Science, Office of Nuclear Physics.

NOMENCLATURE

Aq	Aqueous
bet	Zwitterionic betaine
$[C_2mim][Tf_2N]$	1-ethyl-3-methylimidazolium *bis*(trifluoromethanesulfonyl)imide
$[C_2mim][FSI]$	1-ethyl-3-methylimidazolium *bis*(fluorosulfonyl)imide
$[C_4mim][Tf_2N]$	1-butyl-3-methylimidazolium *bis*(trifluoromethanesulfonyl)imide
$[C_8mim][Tf_2N]$	1-octyl-3-methylimidazolium *bis*(trifluoromethanesulfonyl)imide
$[C_3C_1mim][Tf_2N]$	1-propyl-2,3-dimethylimidazolium *bis*(trifluoromethanesulfonyl)imide
$[C_3C_1pyrr][Tf_2N]$	N-propyl-N-methylpyrrolidinium *bis*(trifluoromethanesulfonyl)imide
D	Distribution ratio
DES	Deep eutectic solvent
ES	Eutectic Solvent
Eq (subscript)	Equilibrium
Eq	Equation
FLNR	Flerov Laboratory of Nuclear Reactions
HBA	Hydrogen bond acceptor
HBD	Hydrogen bond donor
$Hbet^+$	Betainium
HDEHP	Di-(2-ethylhexyl)phosphoric acid
IL	Ionic liquid
Init	Initial

K_a	Acid dissociation constant
K_D	Distribution constant
K_{ext}	Extraction constant
K_{IE}	Constant of ion exchange
K_{IP}	Constant of ion pair formation
K_{sp}	Solubility Product Constant
LLE	Liquid-liquid extraction
MLA	DL-Menthol and lauric acid
MW	Molecular weight
NMR	Nuclear magnetic resonance
Org	Organic
PTE	Periodic table of element
SHE	Superheavy element
TALSPEAK	Trivalent Actinide - Lanthanide Separation by Phosphorus reagent Extraction from Aqueous Komplexes

TABLE OF CONTENTS

Page

LIST OF FIGURES

Page

LIST OF TABLES

Page

1. INTRODUCTION

1.1 Superheavy Elements (SHEs)

The latest version of Periodic Table of Elements (PTE) contains 118 elements (Figure 1), including the four superheavy elements (SHEs) that were officially added in 2016: nihonium (Nh), moscovium (Mc), tennessine (Ts), and oganesson (Og) (Z = 113, 115, 117, and 118, respectively) [1-3]. Although there is no clear definition of SHEs available in the literature, one definition is that the SHEs start with rutherfordium (Z=104) which is also the beginning of the transactinides series [4-6]. This definition was made based on the assumptions that the existence of SHEs is strongly influenced by nuclear shell stabilization and that a chemical element should live for at least 10^{-14} s [4].

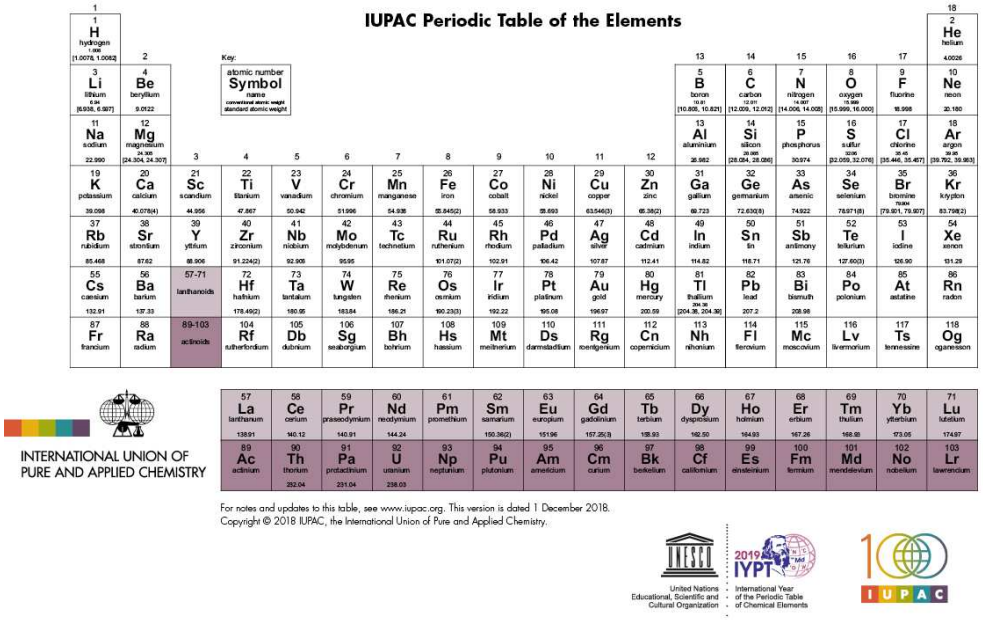

Figure 1. The periodic table of elements as of January 2019. Reprinted from ref. [7].

The SHEs were synthesized through fusion-evaporation reactions. Figure 2 shows the schematic representation of the reaction. There are two types of fusion-evaporation reactions: hot and cold fusion. The characteristics of and the main differences between these two reactions are discussed below.

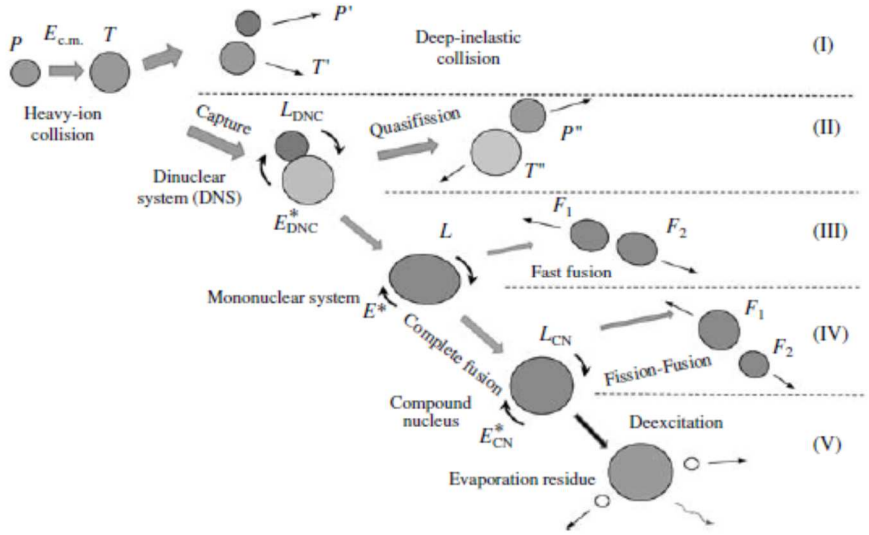

Figure 2. The schematic representation of fusion-evaporation reaction.The initial projectile P and target nuclei T can undergo several processes: (I) deep-inelastic collisions where P' and T' are formed as the products (incomplete momentum transfer), (II) quasifission where P" and T" are formed as the products (total momentum transfer), (III-IV) fusion-fission where F1 and F2 are the fission fragments, and (V) complete fission of P and T. Figure used with permission from ref. [8].

In hot fusion reactions, heavy actinides are used as the target materials and bombarded by light-ion projectiles. The projectiles have to be accelerated to an energy that is adequate to overcome the Coulomb repulsion of the two nuclei of the same charge [9,10]. Seaborgium (Sg, Z=106) is an example of a SHE that was produced in a hot

fusion reaction. The isotope ^{263}Sg was produced through bombardment of a ^{249}Cf target with ^{18}O in a reaction that released 4 neutrons (^{249}Cf(^{18}O,4n)^{263}Sg) [11].

Due to the unfavorable reaction Q-value, the hot fusion reaction produces a compound nucleus with excitation energy on the order of 40 – 50 MeV [9]. The high excitation energy mainly dissipates through evaporation of neutrons and emission of protons and this process always competes with prompt fission [10]. Because of the latter process, the fraction of survival nuclei is only in the order of 10^{-6} – 10^{-8} with a production cross section 10^{-4} – 10^{-2} μb; the higher the charge and mass of the projectiles, the lower the survival rate of the compound nuclei [12,13]. The elements with Z =102 – 106 were synthesized through this route.

Meanwhile, cold fusion reactions use heavier projectiles having atomic masses ≥ 40 to bombard ^{208}Pb (Z=82) or ^{209}Bi targets (Z=83). The compound nuclei produced in this reaction have excitation energies on the range of 12 – 15 MeV due to their very negative Q-values, with emission of only one or two neutrons [10,13]. The probability for the compound nuclei to undergo spontaneous fission is lower compared to hot fusion reactions and thus, their survival probability is higher [10,13,14]. However, cold fusion reactions also have limitations. Because the targets are limited to ^{208}Pb and ^{209}Bi, in order to produce heavier elements, one has to opt for the projectiles with larger atomic number. This leads to lower probability of the formation of the compound nuclei as well as the decrease in their stability due to neutron deficiency in the nucleus [12,13]. The elements with Z = 107 – 112 have been successfully synthesized with this reaction.

To confirm that an element belongs to a particular group in the PTE, its chemical properties have to be carefully characterized. This is particularly important for the SHEs due to the so-called relativistic effect which becomes more pronounced with high Z elements [15]. As a result of having a highly charged nucleus, the electrons in the vicinity of the SHE nucleus within the SHEs accelerate with the velocity approaching the speed of light. Consequently, their mass increase according to Einstein's theory of special relativity as shown in Eq. 1 [15,16]:

$$m = m_0 \cdot \left(1 - \left(\frac{v}{c}\right)^2\right)^{-1/2} \quad \text{Eq. 1}$$

where m is the mass of the electron that moves with velocity v, c is the speed of light and m_0 is the rest mass of the electron. As the mass of the electrons increased, the atomic orbitals are affected in several ways. First, it experiences the relativistic contraction. The radius of an orbital is affected by the mass of the electron according to Bohr radius equation [16]:

$$a_0 = 4\pi\epsilon_0\hbar^2/mZe^2 \quad \text{Eq. 2}$$

where a_0 is the Bohr radius, ϵ_0 is the permittivity free space, $\hbar$ is the reduced Planck's constant, m is the mass of the electron, and Ze is the elementary charge. Based on Eq. 2, as the relativistic mass of the electron, m, increases, the relativistic radius is smaller than the nonrelativistic one. The s orbitals up to the valence shell experience the relativistic contraction almost equally as the speeds of their electron near the nucleus are comparable [16]. The second effect to the atomic orbital is the spin-orbit splitting. The subshells with $l > 0$ split into two subgroups where $j = l \pm ½$. The p subshells split into $p_{1/2}$ and $p_{3/2}$

spinors while the d subshells split into $d_{3/2}$ and $d_{5/2}$ spinors [9,15]. In the heaviest elements, the energetic splitting between the two j values can increase up to a few electronvolts [16]. The third effect is the relativistic self-consistent expansion. The d and f electrons are not directly affected due to their high angular momenta [16]. Thus, they rarely approach the nucleus and the electrons do not gain velocities. However, the contraction of s and p orbitals shields the f and d orbitals from the nuclear charge more effectively. Consequently, the d and f orbitals become expanded and their energies increased (indirect relativistic effect). Because of all these relativistic effects in the atomic orbitals of the SHEs, their chemical properties cannot be simply predicted and extrapolated from their lighter homologues because deviation from the established trend in the PTE is very likely [17,18].

1.1.1 Nihonium

Nihonium (Nh, Z = 113), is the latest member of the group 13 of the PTE and the heavier homolog of boron, aluminum, gallium, indium and thallium. Although it has been assigned officially in group 13 in the PTE, the chemical properties of Nh have not been studied extensively. The experimental data on its chemical properties are very scarce because the synthesis of this element is difficult, the production rates are low, and the isotopes have very short half-lives.

To date, only small quantities of Nh isotopes have been synthesized directly or detected as a decay product of heavier nuclei. The first isotopes of Nh were observed by the research group at the Flerov Laboratory of Nuclear Reactions (FLNR) in Dubna,

Russia in 2004. In that experiment, an ^{243}Am target was bombarded with a ^{48}Ca beam to produce element 115, moscovium (Mc). Two isotopes of Mc were observed: ^{288}Mc and ^{287}Mc. These isotopes subsequently decayed with alpha emission and ^{284}Nh and ^{283}Nh were detected as the decay products [19]. In the same year, the Institute of Physical and Chemical Research, known as RIKEN, in Japan published the results of the nuclear fusion reaction to produce Nh. In that experiment, a ^{209}Bi target was bombarded with a ^{70}Zn beam and one isotope ^{278}Nh was detected as the direct reaction product [20]. The isotope ^{282}Nh was discovered in an experiment performed by the FLNR research group in 2007. In that experiment, ^{282}Nh was produced as the reaction product of a ^{237}Np target with ^{48}Ca as the projectile [21]. Lastly, two isotopes ^{285}Nh and ^{286}Nh were observed in the decay chain of ^{293}Ts and ^{294}Ts, respectively. These Nh isotopes are the granddaughters of Ts isotopes that were produced through ^{48}Ca + ^{249}Bk reaction in FLNR [22]. Table 1 lists all Nh isotopes that have been discovered and identified.

Table 1. List of Nh isotopes produced through nuclear reactions in accelerator facilities in Russia and Japan [19-22].

Isotopes	Half-life	Nuclear reaction	Place	Year
^{284}Nh	~ 0.91 s	^{243}Am(^{48}Ca, 3n)^{288}Mc	FLNR, Russia	2004
^{283}Nh	~ 75 ms	^{243}Am(^{48}Ca, 4n)^{287}Mc	FLNR, Russia	2004
^{278}Nh	~ 0.02 s	^{209}Bi(^{70}Zn, n)^{278}Nh	RIKEN, Japan	2004
^{282}Nh	~ 73 ms	^{237}Np(^{48}Ca, 3n)^{282}Nh	FLNR, Russia	2007
^{286}Nh	~ 9.5 s	^{249}Bk(^{48}Ca, 3n)^{294}Ts	FLNR, Russia	2010
^{285}Nh	~ 4.2 s	^{249}Bk(^{48}Ca, 4n)^{293}Ts	FLNR, Russia	2010

Based on its assigned position in PTE, the ground state electronic configuration of Nh is predicted to be [Rn]$5f^{14}6d^{10}7s^{2}7p^{1}$ [23]. Due to experiencing strong relativistic effect, the 7s orbital is contracted and highly stabilized, making it an inert pair in Nh [9]. Meanwhile, 7p atomic orbital splits; the $7p_{1/2}$ orbital is contracted and stabilized, while the $7p_{1/2}$ orbital is expanded and destabilized [9]. All the current knowledge about the chemical properties of Nh is based on theoretical predictions. Although the common oxidation state of group 13 elements is +3, the main oxidation state of Nh is predicted to be 1+ due to high stabilization of the 7s orbital [24]. Theoretical calculation also predicted that Nh is volatile and less reactive compared to its lighter homologues due to the splitting of the 7p orbital [25]. Molecular calculations suggested that Nh reacts with OH^{-} in a moist oxygen atmosphere to form a stable NhOH compound, which is analog to

TlOH [26]. In addition, interaction between Nh and Au was theoretically studied and compared with that of Tl. The results showed that NhAu bonding is weaker than in TlAu as a consequence of stabilization of the $7p_{1/2}$ orbital and therefore, Nh is expected to be absorbed on Au at lower temperature than Tl [26,27].

There have been some attempts to confirm the theoretical prediction of Nh properties through chemical experiments. In 2014 and 2017, the research group in FLNR reported the results of experiment to determine the volatility and speciation of Nh [23,28] but these results were inconclusive. However, the effort to pursue chemical experiments of Nh and some other SHEs is ongoing. Some researchers have been preparing the baseline data and experimental set up to confirm the results of theoretical studies and to provide evidence of Nh behavior in comparison with its homologues [29,30].

1.1.2 SHE Chemical Experiments

Unlike the traditional chemical experiments, studying the chemistry of SHEs requires a system that meets certain requirements. This includes chemical instrumentation that is sufficiently fast to allow for measurement of isotopes with half-lives in the order of seconds. The current chemical separation apparatus such as gas chromatograph can be used to investigate a SHE isotope with minimum half-life of 1 s [31]. Selectivity of the chemical procedure is also a concern in SHE experiments. The SHEs commonly have low production cross sections and their productions often yield many unwanted reaction products with much larger cross sections that can interfere with the detection of the SHEs. Therefore, the chemical procedure must be highly selective to enhance the quality

of the measurement and accuracy of the results [9]. In addition, SHE's chemical experiment must be done on a one-atom-at-a-time scale due to low production rates [6,17]. To ensure the experimental results are statistically significant, it is required that the SHEs be studied in a system that employs repetitive partition such as chromatography and liquid-liquid extraction systems [32,33]. Since the production of SHEs is a random event, automation of these chemistry systems is inevitable to ensure the chemical separation with the high repetition rate that will lead to detection of the elements. Also, the detection system must be designed such that it provides for an unambiguous interpretation of the results [9]. Finally, it is necessary to study the chemistry of SHEs' lighter homologues under the same chemical system such that their chemical behaviors can be compared and inference about SHEs chemistry can be made.

The chemical experiment setups for the SHEs can be categorized into two: gas-phase chemistry and liquid-phase chemistry [9]. While all of these techniques have been employed for the SHE chemical experiments, the gas-phase chemistry study is more widely used. In liquid phase chemistry, there are two techniques available: liquid-liquid extractions or column-based separation. A more comprehensive overview of all of these techniques can be found in [34-37].

The gas-phase chemical experiments are usually employed to investigate volatile SHEs or their compounds. There are two techniques available: thermochromatography and isothermal chromatography. The basic principles between these two chromatography techniques are shown in Figure 3.

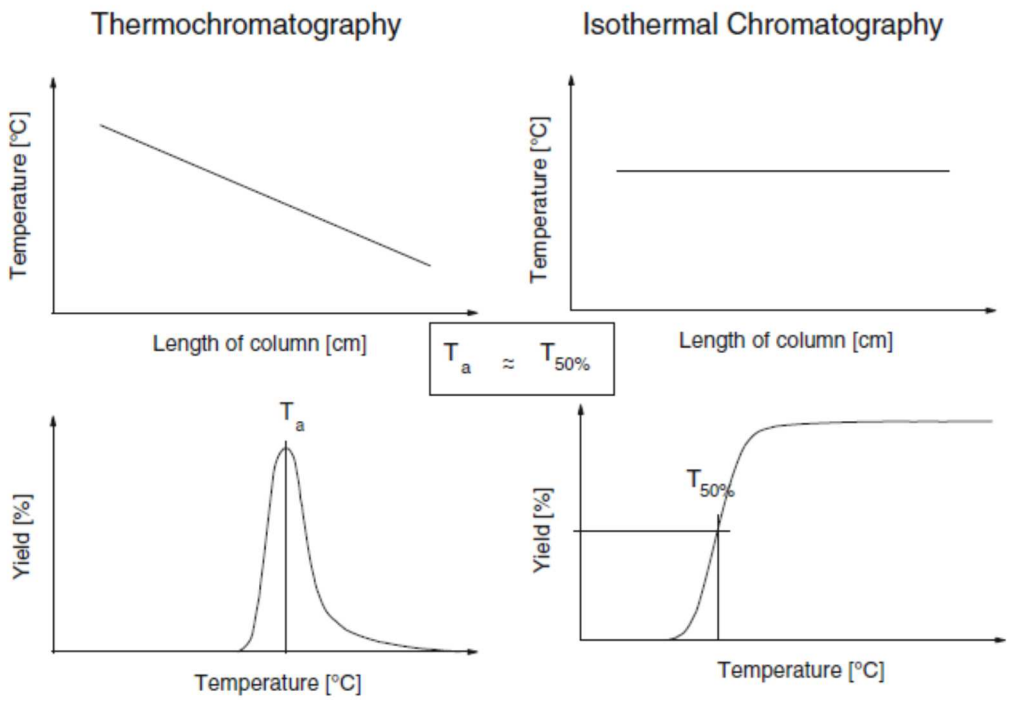

Figure 3. The basic principles of thermochromatography and isothermal chromatography are shown. The upper panel shows the temperature profiles in both techniques while the lower panel shows the deposition peak and integral chromatogram. The figure is used with permission from ref. [38].

1.1.2.1 Thermochromatography

In thermochromatography, the volatile species are injected at the inlet and are transported by a carrier gas through a chromatography column. From the beginning toward the end, the temperature inside the column becomes more negative (see the upper left panel in Figure 3). Consequently, as species traverse downstream, their velocity decrease. Depending on their adsorption entalphy (ΔH_a^0), the species will be deposited at different positions on the column surface. The deposition temperature, T_a, is the quantity that is unique for the species (see the lower left panel in Figure 3).

The thermochromatography separation technique is commonly used to study the SHEs that decay through γ emission, electron capture or β+ decay, or emission of highly energetic particles [38]. The radiation emitted by the nuclides is detected by scanning the length of the column [38]. The detection of nuclides that decay through spontaneous fission (SF) and emission of α-particles is commonly done by inserting solid-state track detector into the column.

On one hand, the thermochromatography separation technique is beneficial because all detectable nuclei contribute to the data as long as they reach the inlet of the column [34]. In addition, both the newly produced element and its homologs are treated identically as long as they are produced simultaneously [34]. This allows scientists to compare the chemical behavior of the new element and its homologs. However, the detection results of the nuclides that decay through SF are not obtained in a real time and therefore, the half-life of the nuclides cannot be determined [34,38].

1.1.2.2 Isothermal Chromatography

In isothermal chromatography, a constant temperature is applied inside the column (see the upper right panel in Figure 3). The species travel slower throughout the column compared to the carrier gas, depending on the applied temperature and the adsorption entalphy (ΔH_a^0) of the species [38,39]. This technique is suitable for separation of volatile short-lived radionuclides from the non-volatile ones. The quantity that is unique for isothermal chromatography is called $T_{50\%}$, that is the temperature at which half of the radionuclides injected in the inlet detectably emerged at the column exit

[38]. The time that the species retained inside the column, also called the retention time, is equal to the half-life of the nuclides.

The main advantage of isothermal chromatography separation technique is the possibility to determine the half-life of the radionuclides and properly identify them [34,38]. However, due to the unknown (ΔH_a^0) of the SHEs, the determination of $T_{50\%}$ requires many measurements at different isothermal temperatures to ensure that most of the nuclides decay inside the column.

1.2 Indium and Thallium Chemistry

Indium (Z = 49) and thallium (Z= 81) are the expected homologues of Nh. Both of these elements have two naturally occurring isotopes: ^{113}In (4.29%) and ^{115}In (95.71%), ^{203}Tl (29.524%) and ^{205}Tl (70.476%). The natural abundance of indium is 2.5 x 10^2 ppb in the continental crust and 3 x 10^{-4} ppb in the ocean. Around 1% of indium occurs in zinc and lead sulphide ores and it is obtained as a by-product in the process of zinc and lead smelting. Annually, 450 tonnes of indium is produced worldwide [40]. Meanwhile, 8.5 x 10^2 ppb of thallium is found in the continental crust and 1.3 x 10^{-2} ppb in the ocean. The amount of thallium found in ores and other sources is considered rare; it is scattered in potash, feldspar and pollucite. Thallium is also obtained as by-product of zinc and lead smelting and H_2SO_4 manufacture [40].

Having the ground state electronic configuration [Kr]$4d^{10}5s^25p^1$, the characteristic formal oxidation state of indium is +3. Lower oxidation states are accessible but not common [40]. In aqueous solution, the indium ions are known to bind with six water

molecules, which means that its coordination number is equal to six [41]. The speciation of indium in aqueous chloride solution has been studied with various techniques. An investigation of indium(III) chloride species by Raman spectroscopy in thirty-one solutions with a chloride-to- indium mole ratio from 0.48 to 15.9 (0.30 – 10.1 M Cl solution) showed the presence of four species: $[InCl(H_2O)_5]^{2+}$ (0.30 – 3.87 M Cl^-), $[InCl_2(H_2O)_4]^+$ (0.30 – 5.05 M Cl^-), $[InCl_3(H_2O)_3]$ (0.61 – 10.1 M Cl^-), and $[InCl_4(H_2O)_2]^-$ (6.50 – 10.1 M Cl^-) [42]. The authors also considered the possibility of the presence of $[InCl_5(H_2O)]^{2-}$ at a very high chloride-to-indium mole ratio. A later study on indium speciation using EXAFS technique showed these indium(III) species are dominant: $[InCl_2(H_2O)_4]^+$ (0 – 1 M HCl), $[InCl_3(H_2O)_3]$ (1 – 6 M HCl), $[InCl_4(H_2O)_2]^-$ (6-10 M HCl), and $[InCl_5(H_2O)]^{2-}$ (10-12 M HCl) [43].

Meanwhile, thallium has a ground state electronic configuration $[Xe]4f^{14}5d^{10}6s^26p^1$. The relativistic effect is more pronounced in thallium due to its heavy mass (its m/m_0 value for the electron in $E^{(Z-1)+}$ ion is 1.24 while for indium is 1.070) [15]. This results in the contraction and stabilization of s- and p-orbitals and subsequently expansion of its d- and f-orbitals. Consequently, the ionization potential of thallium is higher compared to indium [44]. Unlike its lighter homologues in Group 13, the stable oxidation state of thallium is +1 (thallous) but it is readily oxidized to a +3 oxidation state (thallic). The thallium(I) ion is found to be very weakly hydrated in aqueous solution and it does not form strong complexes [45]. However, these species have been found in chloride media: Tl^+, TlCl, $TlCl_2^-$, and $TlCl_3^{2-}$, indicating that the coordination number of

thallium(I) is equal to 4 [46]. Thallium(III) is known to have coordination number approximately 6 [41]. Depending on the chloride concentration, these thallium(III) species may exist in aqueous chloride media: Tl^{3+}, $TlCl^{2+}$, $TlCl_2^{+}$, $TlCl_3$, $TlCl^{4-}$, $TlCl_5^{2-}$ and $TlCl_6^{3-}$. The most stable thallium(III) chloride complex is $TlCl^{4-}$.

1.3 Liquid-liquid Extraction

Liquid-liquid extraction (LLE) has been widely used for separation and purification of organic and inorganic solutes. This technique is based on the preferential distribution of solutes between two immiscible phases which are commonly composed of an aqueous solution and an organic solvent. Prior to the extraction, the solutes are dissolved in one of the phases. For instance, metal salts are always dissolved in the aqueous phase (e.g., mineral acids such as HCl, HNO_3, etc.) and therefore, they are hydrophilic (attracted to water). To be extracted into the organic phase, the hydrophilic solutes must be turned hydrophobic (unfavorable interaction with water) and be electrically neutral [47,48].

The types of organic solvents used in LLE are very diverse depending on the purpose of extraction and the type of solutes being extracted. More details on types and properties of organic solvents can be found in references [47,49,50]. For the purpose of metal extraction, solvents composed of molecules that contain active hydrogen atoms but no donor atoms such as chloroform and some other aliphatic halides are commonly used. In addition, solvents that do not have capability to form hydrogen bonds and do not have donor atoms such hydrocarbons, carbon tetrachloride, are also common. These organic

solvents cannot extract the metal solutes because they do not have the capability to dissolve them. Therefore, the solvents are used as the diluent; that is the material used to dilute the extracting agents [47].

The distribution of a solute in the aqueous and organic phases can be explained based on Nernst's Distribution Law [48]. In a chemical system at equilibrium, one can write a reaction:

$$[A]_{aq} \rightleftarrows [A]_{org} \quad \text{Eq. 3}$$

where $[A]_{aq}$ is the concentration of solute A in the aqueous (aq) phase and $[A]_{org}$ is the concentration of solute A in the organic (org) phase. The distribution constant (K_D) of equilibrium reaction in Eq. 3 can be expressed as:

$$K_D = \frac{[A]_{org}}{[A]_{aq}}. \quad \text{Eq. 4.}$$

The distribution constant (K_D) in Eq. 4 only considers the presence of a single species of solute A and is valid only for pure solvents. In reality, there are several factors that make Eq. 4 impractical. For instance, the mutual solubility of the aqueous and organic phases and the changes of the ionic strength of the aqueous phase [48]. In that case, Eq. 4 must be corrected to take into account the activity coefficients (γ) of solute A in both phases:

$$K_D = \frac{\gamma_{A,org} \cdot [A]_{org}}{\gamma_{A,aq} \cdot [A]_{aq}} \quad \text{Eq. 5.}$$

A metal solute in the aqueous phase could exist in different species. Therefore, Eqs. 4-5 cannot be used to quantify the extraction yield. A more practical expression of the distribution ratio (D) is used as shown in the following equation:

$$D = \frac{[A]_{T,org}}{[A]_{T,aq}} \cdot \frac{V_{aq}}{V_{org}} \quad \text{Eq. 6}$$

where the subscript T denotes the total concentration of all species of solute A in either phase and V is volume of the phase. It is common that the volumes of the phases are equal; thus, the volume term can be eliminated in the calculation. In addition to the distribution ratio (D), a more informative expression, extraction E, is also often used to quantify the extraction yield as shown in the following equation:

$$E = \frac{[A]_{T,org}}{[A]_{T,org} + [A]_{T,aq}} = \frac{D[A]_{T,aq}}{D[A]_{T,aq} + [A]_{T,aq}} = \frac{D}{D+1} \quad \text{Eq. 7}$$

Figure 4 shows a simplified graphical representation of LLE. The temperature setting in the figure (24 ^{o}C) is only an example as LLE can be done at various temperatures depending on the chemistry procedure. The relative positions of the phases are also varied according to the density of the liquids. This figure also shows that, after the aqueous and the organic phase are in contact, the solutions are mixed to increase the interfacial surface contact of the phases and allow the chemical system to reach equilibrium state [51]. This step is often conducted with the aid of a mechanical mixer. The next step is phase settling, commonly accomplished through centrifugation, to allow the two phases to be completely separated. The final step is separation of the phases followed by analysis of the solutes' concentration in each phase.

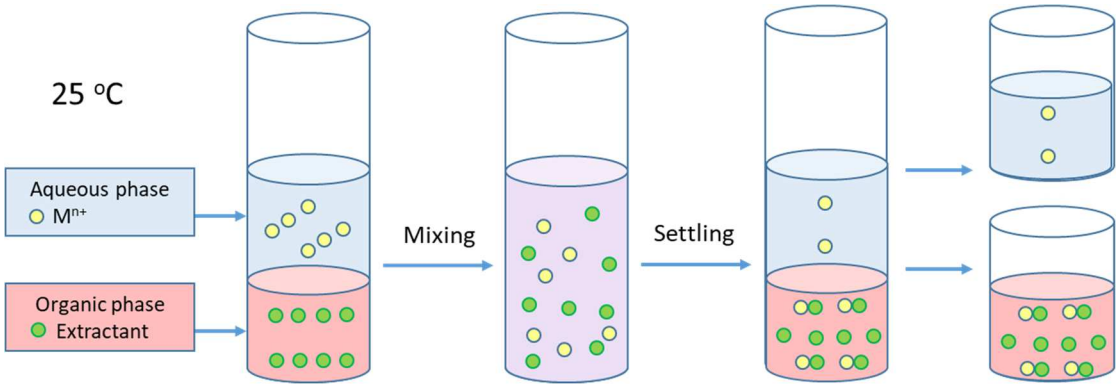

Figure 4. The graphical representation of LLE is shown. After the phase separation, each phase is analyzed to determine the concentration of the analytes and their distribution between the two phases.

1.4 Ionic Liquids and Eutectic Solvents

1.4.1 Ionic Liquids

The use of conventional organic solvents in chemical processes such as LLE have been a concern due to their toxicity, flammability, and/or corrosiveness, which is said to have contributed to environmental pollutions and increased risk to workers [52]. In early 1990, the concept and principles of green chemistry were developed to address the necessity to control the impact of chemical processes to human health and the environment [53]. This includes the need to use sustainable solvents that fulfill the principles of green chemistry (e.g., waste prevention, atom economy, safer solvents and auxiliaries, *etc.* See ref. [52] for more details).

Ionic liquids (ILs) have emerged as an alternative substitution for conventional molecular solvents in chemical processes including LLE owing to their wide liquid range, very low vapor pressure, non-flammability, and ability to solubilize various solutes [54]. IL is a class of solvent that are entirely made of ions (discrete organic cations and weakly

coordinating anions) and have melting points below 100 ^{o}C. The melting points of the ILs are mainly determined by the balance of cation and anion symmetry, length of the alkyl chain of the cation, and the accessibility of the charge [55].

The physicochemical properties, such as thermal stability, hydrophobicity, viscosity, and conductivity of the ILs can be tuned by varying the combination of the cations and anions [56-58]. Because of this tunability property, the ILs are often addressed as "designer solvents". It was reported that this combination can possibly lead to the formation of up to 10^{18} ILs [59]. With many variations of ILs available, they have been applied in various fields such as organic synthesis [60-63], catalysis [64-67], electrochemistry [68], electrocatalysis [69], solid support [70], nanoparticle formation [71], and solvent extraction [72-74].

Although the use of ILs as a green solvent started in the late 1990s, the development of the IL has spanned over 100 years. In 1914, Paul Walden who was a German chemist, developed the ILs through neutralization of ethylamine with concentrated HNO_3 to form ethylammonium nitrate (EAN). The product has melting temperature 13 – 14 ^{o}C [75] and shows water-like physical properties for its clear, colorless, odorless appearance with density 1.21 g/cm^3 and reasonably high viscosity [76]. The electrical conductivity of EAN indicates the liquids are composed of anions and cations [76]. This compound was regarded as the first generation of IL [75,77]. The second generation of IL was reported in 1951 by Frank Hurley and Thomas Weir through the mixing of 1-alkylpyridinium halides and metal halides [78]. They found that a 1-ethylpyridinium bromide-aluminium chloride ([C_2py]Br-$AlCl_3$) mixture with 2:1 molar

ratio was liquid at room temperature [77,78]. Later development revealed that most of the second generation IL were not moisture-stable and that their acidity/basicity was hard to control [79]. The unique liquid-salt characteristic of the ILs furthered the research to overcome the limitation of the second-generation compound. In 1992, Wilkes and Zaworotko reported the synthesis of air- and water-stable 1-ethyl-3-methylimidazolium (EtMeim) based ILs [80]. They obtained two compounds that were liquid at ambient temperature: [EtMeim]BF_4 (m.p. 15 ^oC) and [EtMeim]$MeCO_2$ (m.p. -45 ^oC). This discovery was deemed as the beginning of the development of the current generation of ILs and opened a wide area of opportunity for application of the ILs.

Most of the current ILs are made of a combination of cations such as alkyl-substituted ammonium, phosphonium, imidazolium, pyridinium, and pyrrolidinium, while the anions are usually halides, hexafluorophosphate, tetrafluoroborate, trifluoromethanesulfonate, and bis(trilfuoromethanesulfonyl)imide. Based on its chemical structure, ILs generally can be classified into two categories: protic ILs (proton-donating) and aprotic ILs (nonproton-donating) [76]. Other subclasses also exist based on their distinct structural features, such as chiral ILs, magnetic ILs polymeric ILs, *etc.* [76].

The current research largely focused on the application of aprotic ILs 1-alkyl-3-methylimidazolium *bis*(trifluoromethanesulfonyl)imide (denoted as [$C_n$mim][Tf_2N], here the subscript "n" represents the alkyl group) and N-propyl-N-methylpyrrolidinium *bis*(trifluoromethanesulfonyl)imide (denoted as [C_3C_1mim][Tf_2N]) and a protic IL betainium *bis*(trifluoromethylsulfonyl)imide (herein denoted as [Hbet][Tf_2N]) as the solvents in LLE. Figure 5 shows the structures of aprotic ILs used in this research.

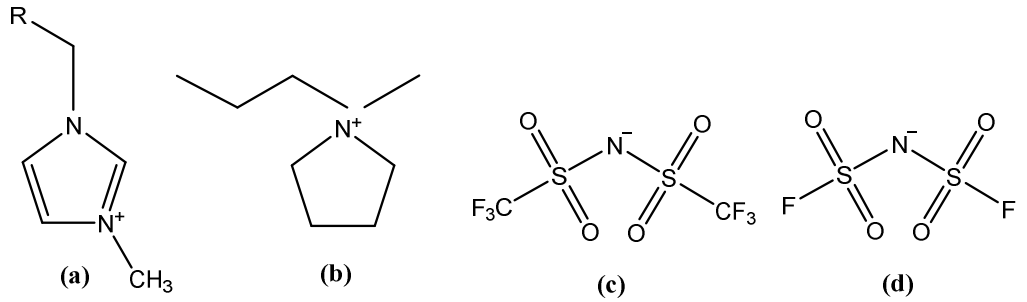

Figure 5. The structures of cations and anion of aprotic ILs used in this research: (a) 1-alkyl-3-methylimidazolium cation (b) N-propyl-N-methylpyrrolidinium cation, (c) *bis*(trifluoromethanesulfonyl)imide anion, (d) *bis*(fluorosulfonyl)imide anion.The imidazolium- and pyrrolidinium-based ILs are commercially available and their physicochemical properties have been characterized [81-84]. Meanwhile, [Hbet][Tf_2N] usually is synthesized in the laboratory because it is not commercially available. The building block of the [$Hbet^+$] cation (also commonly referred to as betainium) is glycine betaine, a zwitterion. By definition, zwitterion is a molecule that naturally possesses both positive and negative charge groups within its structure [85]. Glycine betaine consists of a positively charged tetramethyl-ammonium group and a negatively charged carboxylate group. Protonation to the carboxylate group leads to the formation of [$Hbet^+$] (pK_a = 1.83 [86,87]). Figure 6 shows the structures of zwitterionic betaine and betainium.

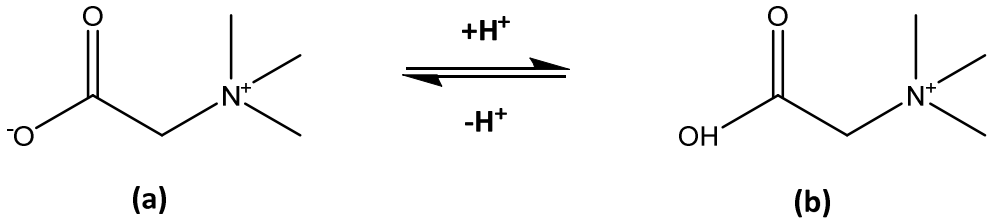

Figure 6. The chemical structure of zwitterionic betaine (a). Protonation of betaine at the carboxylic group leads to the formation of betainium (b).

The IL [Hbet][Tf_2N] was initially developed by Nockemann et al. and they successfully used it to dissolve metal oxides [88]. The carboxylate group on the cationic part has the ability to complex with metal ions, which makes this IL has an advantage over conventional ILs. Some interesting properties of [Hbet][Tf_2N] were reported. For example, the phase separation between [Hbet][Tf_2N] and water is temperature- and pH-dependent [88]. In addition, the [Hbet][Tf_2N] and water mixture exhibits an upper critical solution temperature (UCST) of 55° C [87]. This means that above the UCST, the mixture forms only one phase, while below the UCST, phase separation occurs. These unique properties of [Hbet][Tf_2N] have been exploited for metal extractions through formation of homogenous phases at elevated temperature above the UCST [86,87,89-91].

1.4.2 Eutectic Solvents

Similar to ILs, eutectic solvents (ESs) have also gained interests in the green chemistry process. This type of solvent was introduced by Abbott and co-workers in 2003 and was made from the mixtures of amides and quaternary ammonium salts which are solid in their individual forms [92]. They described that, at stoichiometric mixing ratio, the melting points of the mixtures were much lower than their pure compounds due to the formation of hydrogen bonding between a hydrogen bond donor (HBD) and hydrogen bond acceptor (HBA) [92]. The authors addressed these mixtures as deep eutectic solvents (DESs). This finding has inspired the increasing interest in research on DESs, resulted in more than 1900 DESs related publications registered on ISI Web of Science (as of January 2019). Most of these publications characterized DESs as the analogues

solvents to ILs due to having low vapor pressure, relatively wide-liquid range, and non-flammable but are easier to prepare from cheap materials [93]. However, the definition of DES was criticized and new term was later proposed to define a DES. That is, to qualify as a "deep eutectic solvent", the mixture of the pure compounds must have the eutectic point temperature below an ideal liquid mixture (a mixture that still maintains the physical properties of its pure substances) [94] as shown in Figure 7. This new definition is likely to screen out a lot of references on DESs because most of them deal with eutectic mixtures. Therefore, in this research the terminology ES is used as a generic term for eutectic mixture unless stated otherwise.

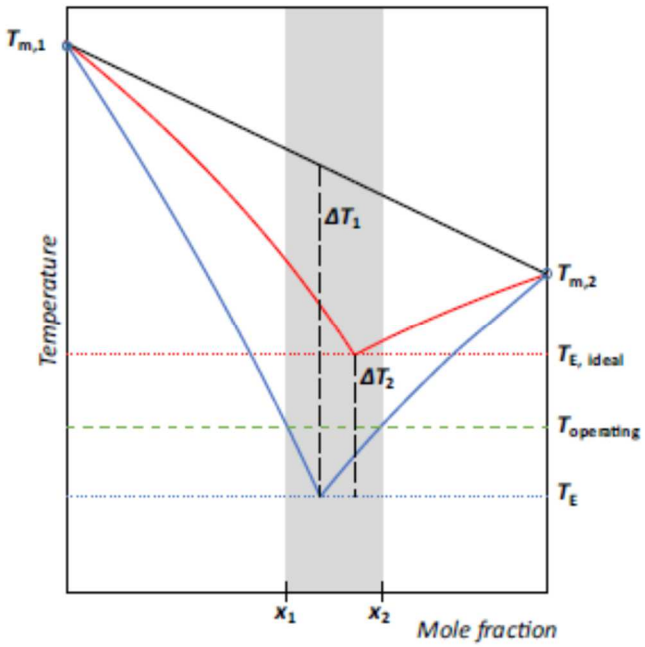

Figure 7. The comparison of the solid-liquid equilibria between a eutectic mixture (red line) and deep eutectic mixture (blue line).Figure used with permission from ref. [94].Most of the ESs are water-soluble but there are few water-immiscible mixture (hydrophobic). Among the hydrophobic ES are the mixtures of DL-menthol as HBA and some carboxylic

acids as HBD, all are biodegradable materials and relatively inexpensive [95]. These mixtures were prepared by combining the individual compounds with a proper molar ratio, then increase the temperature until a liquid mixture is formed at room temperature. Among all the studied ESs, four liquid mixtures that were prepared from the combination of DL-menthol with acetic acid, pyruvic acid, lactic acid, or lauric acid were found to be hydrophobic. The structures of the individual chemical compounds are shown in Figure 8, and the data on their molar ratio and thermal properties from TGA measurement is presented in Table 2. The decomposition temperature, T_{dec}, shows the melting point of the substance, while glass transition temperature, T_g, refers to the temperature at which the physical properties of the materials changes to glassy or crystalline state. It can be seen in the table that all ESs have melting temperatures lower than their individual compounds.

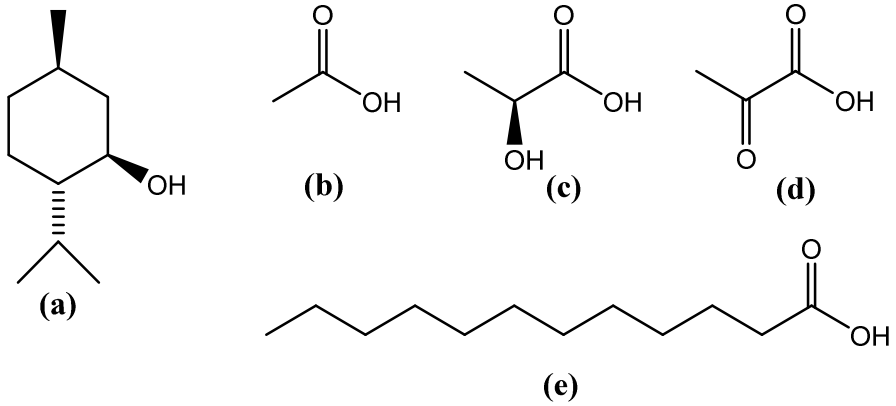

Figure 8. The structures of chemicals used to prepare hydrophobic ES are shown. (a) DL-menthol; (b) acetic acid; (c) L-Lactic acid; (d) pyruvic acid; (e) lauric acid.

Table 2. Molar ratio, decomposition temperature (T_{dec}) and glass transition temperature (T_g) of the hydrophobic ESs. Adapted with permission from "Menthol-based Eutectic Mixtures: Hydrophobic Low Viscosity Solvents" by B. D. Ribeiro et al., ACS Sustainable Chem. Eng. 2015, 3, 10, 2469-2477 [95]. Copyright (2015) American Chemical Society.

Pure compounds	**T_{dec} (ºC)**	**T_g (ºC)**
DL-menthol	168.95	36.82; 44.06
Acetic acid	N/A	16 – 17
Pyruric acid	164.48	11.80
Lactic acid	229.46	16.80
Lauric acid	292.34	43.20
Eutectic mixtures		
DL-menthol: Acetic acid (1:1)	200.79	-7.81
DL-menthol: Pyruric acid (1:2)	218.50	-58.81; -6.78
DL-menthol: Lactic acid (1:2)	228.89	-61.14
DL-menthol: Lauric acid (2:1)	231.49	7.13;13.84

1.4.3 Di-(2-ethylhexyl)phosphoric Acid (HDEHP)

HDEHP (pK_a = 3.24) [96] is an organophosphorus compound widely used as an extracting agent for metal partitioning in solvent extraction techniques. The ability of HDEHP to extract several lanthanides and actinides into mineral acids was reported in 1957 [97]. The best known application of HDEHP is for separation of trivalent minor actinides from the lanthanides produced from nuclear fission in spent nuclear fuel. This process is also known as TALSPEAK (Trivalent Actinide – Lanthanide Separation by Phosphorus reagent Extraction from Aqueous Komplexes) process [98,99]. The structure of HDEHP is shown in Figure 9.

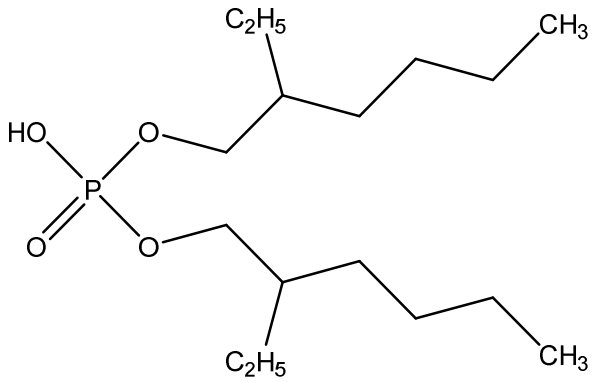

Figure 9. The chemical structure of HDEHP.

Some studies have shown that HDEHP forms a dimer in non-polar solvents and forms a monomer in polar solvents. The extraction mechanism depends on the nature of these diluents [100,101]. However, metal extraction with HDEHP commonly occurs through a cation exchange process, where HDEHP can be a monomeric or dimeric species as shown in Eqs. 7 and 8, respectively.

$$M^{n+}{}_{aq} + n(HA)_{org} \rightleftarrows MA_{n_{org}} + nH^{+}{}_{aq} \quad \text{Eq. 8}$$

$$M^{n+}{}_{aq} + n(HA)_{2_{org}} \rightleftarrows M(AHA)_{n_{org}} + nH^{+}{}_{aq} \quad \text{Eq. 9}$$

where M is the metal ion, HA represents the HDEHP, and the subscripts “aq” and “org” refer to the species in the aqueous and organic phase, respectively.

1.5 Review of Past Studies

There have been some studies of extraction of In and Tl into ILs. Kubota et al. investigated the extraction of In(III) into 1-alkyl-3-methyl imidazolium bis(trifluoromethanesulfonyl)imide, [$C_n$mim][Tf_2N] n= 4, 8, with trioctylphosphine oxide (TOPO) as the extractant [102]. The authors claimed 100% In(III) recovery but no In(III)

was extracted in the absence of TOPO. Another study by Katsuta et al. involved the combination of two ILs trioctylammonium nitrate [TOAH][NO_3] and trioctylammonium bis(trifluoromethanesulfonyl)imide [TOAH][Tf_2N] to extract aluminum(III), gallium(III), and indium(III) from HCl media. Indium(III) was only poorly extracted with an efficiency below 10% [103]. Hoogerstraete et al. extracted In(III) from water by using betaine into betainium bis(trifluoromethanesulfonyl)imide [Hbet][Tf_2N] with D values > 200 [89]. Tereshatov et al. studied In(III), Tl(I), and Tl(III) extraction into [C_4mim][Tf_2N] from HCl media with and without the presence of TBP as the extracting agent [104]. The result showed that Tl(III) was quantitatively extracted into pure IL and D values increased in the presence of TBP. Both Tl(I) and In(III) were not extracted [104]. Extraction of In(III) into 0.1 M TBP dissolved in n-hexyl-trimethylammonium bis(trifluoromethyl-sulfonyl)amide ([N_{1116}][TFSA]) ionic liquid from 1,1,1-trifluoro-N-[(trifluoromethyl)sulfonyl]methane sulfonamide (H[TFSA]) was studied [105]. The authors obtained 100% indium extraction efficiency in the range of pH 1.5 – 4.0. Cubova et al. studied extraction of thallium and indium isotopes into 1-alkyl-3-methylimidazolium bis(trifluoromethansulfonyl)imide ionic liquids ([$C_n$mim][Tf_2N], where n = 2, 4, 6 and 10) and tributylmethylammonium bis(trifluoromethanesulfonyl)imide ([Tbma][Tf_2N]) from hydrochloric acid media [30]. The authors used sodium chlorite, $NaClO_2$, to oxidized Tl(I) to Tl(III). Their results showed that In(III) was not extracted while Tl(III) was effectively extracted into all ILs within 0.2 – 5 M HCl.

The study of In extraction into ESs is more scarce compared to extraction into ILs and no research has been reported on Tl extraction into this media. In 2016, Tereshatov et al. reported the study on In(III) transfer from hydrochloric and oxalic acid into hydrophobic DESs and low-transition-temperature mixtures [106]. These mixtures were composed of quaternary ammonium chloride with decanoic acid, oleic acid and ibuprofen as well as DL-menthol and lauric acid mixture. Their results show the highest distribution ratio value for In(III) was obtained when it was extracted into quaternary ammonium chloride with ibuprofen from 6 M HCl and from the range of 0.01 – 0.1 M oxalic acid (D_{In} > 3000). Meanwhile, indium extraction into a DL-menthol and lauric acid mixture was found to be effective only at low acidity (D_{In} = 20 at 0.001 M HCl).

Literature reports on metal extraction with HDEHP show that this extractant has been effectively used to extract indium from various media. Sato et al. extracted In(III) from HNO_3 and HCl solutions into HDEHP in kerosene [107]. They obtained the highest D_{In} values at HNO_3 concentration below 0.1 M and at 0.2 M HCl with 0.1 M HDEHP (D_{In} 100 and ~40, respectively). In(III) was extracted from H_2SO_4 into various alkylated organophosphates extractants in toluene [108]. Their results showed the extraction into 0.025 M HDEHP is the highest at pH 0.7 with D_{In} = 4. HDEHP was also used for selective extraction of indium from indium tin oxide obtained from LCD screen waste [109,110]. The extraction efficiency of indium was 100% when it was extracted into 1 M HDEHP from < 2 M H_2SO_4 or from < 0.8 M HCl [109]. HDEHP was diluted in a variant of kerosene, marketed as ShellSol 2046 or Exxsol D-80. The other study showed that D_{In} approached 600 when indium was extracted from 0.1 M H_2SO_4 into 0.1 M HDEHP in

kerosene and 200 when it was extracted from 0.1 M HCl into the same media [110]. Separation of no-carrier-added ^{113,117m}Sn and ^{113m,114m}In from natural cadmium target irradiated by alpha particle was investigated by solvent extraction with HDEHP [111]. The extraction was optimized when In(III) was extracted from 0.01 M HCl into 5% HDEHP in cyclohexane.

Limited data on mutual solubility of ionic liquid, in particular [Hbet][Tf_2N], with water are available. Nockemann et al. reported that [Hbet][Tf_2N] contains 13% of water and 15% of the IL dissolved in water [88]. By using various analytical techniques, Onghena et al. also studied mutual solubility of [Hbet][Tf_2N] and water [86]. They reported that the [Hbet][Tf_2N] phase contained 12.9%, 7.6 ± 4.6%, and 15.5 ± 0.5% of water and the water phase contained 13.8%, 14 ± 0.5%, and 14.3 ± 0.5% of [Hbet][Tf_2N] determined with TGA, ^{1}H-NMR, and cloud point titration, respectively. It was also found that the presence of mineral acids or sodium salts can alter the solubility of IL in the water phase [112]. The authors observed IL solubility in water increased in 1 M of mineral acids in the order of H_2SO_4 > HCl > HNO_3 > $HClO_4$. When 1 M sodium salts of these acids were used, the solubilities are lower but increased in the same order.

1.6 Scope and Objectives

This research involves the study of the chemistry of Nh's closest homologues, indium (In) and thallium (Tl), in the liquid phase. This study is designed to provide the basis for a suitable chemistry system that can be used for the potential study of Nh

chemistry in the future. A novel chemical procedure to extract and separate In and Tl effectively was developed by using a liquid-liquid extraction (LLE) technique.

First, the study focused on investigating the ability of imidazolium- and pyrrolidinium- to extract In(III) and Tl (I, III) from hydrochloride acid (HCl) media. Second, mutual solubility of betainium-based IL and water in the presence of HCl and zwitterionic betaine was investigated. The results of this study were important particularly to understand the chemical interactions between the molecules in the system and to explain the mechanism of In and Tl extraction into [Hbet][Tf_2N]. Third, the extraction of In and Tl(I, III) from HCl into [Hbet][Tf_2N] was studied, without and with the presence of zwitterionic betaine as the extracting agent. Fourth, the ability of menthol-based ES to extract In(III) and Tl(I, III) from HCl was investigated, without and with the presence of HDEHP as the extracting agent. Extraction mechanisms of In and Tl into these chemical systems were also explained.

2. EXPERIMENTS

2.1 Chemicals

The chemicals used in all the experiments are described in the next paragraphs. Those chemicals were used as received without further purification. All materials are commercially available, except for the betainium-based IL which was synthesized in the laboratory. The synthesis of this IL is described in section 2.4.

2.1.1 Mutual Solubility of Water and Betainium-based IL

High purity grade betaine anhydrous (N,N,N–trimethylammonium acetate, abbreviated as bet, ≥ 99.0%), betaine hydrochloride (HbetCl, ≥ 99%) and analytical grade deuterium chloride (deutero-hydrochloric acid, DCl, 99 atom% D, 35 wt% in D_2O) were purchased from Sigma-Aldrich. High purity grade lithium bis(trifluoromethylsulfonyl)imide (Li[Tf_2N], 99.9%) was obtained from Solvionic (Toulouse, France). Deuterium oxide (deuterated water, D_2O, 99 atom% D) was purchased from Eurisotop (Gif sur Yvettte, France). Sodium acetate (99.0%) and sodium trifluoroacetate (98.0%) were ordered from Merck (Darmstadt, Germany) and Alfa Aesar (Tewksbury, Massachusetts, USA), respectively. Sodium hydroxide (NaOH) standard solutions were purchased from Carlo Elba (Val-del-Reuil, France). Deionized water (ELGA PURELAB DV25) with a resistivity of 18.2 MΩ cm was used for preparing the aqueous solutions, whereas the NMR samples were prepared by using deutero-hydrochloric acid and/or deuterium oxide.

2.1.2 In and Tl Extraction into Pure Imidazolium- and Pyrrolidinium-based IL

High-purity grade (99.5%) 1-alkyl-3-methylimidazolium bis(trifluoromethanesulfonyl)imide ionic liquids (henceforth indicated as $[C_nmim][Tf_2N]$, where n = 2, 4, and 8), 1-propyl-2,3-dimethylimidazolium bis(trifluoromethanesulfonyl)imide (indicated as $[C_3C_1mim][Tf_2N]$), N-propyl-N-methylpyrrolidinium bis(trifluoromethanesulfonyl)imide (indicated as $[C_3C_1pyrr][Tf_2N]$), 1-ethyl-3-methylimidazolium bis(fluorosulfonyl)imide (indicated as $[C_2mim][FSI]$), and $Li[Tf_2N]$ salt (>99% purity) were purchased from Solvionic (Toulouse, France). Concentrated hydrochloric acid was purchased from Merck (Darmstadt, Germany). Both saturated 3% (w/v) bromine water and 0.3% (w/v) chlorine water were obtained from Ricca Chemical (Arlington, Texas, USA). Thallium(III) chloride hydrate was of analytical grade and purchased from Alfa Aesar (Tewksbury, Massachusetts, USA).

2.1.3 In and Tl Extraction into Betainium-based IL

High-purity grade betaine anhydrous (N,N,N–trimethylammonium acetate, abbreviated as betaine, ≥99.0%) and betaine hydrochloride (HbetCl, ≥99%) were purchased from Sigma (St. Louis, Missouri, USA). High-purity grade lithium bis(trifluoromethylsulfonyl)imide ($Li[Tf_2N]$, ≥98.0%) salt was obtained from TCI America (Portland, Oregon, USA). Concentrated hydrochloric acid was purchased from Merck (Darmstadt, Germany) and 70% (v/v) nitric acid was purchased from BDH chemicals (Sanborn, New York, USA). Both saturated 3% (w/v) bromine water and 0.3%

(w/v) chlorine water were obtained from Ricca Chemical (Arlington, Texas, USA). Indium(III) chloride anhydrous ($InCl_3$) and thallium(III) chloride hydrate ($TlCl_3.xH_2O$) were of analytical grade and purchased from Alfa Aesar (Tewksbury, Massachusetts, USA). Deionized water (ELGA PURELAB DV25) with a resistivity of 18.2 MΩ cm was used for preparing the aqueous solutions.

2.1.4 In and Tl Extraction into DL-menthol-based ES

DL-menthol and lauric acid (> 98% purity) were purchased from VWR. Bis(2-ethylhexyl) phosphate (HDEHP, >95% purity) was purchased from Alfa Aesar (Tewksbury, Massachusetts, USA). Concentrated hydrochloric acid was purchased from Merck (Darmstadt, Germany). Deionized water (ELGA PURELAB DV25) with a resistivity of 18.2 MΩ cm was used for preparing the aqueous solutions.

2.2 Radionuclides

Carrier-free ^{111}In and ^{201}Tl medical radioisotopes were purchased from Mallinckrodt (St. Louis, Missouri, USA). Table 3 shows the production methods and decay characteristics of the radionuclides.

Table 3. Radionuclides used in this work, decay characteristic and production methods Adapted from ref. [104].

Nuclide	Nuclear reaction	Radiopurity	Half-life	γ Energy	Intensity
		(%)	(d)	(keV)	(%)
^{111}In	^{112}Cd(p,2n)^{111}In	99.9	2.80	171.3	90.2
				245.5	94.0
^{201}Tl	^{203}Tl(p,3n)^{201}Pb → ^{201}Tl	98.2	3.04	70.8	46.0
				167.4	10.0

Indium(III) chloride in 0.05 M hydrochloric acid and thallium(I) chloride in 0.9% (w/v) sodium chloride and preserved with 0.9% (v/v) benzyl alcohol. The concentrations of ^{111}In and ^{201}Tl per sample after multistep dilution were below 1×10^{-11} M.

2.3 Instruments and Analytical Techniques

2.3.1 Mutual Solubility of [Hbet][Tf_2N] and Water

2.3.1.1 Nuclear Magnetic Resonance (NMR)

The solubility of [Hbet][Tf_2N] in the aqueous phase was determined by measuring the concentrations of betaine- and bistriflimide- containing species in the aqueous phase with quantitative proton (^{1}H) and fluorine (^{19}F) nuclear magnetic resonance (NMR), respectively. The NMR spectra were recorded using a Bruker Avance 300 MHz NMR spectrometer. An overview on the NMR technique is available in [113] and the detailed procedure on NMR measurement can be found in [106,114].

2.3.1.2 Acid-base Titration

For the mutual solubility study of [Hbet][Tf_2N] and water, the total hydrogen ion concentration in the aqueous phase was determined before and after the aqueous and organic phases were in contact (initial and equilibrium condition). The aqueous phase was titrated using sodium hydroxide with a SCHOTT Instruments Titroline Easy automated titrator.

2.3.1.3 Argentometry

The initial and equilibrium concentration of chloride anion in the aqueous phase was determined by using Mohr method [115]. By using a burette, silver nitrate solution was added gradually into an aliquot of chloride containing aqueous phase until all chloride was precipitated as silver salt. Potassium dichromate was used as an indicator to determine the end point of titration.

2.3.1.4 Karl Fischer Titration

To determine the solubility of water in [Hbet][Tf_2N], the total content of water in the IL phase was measured using a Mettler Toledo 32 Karl Fischer coulometric titrator. The performance of the titrator was tested using a standard solution (Hydranal^{TM}-water, Fluka) containing 1,000 or 10,000 ppm water.

2.3.2 In and Tl Extraction

2.3.2.1 Sodium Iodide Detector

The activity levels of radioactive In and Tl in the aqueous and organic phases after the extraction were measured using 2480 Wizard^{2TM} PerkinElmer automatic gamma counter. This is a high efficiency, 3" well-type NaI(Tl) detector that can be set to count up to 1000 samples [116]. The details on the operational procedure of the instrument can be found in [117] and the principles of radiation detection using a NaI(Tl) detector can be found in [118,119].

2.3.2.2 Inductively Couple Plasma-Mass Spectrometry (ICP-MS)

The determination of stable In and Tl concentrations in the samples was accomplished using a PerkinElmer NexION 300D ICP-MS instrument. The ICP-MS technique has been widely used for elemental analysis due to its high sensitivity, capability to analyze multi-elements, wide linear range, possibility to obtain isotopic information and applicability in various fields [120]. Detailed information about this technique is available in refs. [121,122].

2.3.3 Other Instruments

The pH measurement was conducted by using VWR Symphony SB70P pH meter. Analytical balances Sartorius model BP 2215 and Mettler-Toledo model ML204 with any accuracy of ± 0.1 mg were used to weigh the components.

2.4 Experimental Procedures

2.4.1 Synthesis of [Hbet][Tf_2N]

The IL [Hbet][Tf_2N] was synthesized according to refs. [88,89] with some modifications. Initially, 0.1 mol of betaine hydrochloride (MW 153.61 g/mol) and 0.1 mol of lithium bis(trifluoromethanesulfonylimide) (MW 287.075 g/mol) salts were dissolved in deionized water and then mixed in a beaker. This mixture was stirred for 1 h at room temperature then let to phase-separate. The main source of organic phase impurities came from the salts (Li[Tf_2N] and HbetCl) used for the ionic liquid synthesis and therefore, the ionic liquid purity is at most 99%. The resulting IL was separated from the aqueous phase and washed with small amounts of deionized water several times to remove chloride impurities. An aliquot of the aqueous phase was drawn and treated with silver nitrate after each washing step to check for chloride content. The IL was recovered when there was no more precipitate observed in the aqueous phase.

Initially, an attempt to dry [Hbet][Tf_2N] IL using a rotary evaporator was made. However, it was found that the resulting IL was very hygroscopic and viscous which made it difficult to handle. This limitation has also been addressed in the literature [86]. Therefore, a preconditioning step was taken by pre-saturating [Hbet][Tf_2N] with deionized water. This step was necessary to avoid further water uptake during the partition trials, to minimize changes in the phase ratio, and to lower the viscosity of the organic phase. For most of the experiments with [Hbet][Tf_2N], the IL was used as is after the chloride impurity was removed.

It was reported that the viscosity of water-saturated [Hbet][Tf_2N] at 25 ^oC is 84.7 cP [123]. The preconditioning method used in this study is similar with ref. [123]. Therefore, it is assumed that the viscosity of the water-saturated [Hbet][Tf_2N] in this study is similar to the reported value above. The density of water-saturated [Hbet][Tf_2N] was determined by weighting the IL in a 1 mL volumetric microflask. The measured density at 23 ± 2 ^oC is 1.439 ± 0.014 g/cm^3, and is in good agreement with the literature data (1.453 g/cm^3) [124].

2.4.2 Synthesis of DL-menthol – Lauric Acid ES

The ES was prepared by weighting DL-menthol (MW 156.269 g/mol) and lauric acid (MW 200.318 g/mol) appropriately to obtain a 2 : 1 molar ratio. The solid mixture was heated in a water bath at a temperature of 70 ^oC until liquid mixture was obtained (typically it took 30 minutes). The mixture was cooled to room temperature before it was ready to use.

2.4.3 Mutual Solubility of [Hbet][Tf_2N] and Water

2.4.3.1 Overview of the Experiments

Mutual solubility of [Hbet][Tf_2N] and water was studied in the presence of HCl and zwitterionic betaine. The experiments were carried out at room temperature (23 ± 2 ^oC) by the conventional liquid–liquid extraction technique. Due to its higher density compared to the aqueous phase, in all solubility experiments the IL forms the bottom phase.

To determine the concentrations of the target analytes (betaine-bearing species and sodium acetate internal standard) with quantitative ^{1}H-NMR, it is important to distinguish the proton signal originating from the solvent and from the samples. Therefore, in this study, deutero-hydrochloric acid (DCl) and deuterium oxide (D_2O) were used in place of HCl and H_2O, respectively. The use of deuterium in place of light hydrogen was assumed not to affect solute partition behavior in the biphasic system under study.

In addition, this mutual solubility study required the analysis of the concentration of the analytes in the organic and aqueous phases before and after the phase contact. Thus, the following experimental details are defined for clarity. First, the concentrations are expressed as molarities (mol/dm^3). Second, the initial concentration specifically refers to the concentration of a species before the organic and aqueous phase are put in contact (prior to the formation of biphasic system). Meanwhile, the equilibrium concentration describes the concentration of a species after the formation and separation of the biphasic system. The subscripts “init” and “eq” are used to denote the initial and equilibrium concentrations, respectively. Third, the experiment involved organic (IL) and aqueous phases. The subscripts “org” and “aq” are used to address the species in the IL and aqueous phase, respectively. Fourth, since the analysis with ^{1}H-NMR uses deuterated solvents, deuterium (^{2}H, D) from these solvents is also present in the aqueous phase in addition to proton (^{1}H) from the solutes. Therefore, for simplicity, a generic notation H^+ is used to address the acidic proton from either source.

2.4.3.2 Sample Preparation

The aqueous acidic phase was prepared by diluting concentrated deutero-hydrochloric acid (DCl) with D_2O appropriately to obtain the DCl concentrations in the range of 0.01 – 8 M. The samples were prepared by adding equal volumes of water-saturated IL and aqueous phase (typically 800 μL) into a 2-mL Eppendorf centrifugation tubes. The required mass of IL was calculated using the density and weighed precisely to obtain the required volume. The aqueous phase was added into the tube by an Eppendorf Research precision pipette. Then, biphasic samples were vigorously mixed for 5 min at 1,500 rpm using a mechanical shaker (IKA vibrax VXR basic). After the mixing, the samples were centrifuged for 5 min at 3,000 rpm (Micro Star 12, VWR) in order to promote phase separation.

Subsequently, the aqueous phase was analyzed to determine the equilibrium concentration of the IL cation and anion, proton, and chloride ions in the aqueous phase using techniques described in sections 2.3.1.1 – 2.3.1.3. Meanwhile, the organic phase was analyzed to determine the equilibrium concentration of water based the technique described in section 2.3.1.4.

2.4.3.3 Sample Analysis

For analysis of samples with quantitative ^{1}H-NMR and ^{19}F-NMR, an aliquot of the equilibrium aqueous phase was taken and mixed with sodium acetate and sodium trifluoroacetate solutions as internal standards (δH = 1.90 ppm and δF = -76.5 ppm,

respectively). This solution was diluted with D_2O to the required volume (typically 600 μL), then shaken in order to assure homogeneity and placed into the NMR tube. The concentrations of the analytes were calculated using the following equation:

$$C_x = \left(\frac{I_x}{I_{std}}\right)\left(\frac{N_{std}}{N_x}\right)\left(\frac{V_{std}}{V_x}\right)C_{std} \quad \text{Eq. 10}$$

where C, I, N, and V are concentration, integral area, number of nuclei per molecule, and volume of the analyte (x) and internal standard (std), respectively [106].

2.4.4 In and Tl Extraction into Pure Imidazolium- and Pyrrolidinium-based ILs

2.4.4.1 Sample Preparation

The aqueous hydrochloric acid (HCl) stock solutions were prepared by appropriate dilution of concentrated HCl to obtain the solutions with the concentration of 0.01 – 8 M (mol/L). The organic phase was prepared by carefully weighing the IL to obtain a volume of 500 μL in a test tube (the density and other properties of the ILs are listed in Table 4). An equal volume of aqueous phase composed of HCl and an aliquot of In or Tl stock solution was added into the tube using an Eppendorf Reference precision pipette. For the study of the extraction of Tl(III), an aliquot of bromine (Br_2) or chlorine (Cl_2) water was added in order to oxidize Tl(I) to Tl(III).

After adding the organic and aqueous phase, the biphasic sample was shaken vigorously with a VWR Signature digital vortex mixer at 3000 rpm for 5 min (except for the kinetic study, in which the time was varied) at 23 ± 2 °C. Then, it was centrifuged at 4400 rpm for 1 min (Eppendorf model 5702) in order to promote phase separation.

Finally, an aliquot was taken from each phase to determine the indium or thallium concentration or activity.

Table 4. Properties of the ionic liquids. The molar masses, melting points, densities, and viscosities were obtained from the manufacturer. Meanwhile, the solubility of ILs in H_2O and the cation hydrophobicity were obtained from refs. [114,125]. Adapted with permission from "Thallium Transfer from Hydrochloric Acid Media into Pure Ionic Liquids" by E. E. Tereshatov et al., 2016. Journal of Physical Chemistry B, 120, 2311-2322, https://doi.org/10.1021/acs.jpcb.5b08924. Copyright [2016] by American Chemical Society.

Ionic liquid	**Molar mass, g/mol**	**Melting point, °C**	**Density, g/mL**	**Viscosity, cP**	**Solubility in H_2O, g/L**	**Cation hydrophobicity, log $k_{0,c}$***
[C_2mim][FSI]	291.30	–13	1.39	24.5	26.7 ± 2.7	0.22
[C_2mim][Tf_2N]	391.31	–16	1.52	35.55	18.8 ± 1.1	0.22
[C_4mim][Tf_2N]	419.36	–4	1.43	61.14	6.6 ± 0.4	0.67
[C_3C_1pyrr][Tf_2N]	408.40	+12	1.40	71.23	10.5 ± 0.6	< 0.57
[C_3C_1mim][Tf_2N]	419.36	+15	1.40	78.4	6.8 ± 0.4	–
[C_8mim][Tf_2N]	475.47	< +20	1.32	104	0.73 ± 0.05	1.8

*log $k_{0,c}$ = log capacity factor; related with the activity coefficient of IL's cation in the mobile phase at the beginning of the gradient. See ref. [125] for more details.

2.4.4.2 Sample Analysis

After phase separation, the organic and aqueous phase were analyzed to determine the activity level (or concentration, in the case of stable metal analytes) of In or Tl in each phase. For radioactive samples, the activity of the metal in the organic phase was counted before the aqueous phase, and the activity in the latter phase was corrected for radioactive

decay. Background correction was applied to the activity in both phases; then, the extraction yield is quantified as distribution ratio (D) according to Eq. 6.

To ensure that the count rate obtained from the measurement with the NaI detector is statistically meaningful, a minimum detectable amount (MDA) is set for every measurement. The MDA (α) is calculated based on the following equation [118]:

$$\alpha = \frac{N_D}{f \cdot \epsilon \cdot T} \quad \text{Eq. 11}$$

where N_D is minimum amount of counts from the source that is required to ensure that false-negative rate not more than 5% when the system is operated with a critical level (or a trigger point that ensure the false-positive rate < 5%), f is the radiation yield per disintegration, ε is absolute detection efficiency, and T is the counting time per sample. N_D can be calculated according to equation below [118]:

$$N_D = 4.653\ \sigma_{N_B} + 2.706 \quad \text{Eq. 12}$$

where σ_{N_B} is error of the background count.

2.4.5 In and Tl Extraction into Betainium-based IL

In this extraction experiment, In(III) and Tl (I, III) were extracted into [Hbet][Tf_2N] without and with the presence of zwitterionic betaine. [Hbet][Tf_2N] IL was synthesized according the procedure in section 2.4.1. The experimental procedure for the partition experiment was identical with that described in section 2.4.4, with an additional procedure for the system that contained additional zwitterionic betaine. For the latter system, HCl containing betaine (typically 15% unless stated otherwise) was prepared

prior to the phase mixing. This solution was prepared by weighing the appropriate amount of zwitterionic betaine (MW 117.148 g/mol) in a tube and adding HCl into it volumetrically.

To study the dependency of In(III) and Tl(III) extraction on Li[Tf_2N] concentration, stock solutions of the salt were prepared. A known amount of Li[Tf_2N] salt was dissolved in 0.05 M HCl and diluted gradually to obtain stock solutions with the concentration ranging from 0.004 – 0.6 M. This experiment was carried out using stable $InCl_3$ salt or $TlCl_3$ hydrate and the aqueous phase samples were analyzed using ICP-MS (see section 2.3.2.2).

2.4.6 In and Tl Extraction into DL-menthol-based ES

The ES composed of DL-menthol and lauric acid were synthesized according to procedure described in section 2.4.2. The density of dry DL-menthol and lauric acid ES at 25 ^oC is 0.894 g/cm^3 [95]. Therefore, in this system, the aqueous phase forms the denser phase. HDEHP as the extracting agent was added into the organic phase prior to the phase mixing. The partition experiment was carried out according to the procedure described in section 2.4.4.

3. MUTUAL SOLUBILITY OF [Hbet][Tf_2N] AND WATER*

This chapter focuses on the results of the mutual solubility study of [Hbet][Tf_2N] ionic liquid and water in the presence of HCl and zwitterionic betaine. Hydrochloric acid was used as the aqueous phase media in the study of In(III) and Tl(I, III) extraction into [Hbet][Tf_2N]. In addition, zwitterionic betaine was used as an additive or extractant to improve the extraction yield of the metals in that chemical system. In order to understand the extraction mechanism of In(III) and Tl(I, III) into [Hbet][Tf_2N], the chemical interactions between the molecules in the system have to be understood. The results of this mutual solubility study give an insight into it.

The analysis of the samples was carried out using several analytical techniques as described in section 2.3. Table 5 provides the uncertainties of the techniques used in the study. Additionally, as mentioned in section 2.4, deutero-hydrochloric acid (DCl) was used in place of HCl for the purpose of ^{1}H-NMR measurement and this substitution was assumed not to affect the chemical behavior of the solutes of interest.

* Reprinted with permission from "Effect of aqueous hydrochloric acid and zwitterionic betaine on the mutual solubility between a protic betainium-based ionic liquid and water" by M. F. Volia et al., 2018. Journal of Molecular Liquids, 276, 296-306, https://doi.org/10.1016/j.molliq.2018.11.136. Copyright [2018] by Elsevier B.V.

Table 5. The uncertainties of the analytical techniques used in the mutual solubility study are presented.

Phase	Species	Technique	Uncertainty (%)
Aqueous	H^+, D^+	Acid-base titration	2
	Cl^-	Argentometry	10
	[$Hbet^+$]	Quantitative ^{1}H-NMR	10
	[Tf_2N^-]	Quantitative ^{19}F-NMR	5
Organic	Water	Karl Fischer	5

3.1 Solubility of [Hbet][Tf_2N] in Water

To determine the solubility of [Hbet][Tf_2N] in water, a series of measurements was conducted to quantify the concentrations of the IL's cation and anion as well as proton and chloride ion in the aqueous phase. The equilibrium concentrations of the IL's cation ([$Hbet^+$]) and anion ([Tf_2N^-]) were measured by using ^{1}H-NMR and ^{19}F-NMR techniques, respectively. Meanwhile, the aqueous phase was titrated separately by using NaOH and $AgNO_3$ prior to and after being in contact with [Hbet][Tf_2N] to determine the initial and equilibrium concentration of H^+ and Cl^- ions. These measurements give the total equilibrium concentrations of all betaine-, bistriflimide-, and proton-containing species as well as the equilibrium concentration of Cl^- ion in the aqueous phase. In

addition, the concentration of free hydrogen ion in water was determined by using a pH meter.

Prior to analyzing the data, it is important to understand the underlying chemical reactions of [Hbet][Tf_2N] solubility in the aqueous phase. After [Hbet][Tf_2N] IL was mixed and separated with the aqueous phase, the IL was expected to partially distribute into the aqueous phase and dissociate into betainium and bistriflimide ions according to Eq. 13:

$$[\mathrm{Hbet}][\mathrm{Tf_2N}]_{\mathrm{org}} \rightleftarrows [\mathrm{Hbet^+}]_{\mathrm{aq}} + [\mathrm{Tf_2N^-}]_{\mathrm{aq}} \quad \text{Eq. 13.}$$

In the aqueous phase, betainium (pK_a = 1.83) [86,87] dissociates to form proton and zwitterionic betaine (bet):

$$[\mathrm{Hbet^+}]_{\mathrm{aq}} \rightleftarrows \mathrm{H^+}_{\mathrm{aq}} + [\mathrm{bet}]_{\mathrm{aq}} \quad \text{Eq. 14.}$$

In the presence of proton, bistriflimide anion undergoes protonation to form HTf_2N acid (pK_a = 0.16) [103] *via* the imide nitrogen sites:

$$\mathrm{H^+}_{\mathrm{aq}} + [\mathrm{Tf_2N^-}]_{\mathrm{aq}} \rightleftarrows [\mathrm{HTf_2N}]_{\mathrm{aq}} \quad \text{Eq. 15.}$$

Since the results from the NMR measurements and NaOH titration give only the total concentration of all betaine-, bistriflimide-, and proton-containing species, the concentrations of individual species as the reaction products in the aqueous phase shown in Eqs. 13 – 15 cannot be deduced directly from these measurement data. Therefore, a system of linear equations was developed to evaluate the individual concentrations of these species.

The system of linear equations is comprised of the mass balance equations of the proton-, betaine-, bistriflimide-bearing species (Eqs. 16 – 18), the dissociation constants

(K_a) of [$Hbet^+$] and [HTf_2N] (Eqs. 19– 20), and the relationship that shows the dependence of the activity coefficient $\gamma_{HCl\pm}$ on the H^+ concentration (Eq. 21). Hereinafter, proton-, betaine-, bistriflimide-bearing species are referred to as $H_{Titrated}$, Bet_{NMR}, and F_{NMR}, respectively.

$$[H^+]_{aq} + [Hbet^+]_{aq} + [HTf_2N]_{aq} = [H_{Titrated}] \quad \text{Eq. 16.}$$

$$[Hbet^+]_{aq} + [bet]_{aq} = [Bet_{NMR}] \quad \text{Eq. 17.}$$

$$[Tf_2N^-]_{aq} + [HTf_2N]_{aq} = [F_{NMR}] \quad \text{Eq. 18.}$$

$$\frac{\gamma_{HCl\pm}[H^+]_{aq}[bet]_{aq}}{[Hbet^+]_{aq}} = K_{a_{[Hbet^+]}} \quad \text{Eq. 19.}$$

$$\frac{\gamma_{HCl\pm}[H^+]_{aq}[Tf_2N^-]_{aq}}{[HTf_2N]_{aq}} = K_{a_{[HTf_2N]}} \quad \text{Eq. 20.}$$

$$\gamma_{HCl\pm} = f([H^+]_{aq}) \quad \text{Eq. 21.}$$

The system of equations used the mean ionic activity coefficient of HCl ($\gamma_{HCl\pm}$) in Eqs. 19 – 20 for the activity coefficient of the protons, with the assumption that this quantity is not affected by the presence of other ions dissolved in the aqueous phase [126,127]. It also has to be noted that the presence of various ions in the aqueous phase is likely to change the ionic strength of the solution especially when the HCl concentration is high. Since the concentration of [H^+] was varied, the effect of the ionic strength on the activity coefficient is indirectly accounted for in the system of equations. The dependence of the activity coefficient $\gamma_{HCl\pm}$ on the H^+ concentration in Eq. 21 was implemented using a lookup table based on literature data combined with linear interpolation [126]. It is also known that, in the presence of hydrochloric acid, [$Hbet^+$] interacts with Cl^- ion to form

[Hbet]Cl species (one of the precursors of [Hbet][Tf_2N]). However, this species was considered to be completely dissociated and was not included in the system of linear equations above.

3.1.1 Evaluation of the Solubility of the [Hbet][Tf_2N] in the Absence of DCl

The solubility of [Hbet][Tf_2N] in the absence of DCl is discussed in this section. The chemical systems that were evaluated consisted of pre-equilibrated [Hbet][Tf_2N] as the organic phase, and pure water or water containing initially 15 % (w/v) bet (1.28 M) as the aqueous phase. The data from ^{1}H-NMR, ^{19}F-NMR, titration and pH measurements for these systems were collected, then the equilibrium concentrations of individual species were calculated using the system of equations (Eqs. 16 – 21). The results are shown in Table 6. The uncertainties of the calculated values in Table 6 were estimated by using the values of uncertainties of the corresponding species in Table 5. Hereinafter, “measured” concentrations refer to the experimentally measured values and “calculated” concentrations refer to the concentration of individual species evaluated by the system of equations.

Table 6. Experimentally measured values and the calculated concentrations of individual species in the equilibrium aqueous phase based on the results from solving the system of equations. The chemical systems that were evaluated consisted of pre-equilibrated [Hbet][Tf_2N] as the organic phase, and pure water (denoted as "Water" in the table below) or water containing initially 15 % (w/v) bet (1.28 M) (denoted as "Water + bet") as the aqueous phase. Note that the presence of $[H^+]_{aq}$ in pure water was due to the solubility of [Hbet][Tf_2N] in the aqueous phase.

Experimentally measured values			**Calculated values**		
Species	**Water (M)**	**Water + bet (M)**	**Species**	**Water (M)**	**Water + bet (M)**
$\mathbf{[H^+]_{aq}}$	0.045 ± 0.004	(3.35 ± 0.33)·10^{-3}	$\mathbf{[H^+]_{aq}}$	0.048 ± 0.005	(6.2 ± 0.6)·10^{-3}
$\mathbf{[H_{Titrated}]}$	0.313 ± 0.031	0.296 ± 0.030	$\mathbf{[Hbet^+]_{aq}}$	0.251 ± 0.025	0.288 ± 0.029
$\mathbf{[Bet_{NMR}]}$	0.344 ± 0.034	1.030 ± 0.100	$\mathbf{[bet]_{aq}}$	0.093 ± 0.009	0.750 ± 0.080
$\mathbf{[F_{NMR}]}$	0.274 ± 0.014	0.260 ± 0.013	$\mathbf{[Tf_2N^-]_{aq}}$	0.259 ± 0.013	0.258 ± 0.013
			$\mathbf{[HTf_2N]_{aq}}$	(1.47± 0.07)·10^{-2}	(2.10 ± 0.11)·10^{-3}

As seen in Table 6, the experimentally measured hydrogen ion concentration in water ($[H^+]_{aq}$ = 0.045 ± 0.004 M) is in a good agreement with the calculated value ($[H^+]_{aq}$ = 0.048 ± 0.005 M). This result suggests that the proposed system of equation is adequate to describe the real concentration of the species. However, the calculated concentration of the same species in water containing 15 % (w/v) bet is two times larger than the measured value ((6.2 ± 0.6)·10^{-3} M vs (3.35 ± 0.33)·10^{-3} M). This discrepancy may result from the change of the chemical potential in the solution due to the presence of zwittterionic betaine in water. The effect of the change of the chemical potential is unknown and was not taken into account in the system of equations. In addition, betaine solution is known to pose challenges in pH measurement due to its low ionic strength which affect the accuracy in the measurement [128]. Therefore, it is likely that both the measured and calculated values for H^+ species in this chemical system have additional unquantified systematic errors.

The effect of addition of zwitterionic betaine in water was analyzed further. The calculated equilibrium concentrations of cationic and anionic species, [$Hbet^+$] and [Tf_2N^-], shown in Table 6, in pure water and water containing 15 % (w/v) bet are comparable. Meanwhile, for zwitterionic betaine species (bet), the calculated equilibrium concentration in the aqueous phase was found to be 0.750 ± 0.080 M, which was lower than the initial one (1.28 M). This finding indicated that this species was partially transferred into the organic phase. In has been suggested that neat [Hbet][Tf_2N] is able to dissolve up to 60 mol % of zwitterionic betaine [129]. The presence of an additional 15 % (w/v) bet in water also affected the amount of HTf_2N species. In Table 6, it can be seen

that the calculated equilibrium concentration of this species is lower than that in the pure water system. HTf_2N is the product of [Tf_2N^-] protonation and this reaction is possible due to the presence of free proton liberated from [$Hbet^+$] according to Eq. 14. The presence of bet in excess would suppress the dissociation of the cationic species [$Hbet^+$] (see Eq. 14) and thus, lower the amount of free proton that was available to protonate [Tf_2N^-] in this chemical system. Consequently, the amount of HTf_2N in the aqueous phase also decreased.

Most of the reports on IL solubility are based on the measurement of the aqueous equilibrium concentration of the IL cation [86,103,112]. For instance, the reported value of the solubility of [Hbet][Tf_2N] based on ^{1}H-NMR measurement is 14 ± 0.5 wt % [sic] [86], which is equal to 0.371 ± 0.010 M (assuming the density of the pre-equilibrated IL is 1.453 g/cm^3). The experimental result on [Hbet][Tf_2N] solubility in water obtained in this work is 0.344 ± 0.034 M, in good agreement with the literature data.

3.1.2 Evaluation of Solubility of [Hbet][Tf_2N] in the Presence of DCl

The effect of the presence of DCl on the solubility of [Hbet][Tf_2N] in the aqueous phase was evaluated. The chemical systems consisted of pre-equilibrated [Hbet][Tf_2N] as the organic phase, and DCl or DCl containing initially 15 % (w/v) bet (1.28 M) as the aqueous phase. The DCl concentration was varied in the range of 0.01 – 8 M and 0.009 – 6.8 M in the absence and the presence of betaine, respectively. The aqueous phase samples were analyzed with analytical procedures similar to the water-based system

discussed previously. The equilibrium concentrations of the individual species were calculated using the system of equations (Eqs. 16 – 21).

The dependency of experimental and calculated equilibrium concentrations of betaine-containing species on aqueous phase acidity are presented in Figure 10. It can be seen that, in the absence of betaine, the concentration of all betaine-containing species (Bet_{NMR}) increased with increasing aqueous phase acidity (Figure 10a). A similar trend was also observed for the calculated equilibrium concentration of [$Hbet^+$]. Meanwhile, in this chemical system, bet species only existed at <0.5 M DCl. Above this acid concentration, bet is fully protonated. This is evident from the figure where bet concentrations above 0.5 M DCl approach zero values while the concentrations of protonated [$Hbet^+$] species overlap with the measured Bet_{NMR} values, indicating that only [$Hbet^+$] species existed at high acid concentrations.

Furthermore, when 15% (w/v) bet (1.28 M) was added into the aqueous phase, the equilibrium aqueous concentration of Bet_{NMR} at low acidity (<1 M) was found to be lower than the initial bet concentration and it was independent of DCl concentration (Figure 10b). This finding suggested that some betaine-containing species was transferred into the organic phase. The results from solving the system of equations indicated that this species is zwitterionic betaine (bet). Figure 10b shows that, below 1 M initial DCl concentration, the calculated equilibrium concentrations of bet are indeed higher than [$Hbet^+$]. The presence of higher acid concentration resulted in the protonation of bet. Consequently, [$Hbet^+$] increased with increasing acidity. Additionally, it is noteworthy that at high acidity (>1 M DCl) the concentrations of Bet_{NMR} are greater than that of

initial bet. This leads to the conclusion that the presence of zwitterionic betaine in a very acidic aqueous solution increases the solubility of [Hbet][Tf_2N] significantly.

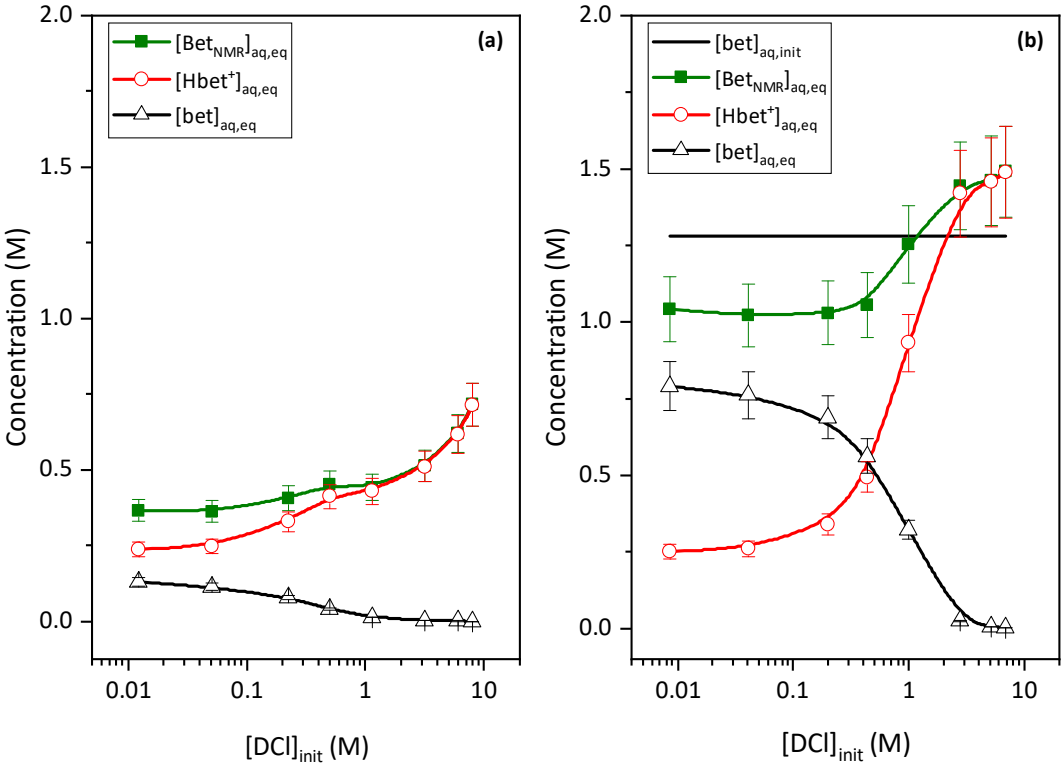

Figure 10. The dependency of betaine-containing species concentration on the aqueous phase to acidity. The aqueous phase only contains DCl (a) and contains DCl and $[bet]_{aq,\ init}$ = 15% w/v (1.28 M) (b). The closed and open symbols are experimental data and calculation results obtained by using the system of equations, respectively. The lines are drawn to guide the eye.

The effect of DCl concentration on the equilibrium concentration of bistriflimide-bearing species in the absence and presence of zwitterionic betaine is presented in Figure 11a and 11b, respectively. In both figures, it can be seen that [F_{NMR}] decreased with increasing acid concentration but it experienced a steeper decline in the chemical system

containing additional betaine (Figure 11b). As expected, at low acid region (<1 M DCl) the bistriflimide-bearing species was mostly [Tf_2N^-] anion, but as the acid concentration increased, the protonated species, HTf_2N, was the dominant one in the aqueous phase.

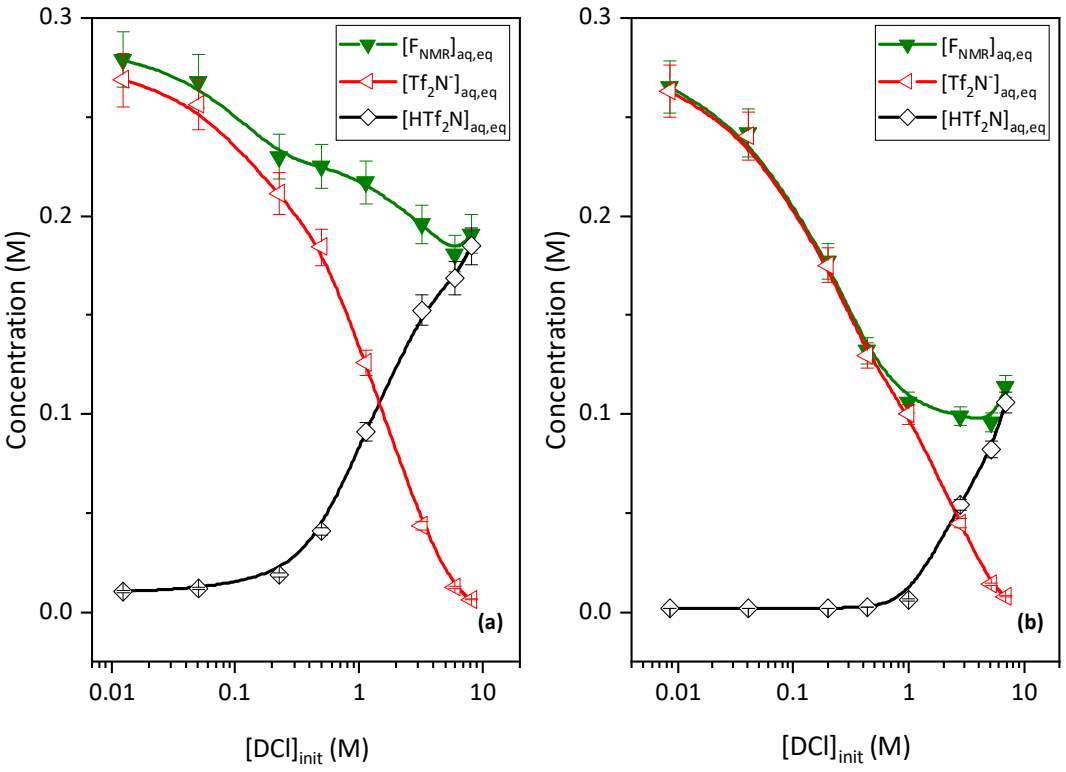

Figure 11. The dependency of bistriflimide-containing species concentration to the aqueous phase to acidity. The aqueous phase only contains DCl (a) and contains DCl and $[bet]_{aq,\ init}$ = 15% w/v (1.28 M) (b). The closed and open symbols are experimental data and calculation results obtained by using the system of equations, respectively. The lines are drawn to guide the eye.

The equilibrium concentrations of betaine- and bistriflimide-containing species in the aqueous phase that are shown above gave some important details about the distribution of the species originated from the IL between the two phases. For instance,

while the IL's cation and anion dissolved simultaneously into the aqueous phase as an ion pair (see Eq. 13), their equilibrium concentrations were not always the same. In the aqueous phase containing only water, shown in Table 6, the equilibrium concentrations of Bet_{NMR} and F_{NMR} are approximately equal. However, in the presence of DCl, the amount of Bet_{NMR} is higher than F_{NMR} (Figure 10a and 11a). The difference between the equilibrium concentrations of these species are more pronounced as the concentration of DCl increased. Moreover, it was also observed that the presence of additional betaine at high acidity suppressed the equilibrium concentration of F_{NMR} even lower compared to the system containing only DCl (Figure 11) but the effect of betaine addition to Bet_{NMR} was the opposite (Figure 10b).

The difference between the equilibrium concentrations of Bet_{NMR} and F_{NMR} due to the acidity of the aqueous phase can be explained from the preferential distribution of their speciation products either to the aqueous or the organic phase. As the acidity increased, there are more free protons available to form [$Hbet^+$] and H[Tf_2N]. However, while [$Hbet^+$] is known to be highly solvated by water molecules [130] and likely to stay in the water-rich phase, H[Tf_2N] contains a hydrophobic anion and has a higher affinity to the IL phase [112]. Thus, the latter species would likely to be transferred into the organic phase. Consequently, the equilibrium concentrations of these two species in the aqueous phase are no longer equal.

The apparent decrease of F_{NMR} at high acidity due to the presence of zwitterionic betaine compared to the system containing pure DCl (Figure 11) seems to be strongly related with increasing amounts of the protonated betaine-containing species, [$Hbet^+$].

According to Le Châtelier's principle, changing the condition of a chemical system at equilibrium (which also means applying a stress) will force the system to shift the equilibrium to the direction that reduces the stress [131]. This means that, increasing amounts of [$Hbet^+$] as the reaction product of bet protonation will reduce the solubility of [Hbet][Tf_2N] according to Eq. 13. As a result, the amount of [Tf_2N^-] in the aqueous phase decreased.

The analysis of the equilibrium concentrations of proton-containing species gives further insight into the solubility behavior of [Hbet][Tf_2N] in DCl. Figure 12 shows the equilibrium concentrations of total proton ($H_{Titrated}$) as a function of initial DCl concentration. The broken lines in Figure 12a and 12b indicate the reference value when the initial and equilibrium concentration of $H_{Titrated}$ are equal. In reality, it can be seen in the figures that, below 1 M DCl, [$H_{Titrated}$] are above the reference lines. The increase of equilibrium concentration of total proton species was possible only due to the dissolution of [Hbet][Tf_2N] in the aqueous phase. As shown in the figures, [$Hbet^+$] is the dominant species in that acid region. Above 1 M DCl, the equilibrium concentrations of $H_{Titrated}$ are equal to the initial ones.

The presence of zwitterionic betaine has several effects on the speciation of proton-containing species in the aqueous phase (Figure 12b). The amount of [$Hbet^+$] at low acid concentration is approximately the same with the system without betaine added (Figure 12a), but it increases significantly at higher acidity. Due to the protonation of zwitterionic betaine that is present in excess in the aqueous phase, the equilibrium concentrations of free proton, H^+, are generally lower in the entire acid region. As a

result, the amounts of H[Tf_2N] are also lower compared to the system without betaine added.

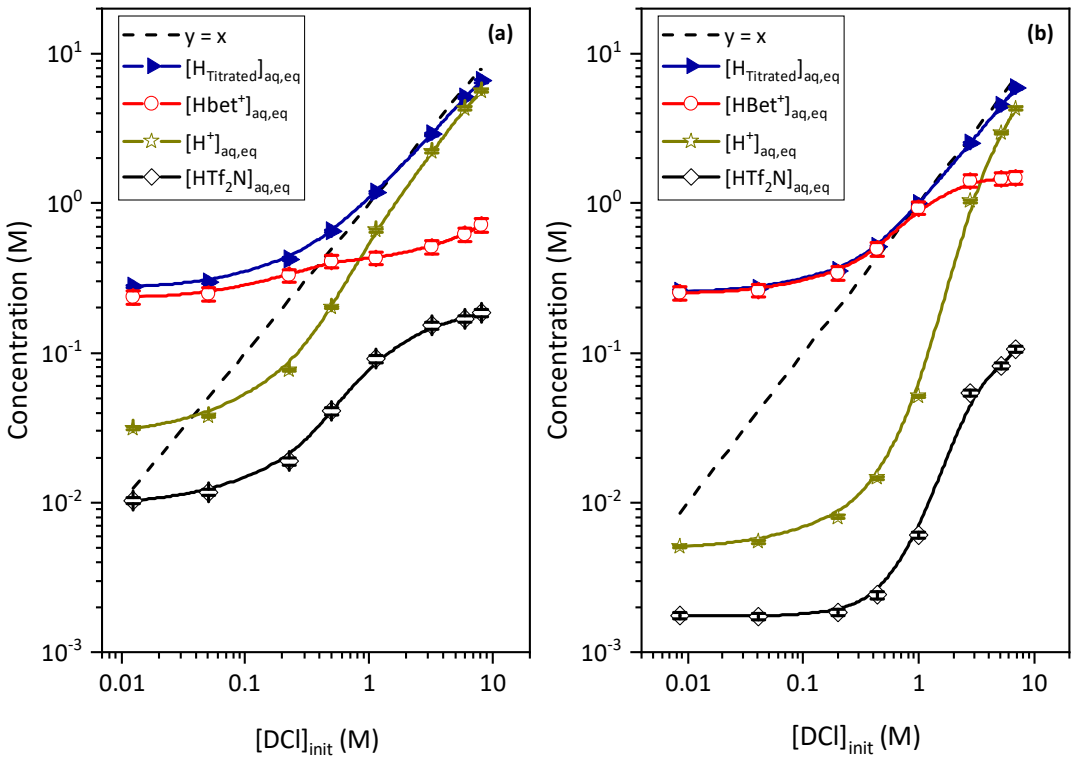

Figure 12. The dependency of proton-containing species concentration to the aqueous phase to acidity. The aqueous phase only contains DCl (a) and contains DCl and $[bet]_{aq,init}$ = 15% w/v (1.28 M) (b). The dashed line (y = x) indicates the reference value when the initial and equilibrium H^+ concentrations are equal. The closed and open symbols are experimental data and calculation results obtained by using the system of equations, respectively. The lines are drawn to guide the eye.

3.2 Solubility of Water in [Hbet][Tf_2N]

Prior to contact with the acidic aqueous phase, the water content in pre-equilibrated [Hbet][Tf_2N] IL was analyzed by using the Karl Fischer titration technique.

It was found that the IL contained 13.8 ± 0.5 wt % water, consistent with reported values in the literature [86,87,112]. In addition, the pre-equilibrated [Hbet][Tf_2N] was also contacted with water containing 15 % (w/v) bet and the IL phase was analyzed further. The amount of water in the IL phase in the presence of additional betaine was found to be 13.8 ± 0.5 wt %, leading to conclusion that the extra betaine in the aqueous phase did not affect the solubility of water in [Hbet][Tf_2N].

Figure 13 shows the effect of aqueous phase acidity on the solubility of water in [Hbet][Tf_2N] IL. The solid horizontal line indicates the measured water content in the pre-equilibrated IL phase prior to contact with the aqueous phase. After the formation of the biphasic system with DCl < 1 M, the equilibrium water content in the IL was constant. However, it decreased when the aqueous phase acidity was higher. Interestingly, the equilibrium water content in the IL phase was generally lower than the initial ones after it was contacted with DCl containing 15 % (w/v) bet. Further decrease was observed when the aqueous phase acidity was above 3 M.

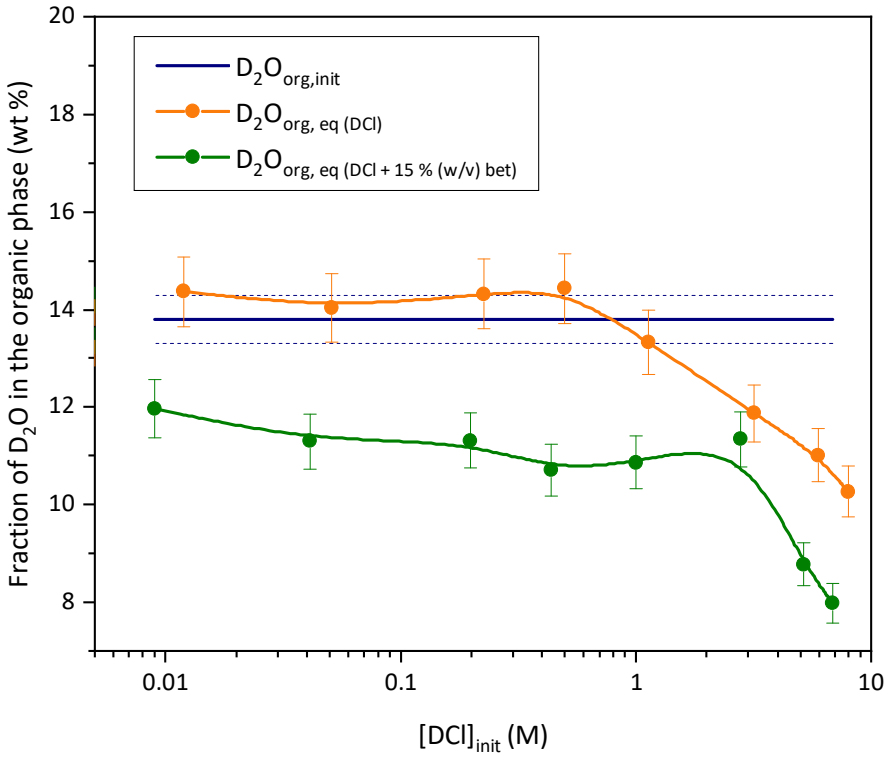

Figure 13. The amount of equilibrium water content in the IL phase as a function of initial aqueous DCl concentration. The solid horizontal line represents the water content in pre-equilibrated [Hbet][Tf_2N] (initial water concentration), while the dashed horizontal lines represent its error values. The lines are drawn to guide the eye.

The decrease of equilibrium water content in the IL phase that is observed in the figure above is a clear indication of transfer of water from the pre-equilibrated IL phase into the aqueous phase. This phenomenon is likely due to high concentration of ions in the aqueous phase that attract water molecules into it. Water is a polar molecule and it interacts strongly with ions [131]. At high DCl concentration and the presence of 15 % (w/v) zwitterionic betaine, the aqueous phase was populated by ions *e.g.*, proton, chloride ion and betaine. Due to its high charge density, chloride ion in the aqueous phase is

strongly solvated by water molecules [112]. Meanwhile, betaine has both hydrophilic carboxylate and hydrophobic methyl groups [132,133] and water molecules are strongly bonded to the carboxylic acid group through the hydrogen atom [133,134]. These facts are also supported by a theoretical study which suggests an increase of water solvation around the betaine's molecule is observed when betaine is present in excess [130].

The relationship between the amount of water transferred into the aqueous phase (D_2O_{aq}) and betaine behavior as a function of acid concentration is shown in Figure 14. Both the equilibrium concentrations of Bet_{NMR} and D_2O_{aq} (Figure 14a and 14c, respectively) are constant in the presence of pure aqueous DCl up to 1 M. Above this acid concentration, the amount of D_2O_{aq} increased. Similar tendency was also observed in the case of Bet_{NMR}. The presence of high H^+ and Cl^- concentrations is likely to reduce the amount of free water available in the aqueous phase due to solvation of these ions and thus, prompted the transfer of water from the IL phase to the aqueous phase.

The solvation effect is more pronounced when an additional 15 % (w/v) bet was dissolved in DCl. It can be seen in Figure 14d that D_2O_{aq} was much higher in this chemical system compared to pure DCl. An increase in the amount of Bet_{NMR} and D_2O_{aq} in the aqueous phase was observed at very high acid concentration (Figure 14b and 14d). This is likely the effect of even lower free water available in the aqueous phase due to betaine solvation, in addition to high H^+ and Cl^- concentrations that also existed in the aqueous phase.

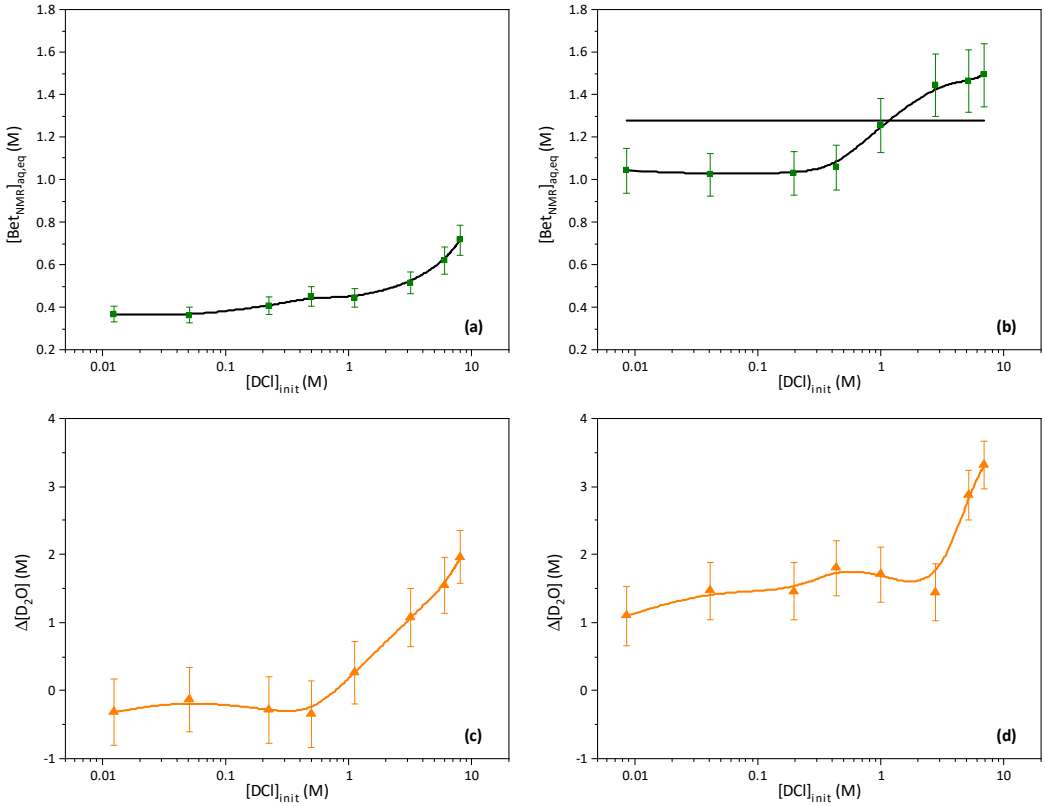

Figure 14. The measured equilibrium concentration of betaine species ($[Bet_{NMR}]_{aq,eq}$) and amount of water transferred into the aqueous phase ($[D_2O]_{aq,eq}$) as a function of aqueous phase acidity. The aqueous phase contains DCl (a) and (c), and contains DCl and 15 % (w/v) bet (b) and (d). The lines are drawn to guide the eye.

3.3 Extraction of Species into [Hbet][Tf_2N]

In the previous section, it was shown that the equilibrium concentrations of Bet_{NMR} and F_{NMR} were not equal (see Figure 10 and 11). The presence of DCl increased $[Bet_{NMR}]$ but its effect to $[F_{NMR}]$ was the opposite. The difference between the equilibrium concentrations of these species was assumed to occur due to the transfer of the hydrophobic H[Tf_2N] species into the organic phase. Meanwhile, in the presence of 15 % (w/v) bet in DCl, betaine species was also found to be partially transferred into the

organic phase (Figure 10b) particularly in less than 1 M DCl. This section discusses the possible chemical reactions involved in the process and estimates the concentrations of the transferred species.

The following analysis was made with the assumption that the intermolecular interaction in the organic phase is weak, such that the activity coefficients of betaine- and bistriflimide-containing species is assumed to be equal to 1. First, a cation exchange process between the aqueous and the organic phase was considered to have taken place, followed by extraction of [HTf_2N] species into the organic phase:

$$H^+_{aq} + [Hbet^+]_{org} \rightleftarrows H^+_{org} + [Hbet^+]_{aq} \quad \text{Eq. 22}$$

$$H^+_{aq} + [Tf_2N^-]_{aq} \rightleftarrows [HTf_2N]_{org} \quad \text{Eq. 23}$$

Second, a mass balance equation was proposed based on the difference of the equilibrium concentration of Bet_{NMR} and F_{NMR}. A correction factor (see the parameter in the parenthesis below) was applied to account for the change of the concentration of betaine species due to protonation:

$$[Bet_{NMR}]_{aq,eq} - [F_{NMR}]_{aq,eq} = [H^+]_{org,eq} + [HTf_2N]_{org,eq} + [bet]_{org,eq} \cdot \left(1 + \frac{\gamma_{HCl\pm} \cdot [H^+]_{aq,eq}}{K_{a\,[Hbet^+]}}\right) \quad \text{Eq. 24}$$

Third, the concentrations of proton and H[Tf_2N] species that were extracted into the organic phase were quantified. The calculation was made based on the difference in the equilibrium concentrations of Bet_{NMR} and F_{NMR} in the presence and absence of acid:

$$[H^+]_{org,eq} = [Bet_{NMR}]_{aq,eq,DCl} - [Bet_{NMR}]_{aq,eq,D_2O} \quad \text{Eq. 25}$$

$$[HTf_2N]_{org,eq} = [F_{NMR}]_{aq,eq,DCl} - [F_{NMR}]_{aq,eq,D_2O} \quad \text{Eq. 26}$$

Finally, the concentration of betaine that was extracted into the organic phase can be obtained from Eq. 24, taking into account the results from Eqs. 25 and 26:

$$[\mathrm{bet}]_{\mathrm{org,eq}} = \left([\mathrm{Bet}_{\mathrm{NMR}}]_{\mathrm{aq,eq}} - [\mathrm{F}_{\mathrm{NMR}}]_{\mathrm{aq,eq}} - [\mathrm{H}^+]_{\mathrm{org,eq}} - [\mathrm{HTf_2N}]_{\mathrm{org,eq}}\right) \cdot \left(1 + \frac{\gamma_{HCl\pm} \cdot [\mathrm{H}^+]_{\mathrm{aq,eq}}}{\mathrm{K_a}\,[\mathrm{Hbet}^+]}\right)^{-1} \quad \text{Eq. 27}$$

The results of the calculation of the extracted species concentrations based on Eqs. 25 - 27 are presented in Figure 15. This figure is a visual confirmation that shows the transfer of H^+, $H[Tf_2N]$ and betaine species into the organic phase as described in the previous section. Figure 15a shows the extraction of species from the aqueous phase into the organic phase in the absence of betaine. It can be seen that the betaine species was not extracted since the values approach zero in all acid concentrations that were studied. Conversely, the concentrations of H^+ and $H[Tf_2N]$ increased with increasing acidity (Figure 15b). Similar results were obtained for the extraction H^+ and $H[Tf_2N]$ species in the system containing 15 % (w/v) betaine. Interestingly, betaine species was shown to be extracted into the organic phase from acid concentrations below 3 M. The error bars on $[H^+]$ data points were estimated by extrapolating the error values of betaine-containing species in the absence and the presence of acid (see Eq. 25). Because there was a large amount of betaine presented in the aqueous phase, the estimated errors on the H^+ concentrations also appeared to be large.

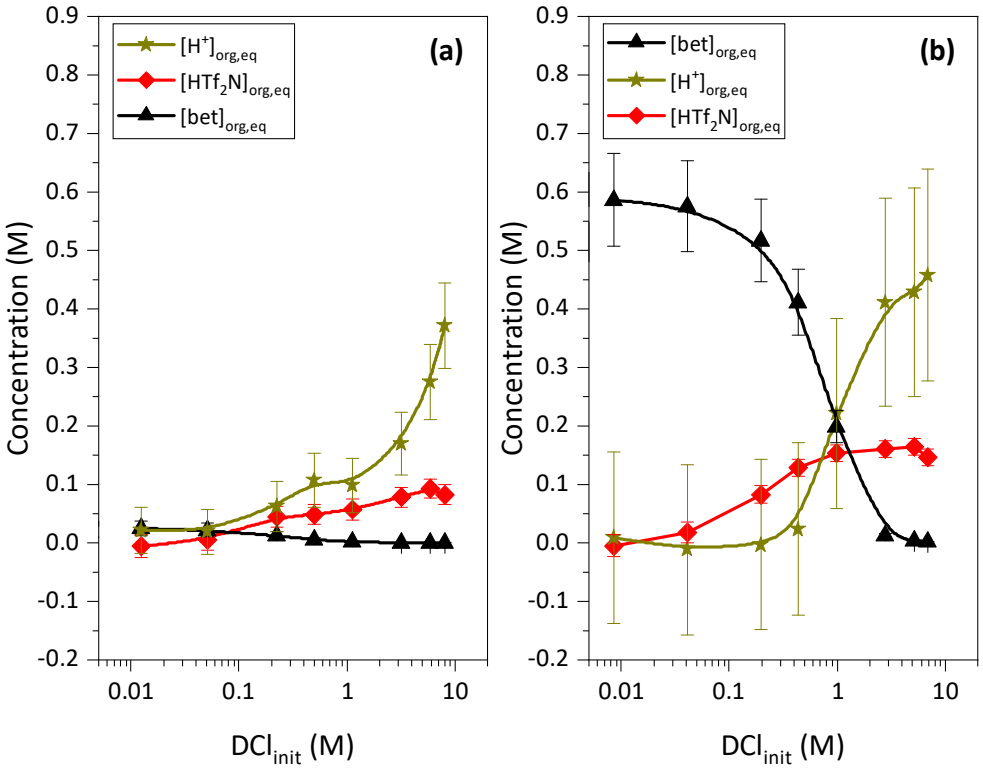

Figure 15. The calculated concentrations of proton, H[Tf_2N], and bet species that were extracted into the organic phase as a function of initial acid concentration. The aqueous phase contains pure DCl (a) and contains DCl and 15 % (w/v) bet (b). The lines are drawn to guide the eye.

3.4 Conditional Solubility Product Constant

Some studies suggested that the mechanism of metal extraction into an IL is governed by the solubility of the IL in the aqueous phase [103,106,135,136]. Therefore, the solubility product constant (K_{sp}) becomes an important parameter that allows for determination of the concentrations of the IL cation and anion in the aqueous phase and explain the metal extraction mechanism [135]. This section discusses an approach to estimate the K_{sp} of [Hbet][Tf_2N] in the aqueous phase.

According to the dissolution reaction in Eq. 13 the K_{sp} of [Hbet][Tf_2N] can be written as follows:

$$K_{sp} = [Hbet^+]_{aq} \cdot [Tf_2N^-]_{aq} \quad \text{Eq. 28}$$

However, both of the IL's cation and anion experienced deprotonation and protonation reaction in the aqueous phase. Therefore, Eq. 29 has to be modified and as a consequence, the obtained result is the *conditional* solubility product constant (K_{sp}'):

$$K_{sp}' = \left([Hbet^+]_{aq,eq} + [bet]_{aq,eq}\right)\left([Tf_2N^-]_{aq,eq} + [HTf_2N]_{aq,eq}\right) \quad \text{Eq. 29}$$

Equation 29 is modified further to take into account the dissociation constants of [$Hbet^+$] and H[Tf_2N] as well as the activity coefficients for all charged species ($\gamma_{IL\pm}$):

$$K_{sp}' = \gamma_{IL\pm}^2 \cdot [Hbet^+]_{aq,eq} \left(1 + \frac{K_{a[Hbet^+]}}{\gamma_{HCl\pm} \cdot [H^+]_{aq,eq}}\right)\left(1 + \frac{\gamma_{HCl\pm} \cdot [H^+]_{aq,eq}}{K_{a[HTf_2N]}}\right) [Tf_2N^-]_{aq,eq}$$

Eq. 30

The charge balance in the aqueous solution at equilibrium is shown in the following equation:

$$[H^+]_{aq,eq} + [Hbet^+]_{aq,eq} = [Tf_2N^-]_{aq,eq} + [Cl^-]_{aq,eq} \quad \text{Eq. 31}$$

Based on the equation above, the sum of equilibrium concentrations of the cations was plotted as a function of the sum of equilibrium concentrations of the anions. The results are shown in

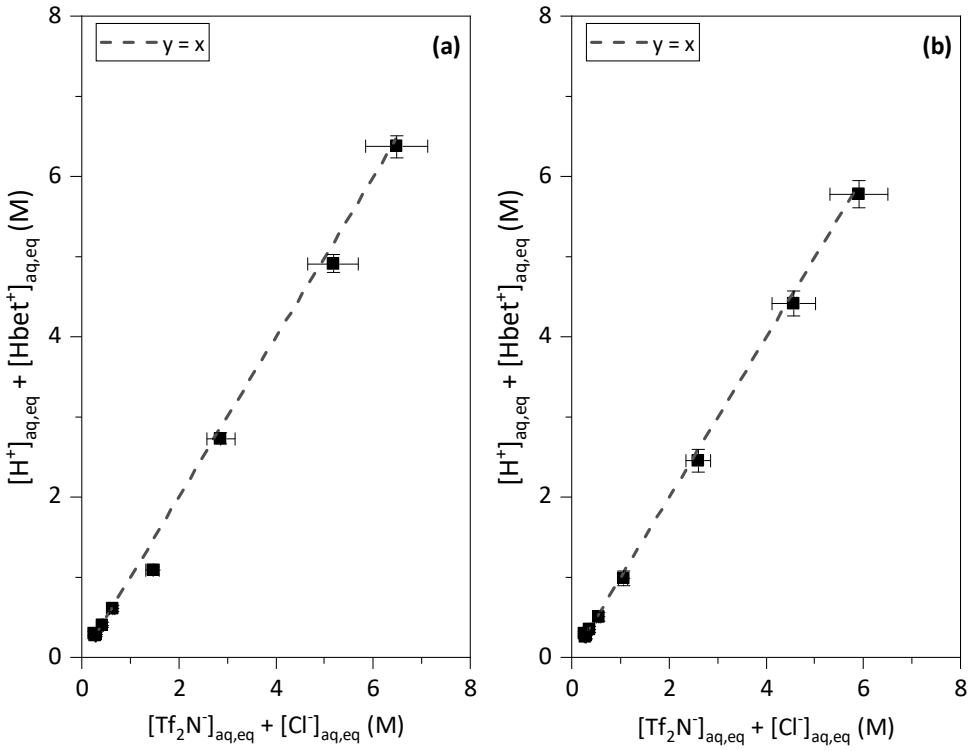

Figure 16. The dashed lines in the figure show the expected trend for perfect agreement between the cation and anion concentrations. It can be seen that the data points on both plots follow the expected trend. This confirms the validity of Eq. 31.

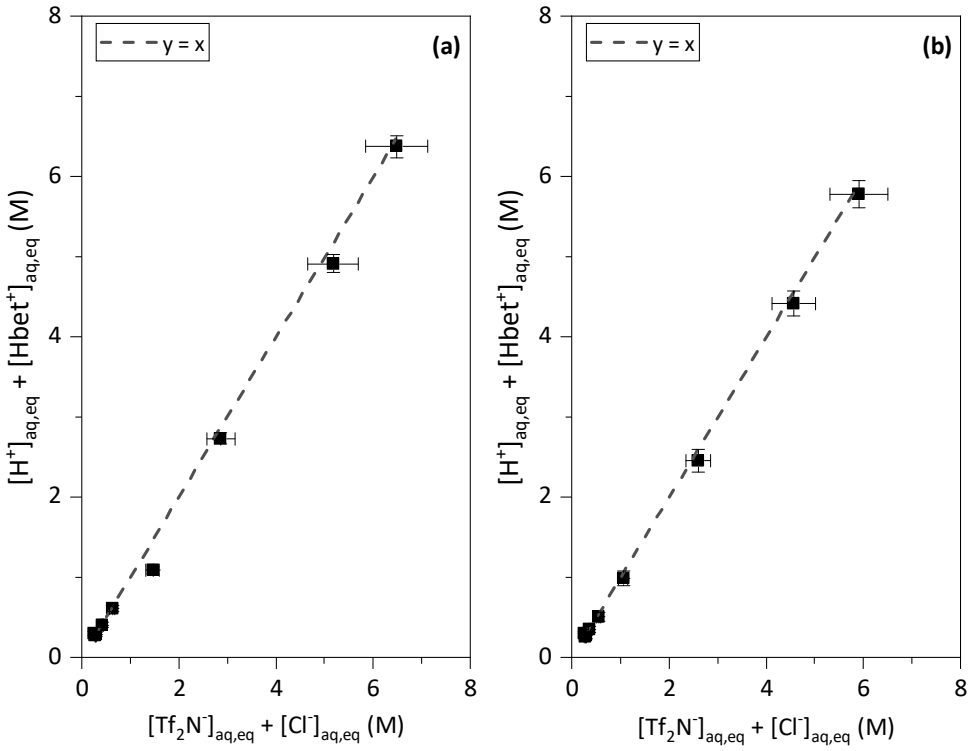

Figure 16. The plot of equilibrium concentrations of cations as a function of equilibrium concentrations of anions in the aqueous phase containing DCl **(a)** and aqueous phase containing DCl with 15 % (w/v) bet **(b)**. The dashed line shows the trend expected for perfect agreement between the cation and anion concentrations.

Furthermore, the combination of Eqs. 30 and 31 leads to a quadratic equation either for $[\mathrm{Hbet}^+]_{\mathrm{aq,eq}}$ or $[\mathrm{Tf_2N}^-]_{\mathrm{aq,eq}}$ species, for example:

$$\mathrm{K_{sp}}' = \gamma_{IL\pm}^2 \cdot [\mathrm{Hbet}^+]_{\mathrm{aq,eq}} \left(1 + \frac{\mathrm{K_{a[Hbet^+]}}}{\gamma_{HCl\pm} \cdot [\mathrm{H}^+]_{\mathrm{aq,eq}}}\right)\left(1 + \frac{\gamma_{HCl\pm} \cdot [\mathrm{H}^+]_{\mathrm{aq,eq}}}{\mathrm{K_{a[HTf_2N]}}}\right) \left([\mathrm{H}^+]_{\mathrm{aq,eq}} + [\mathrm{Hbet}^+]_{\mathrm{aq,eq}} - [\mathrm{Cl}^-]_{\mathrm{aq,eq}}\right) \quad \text{Eq. 32}$$

Solving Eq. 32 for $[\mathrm{Hbet}^+]_{\mathrm{aq,eq}}$ leads to:

$$[\mathrm{Hbet^+}]_{\mathrm{aq,eq}} =$$

$$\frac{[\mathrm{Cl^-}]_{\mathrm{aq,eq}} - [\mathrm{H^+}]_{\mathrm{aq,eq}} + \sqrt{\left([\mathrm{Cl^-}]_{\mathrm{aq,eq}} - [\mathrm{H^+}]_{\mathrm{aq,eq}}\right)^2 + 4 \cdot K'_{sp} \cdot \gamma_{IL\pm}^{-2} \cdot \left(1 + \frac{\mathrm{K_{a[Hbet^+]}}}{\gamma_{HCl\pm} \cdot [\mathrm{H^+}]_{\mathrm{aq,eq}}}\right)^{-1} \cdot \left(1 + \frac{\gamma_{HCl\pm} \cdot [\mathrm{H^+}]_{\mathrm{aq,eq}}}{\mathrm{K_{a[HTf_2N]}}}\right)^{-1}}}{2}$$

Eq. 33

Since the activity coefficients of the ionic liquid species are unknown, the equation above was used to fit the experimental data only in the low acid region (up to 0.2 M) where it can be assumed that $\gamma_{IL\pm} \approx 1$. To allow the variation of $[\mathrm{Hbet^+}]_{\mathrm{aq,eq}}$ in Eq. 33 only as a function of $[H^+]_{aq,eq}$, an empirical relation between $[Cl^-]_{aq,eq}$ and $[H^+]_{aq,eq}$ was developed such that the term $[Cl^-]_{aq,eq}$ can be substituted with $[H^+]_{aq,eq}$. Using the data on the equilibrium concentrations of $[H^+]_{aq}$ and $[Cl^-]_{aq,eq}$ in the absence of betaine, the empirical relation between those two quantities is shown below:

$$\log\left([\mathrm{Cl^-}]_{aq,eq}\right) = 1.804 \cdot \left(\log([\mathrm{H^+}]_{aq,eq}) + 1.503\right)^{0.472} - 1.900 \qquad \text{Eq. 34}$$

Meanwhile, using the data on the equilibrium concentrations of $[H^+]_{aq}$ and $[Cl^-]_{aq,eq}$ in the presence of 15 %(w/v) bet, the following relationship was obtained:

$$\log\left([\mathrm{Cl^-}]_{aq,eq}\right) = 2.300 \cdot \left(\log\left([\mathrm{H^+}]_{aq,eq}\right) + 2.294\right)^{0.245} - 2.293 \qquad \text{Eq. 35}$$

Figure 17 shows the experimental data fitting for [Hbet$^+$] and [Tf_2N^-] as the function of equilibrium [H^+]. The K_{sp}' value seems to increase in the presence of 15 % (w/v) bet compared to the system without betaine added.

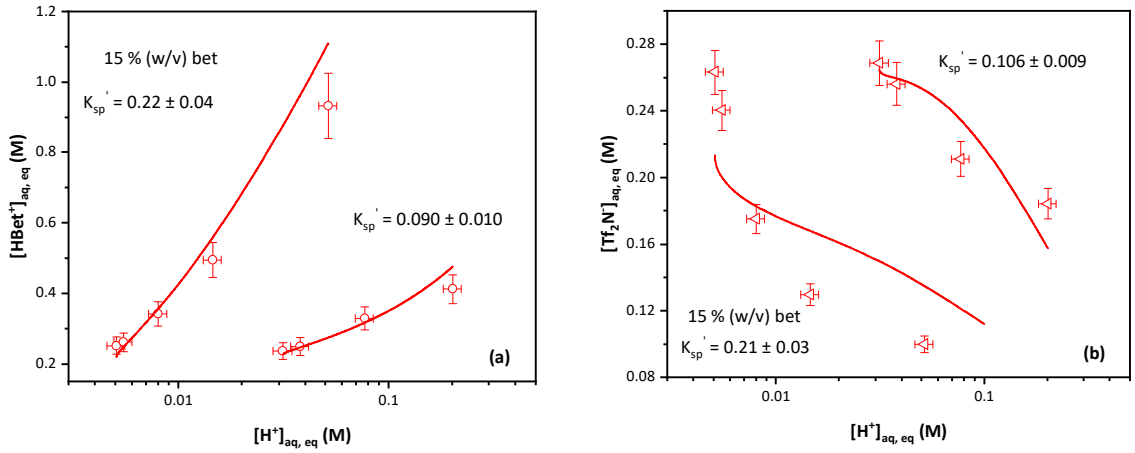

Figure 17. The concentration of [Hbet$^+$] as a function of [H$^+$] (a) and the concentration of [Tf_2N^-] as a function of [H$^+$] (b). Both figure panels show data in the presence and absence of bet. The red lines are fits based on Eq. 32, which allows for the determination of the conditional solubility product constant (K_{sp}') of [Hbet][Tf_2N].

The K_{sp}' of [Hbet][Tf_2N] can also be estimated by using the experimental results of the equilibrium concentration of betaine- and bistriflimide-containing species:

$$K_{sp}' = [Bet_{NMR}][F_{NMR}] \quad \text{Eq. 36}$$

Expressing Eq. 36 in term of [Bet_{NMR}]:

$$[Bet_{NMR}] = K_{sp}' \cdot 1/[F_{NMR}] \quad \text{Eq. 37}$$

Figure 18 shows the plot of [Hbet$^+$] as the function of the reciprocal of the equilibrium [F_{NMR}] based on Eq. 37. The slope in the figure indicates the K_{sp}' of [Hbet][Tf_2N]. The results of K_{sp}' calculated using this approach are in agreement with the results from the fitted parameter shown in Figure 17. Unfortunately, the K_{sp}' of [Hbet][Tf_2N] in aqueous phase containing 15 % (w/v) betaine cannot be estimated. This

chemical system contains higher concentration of ions, and the activity coefficients of the ionic liquid species, which is part of the K_{sp}' equation, can no longer assumed to be equal to 1.

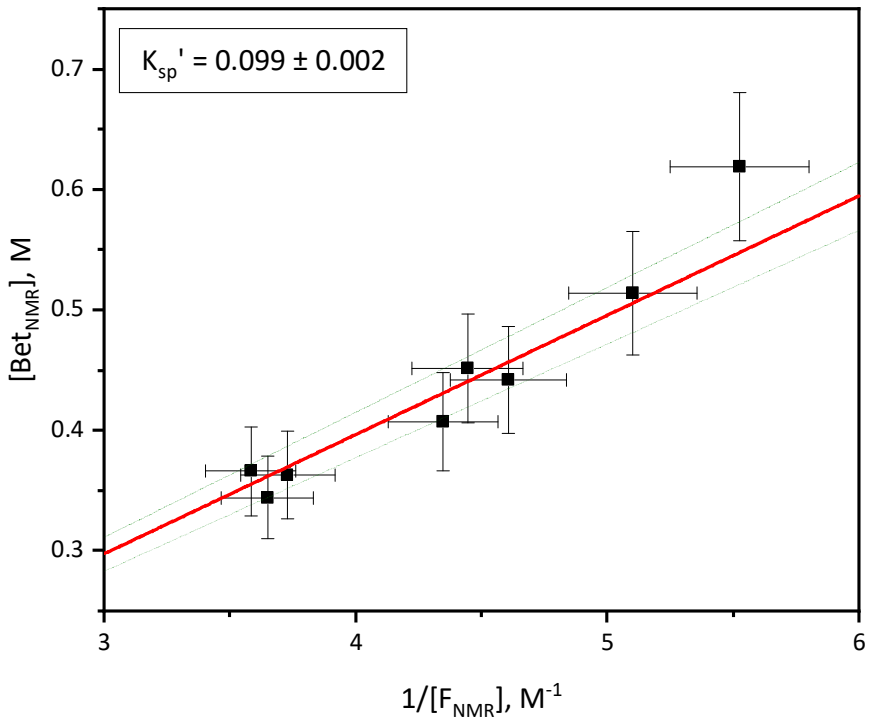

Figure 18. [Bet_{NMR}] as a function of inverse [F_{NMR}] based on Eq. 37. The red line is a linear fit and the green lines represent the 95 % confidence interval.

Based on the findings from these mutual solubility experiments, the extraction behaviors of In(III) and Tl(I, III) extraction into betainium-based IL can be better understood. The extraction experiments and the results are discussed in Chapter 4.

4. INDIUM AND THALLIUM EXTRACTION INTO IONIC LIQUIDS AND EUTECTIC SOLVENTS*

This chapter focuses on the results of indium and thallium extraction into various chemical systems consisted of ILs or ESs as the organic phase and HCl as the aqueous phase media. First, the results of In(III) and/or Tl(I, III) extraction into aprotic ILs, imidazolium- and/or pyrrolidium-based ILs, as well as into protic betainium-based IL are presented and discussed. The mechanisms of metal extraction into some of these chemical systems are also shown. This chapter also includes the result of In(III) and Tl(I, III) extraction into DL menthol-based ES, in the presence and absence of HDEHP as the extracting agent. The data on Tl(I, III) extraction into pure imidazolium- and pyrrolidinium-based ILs have been published in and used with permission from the Journal of Physical Chemistry B [136]. Meanwhile, the results of In(III) and Tl(I, III) extractions into betainium-based IL have been submitted for publication.

The samples for these experiments were prepared according to the procedures described in sections 2.4.4 – 2.4.6. Unless stated otherwise, carrier-free ^{111}In and ^{201}Tl radionuclides were used as the metal sources and the sample analyses were carried out using a NaI(Tl) gamma counter.

---

* Reprinted with permission from "Thallium Transfer from Hydrochloric Acid Media into Pure Ionic Liquids" by E. E. Tereshatov et al., 2016. Journal of Physical Chemistry B, 120, 2311-2322, https://doi.org/10.1021/acs.jpcb.5b08924. Copyright [2016] by American Chemical Society.

4.1 Tl Extraction into Pure Imidazolium- and/or Pyrrolidium-based Ionic Liquid

This section discusses the capability of various imidazolium- and/or pyrrolidinium-based ILs to extract Tl(I) and Tl(III). In an earlier paragraph it was mentioned that thallium has two oxidation states: +1 and +3. The ^{201}Tl radionuclide that was purchased from the manufacturer was in the form of Tl(I). Therefore, for the experiments involving Tl(III), an oxidizing agent, bromine (Br_2) water or chlorine (Cl_2) water was used to oxidize Tl(I). This section also discuss the kinetics of Tl(III) extraction and Tl(I, III) extraction mechanism.

4.1.1 Tl(I) Extraction into Pure Imidazolium- and/or Pyrrolidinium-based Ionic Liquid

Thallium(I) extraction into various imidazolium- and/or pyrrolidinium-based ionic liquids was investigated. First, the influence of the cation's alkyl chain on Tl(I) extraction yield was studied by varying the alkyl length of the imidazolium cation's with 2, 4, and 8 carbons. These ILs have the same anion group. The results are shown in Figure 19.

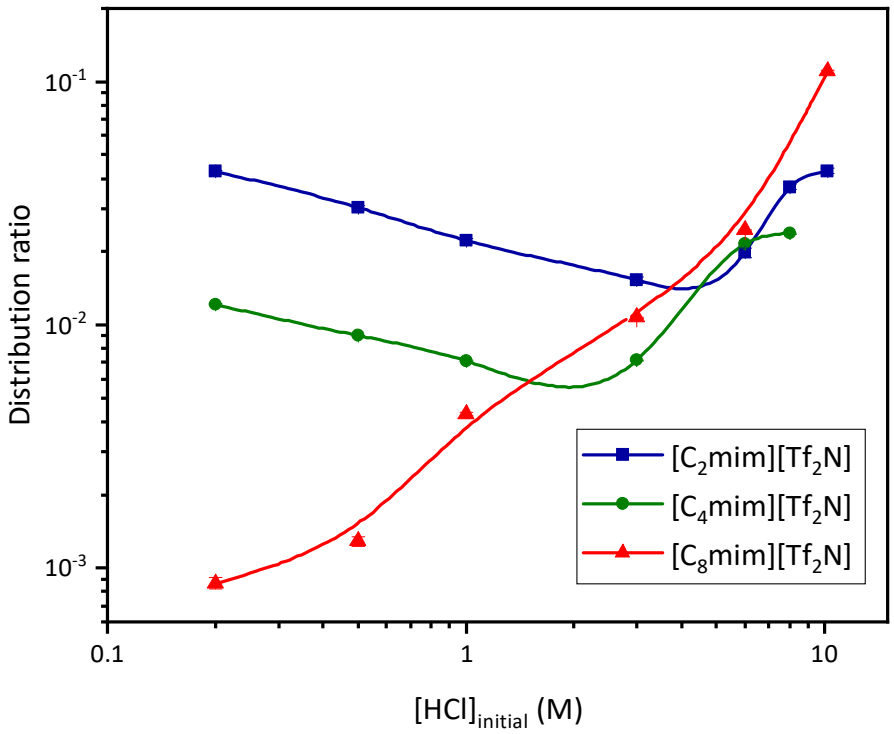

Figure 19. Thallium(I) extraction into [$C_n$mim][Tf_2N] where n = 2, 4, and 8. The lines are drawn to guide the eye.

The results in Figure 19 show that the length of the alkyl chain on the IL cation group affects Tl(I) extraction especially at lower acidity (≤ 1 M HCl). At any given acid concentration at that acid region, the extraction yield of Tl(I) decreases as the alkyl chain increases in length: [C_2mim][Tf_2N] > [C_4mim][Tf_2N] > [C_8mim][Tf_2N]. Also in the same acid region, *D* values of Tl(I) extracted with [$C_n$mim][Tf_2N] (n = 2 and 4) decreased with increasing acidity, while that with [C_8mim][Tf_2N] increased steadily. Above 3 M HCl, $D_{Tl(I)}$ values increased regardless of the IL's structure.

In general, the results above show that Tl(I) was poorly extracted into these ILs ($[C_nmim][Tf_2N]$, n = 2, 4, and 8). $D_{Tl(I)}$ values were mostly below 0.1 in the entire range of HCl that was studied. However, the behavior of Tl(I) extracted into these ILs can give an insight into the extraction mechanism, which is strongly correlated with Tl(I) speciation in the aqueous phase.

When it is dissolved in aqueous chloride media with different concentrations, a series of Tl(I) species exists in the aqueous phase [46]. At low chloride concentration, the predominant species is Tl^+ [46]. This is a hydrophilic ion, and is likely to stay in the aqueous phase where it is better solvated. In the chemical systems under study, below 1 M HCl, Tl(I) was most likely extracted through ion exchange mechanism between Tl^+ species with the IL's cation as described in Eq. 38 below:

$$[Tl^+]_{aq} + [C_nmim^+]_{org} \rightleftarrows [Tl^+]_{org} + [C_nmim^+]_{aq} \qquad \text{Eq. 38}$$

The reaction in Eq. 38 above indicates that the IL's cation has to dissolve in the aqueous phase to allow for the exchange reaction with Tl^+ to occur. The decrease of Tl(I) extraction yield with increasing length of the cation's alkyl chain shown in Figure 19 is likely the consequence of increasing cation solubility in the aqueous phase. This hypothesis is supported by the solubility values obtained from the literature. As shown in Table 4 (see section 2.4.4) the solubility of the IL's cations decreases with increasing the length of the alkyl chain: $[C_2mim^+] > [C_4mim^+] > [C_8mim^+]$. Likewise, the cation's hydrophobicity increases in the same order.

Meanwhile, Figure 19 shows that the extraction of Tl(I) at higher acidity (> 3 M) was not affected by the structure of the IL cations. At this acid region, the predominant Tl(I) species is the anionic complex $TlCl_2^-$ [46]. Since the extraction is independent of the cation's structure, most likely Tl(I) was transferred to the organic phase via an anion exchange mechanism:

$$[TlCl_2^-]_{aq} + [Tf_2N^-]_{org} \rightleftarrows [TlCl_2^-]_{org} + [Tf_2N^-]_{aq} \quad \text{Eq. 39}$$

In addition to the mechanism reaction above, ion pair formation between $TlCl_2^-$ and IL cations, and/or extraction of neutral TlCl species is also possible.

The influence of IL anion on Tl(I) extraction was also studied. Figure 20 shows the distribution ratio of Tl(I) extraction into $[C_2mim][Tf_2N]$ and $[C_2mim][FSI]$ as a function of aqueous phase acidity. The structure of the IL anions is similar, but with different number of fluorine ions in their molecules (the anion $[Tf_2N^-]$ has six fluorine ions while $[FSI^-]$ has two; see the anion's structures in Figure 5, section 1.4.1). As can be seen in Figure 20, in the entire HCl concentration that was studied, the *D* values of Tl(I) extracted into $[C_2mim][FSI]$ are slightly higher than $[C_2mim][Tf_2N]$. It is believed that the same extraction mechanisms that are described in the paragraphs above also occurred in both of these chemical systems. There are evidences that aqueous solubility of the IL is one of the determining factors for the extraction of metal into IL [135]. The difference in $D_{Tl(I)}$ values that are observed in Figure 20 is likely due to higher aqueous solubility of $[C_2mim][FSI]$ compared to $[C_2mim][Tf_2N]$ (see Table 4).

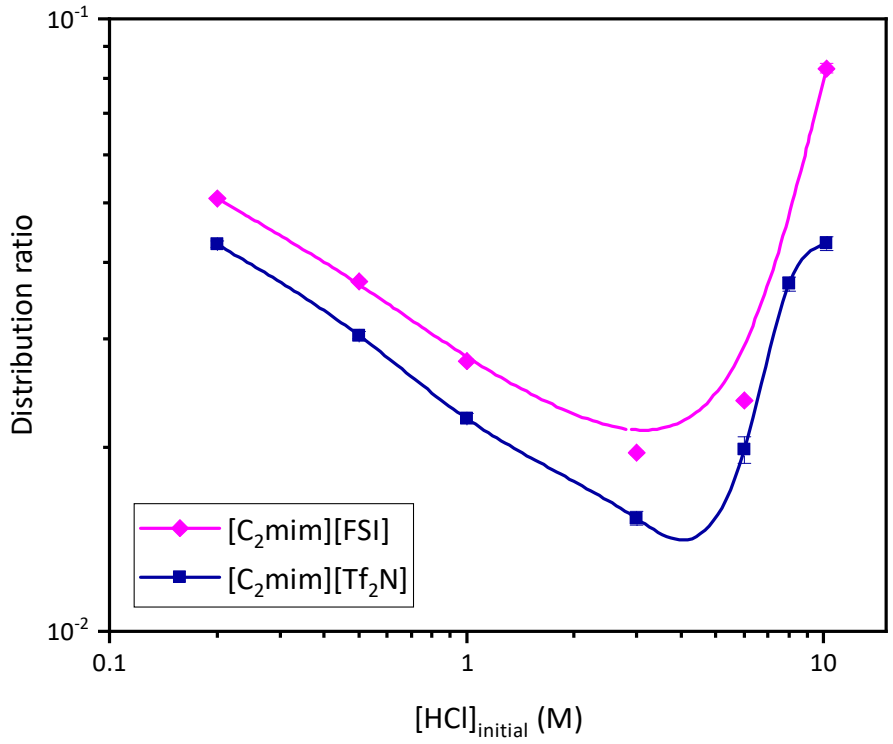

Figure 20. Thallium(I) extraction into [C_2mim][FSI] and [C_2mim][Tf_2N]. The lines are drawn to guide the eye.

Further effect of IL's structures and solubility on the extractability of Tl(I) can also be seen in Figure 21. Tl(I) was extracted into ILs with different cation and anion groups: [C_2mim][FSI], [C_4mim][Tf_2N], [C_3C_1mim][Tf_2N] and [C_3C_1pyrr][Tf_2N].

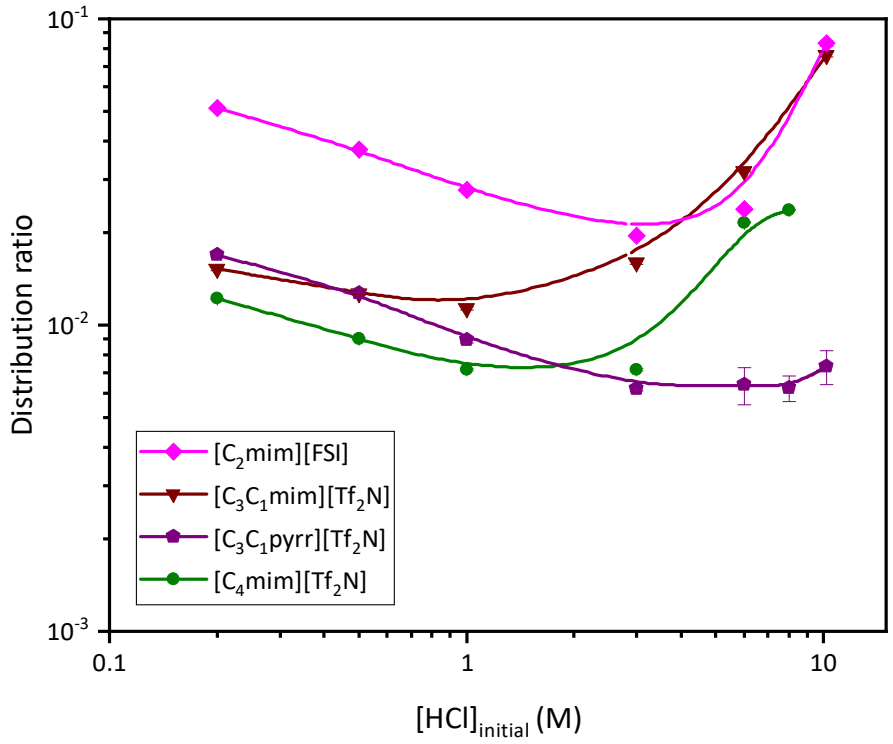

Figure 21. Thallium(I) extraction into imidazolium- and pyrrolidinium-based ILs with different anions groups. The lines are drawn to guide the eye.

It can be seen it Figure 21 that the shape of Tl(I) extraction curves are generally similar with those in Figure 19 and 20. The $D_{Tl(I)}$ values have the tendency to decrease with increasing acidity until up to 3 M HCl, then they increase above this acid concentration. The exception was found for Tl(I) extraction into $[C_3C_1pyrr][Tf_2N]$, where the *D* values did not improve even at very high acid concentrations. This leads to the conclusion that the same extraction mechanism as described in Eqs. 38 – 39 also occurred in these chemical systems. The difference in the $D_{Tl(I)}$ values that are observed in Figure 21 is believed to be the effect of different IL solubility in the aqueous phase. Based on

Table 4, the IL solubility in water decreases in the order $[C_2mim][FSI]$ > $[C_3C_1pyrr][Tf_2N]$ > $[C_3C_1mim][Tf_2N]$ > $[C_4mim][Tf_2N]$. The decrease in $D_{Tl(I)}$ values also follow the same order except for the system with $[C_3C_1pyrr][Tf_2N]$. The latter system shows that the $D_{Tl(I)}$ values continuously decrease even lower than $[C_3C_1mim][Tf_2N]$ and $[C_4mim][Tf_2N]$ despite its higher solubility compared to these two ILs. It is possible that $[C_3C_1pyrr^+]$ cation is attracted stronger to $[Tf_2N^-]$ anion in the aqueous phase, which leads to lower amount of IL's anion available to exchange with the metal ion and allow it to be extracted into the organic phase.

4.1.2 Tl(III) Extraction into Pure Imidazolium- and/or Pyrrolidinium-based Ionic Liquid

The effectiveness of Br_2 water and Cl_2 water to oxidize Tl(I) was studied by varying the volume of the oxidizing agents in the aqueous phase. Thallium(III) was extracted from 1 M HCl into $[C_nmim][Tf_2N]$, where n = 2, 4, and 8. The volumes of Br_2 water and Cl_2 water were varied from 5 to 50 μL, and the total volume of the aqueous phase was 500 μL. The obtained results are presented in Figure 22.

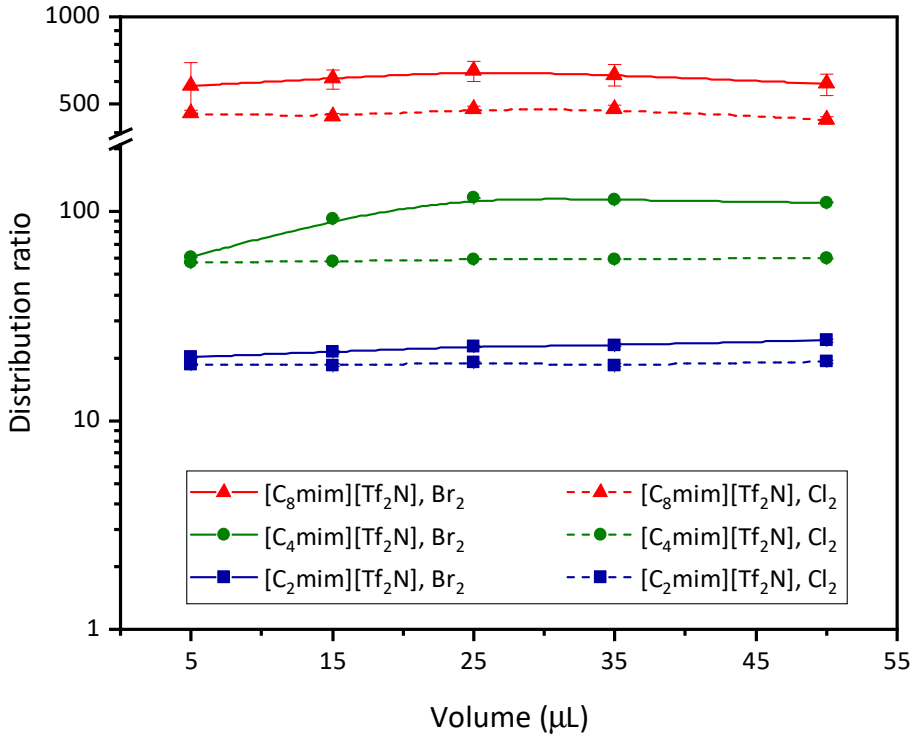

Figure 22. The effect of oxidizing agents, Br_2 water and Cl_2 water, to the distribution ratio of Tl(III). The metal was extracted from 1 M HCl into $[C_nmim][Tf_2N]$, where n = 2, 4, and 8. The solid and dashed lines are drawn to guide the eye.

Of all the ILs that were studied, $D_{Tl(III)}$ values are generally higher when thallium was oxidized by using Br_2 water (see Figure 22). The $D_{Tl(III)}$ values initially increased and reached saturation when 25 µL or more bromine water was added into the aqueous phase. Meanwhile, the volume of Cl_2 water does not affect $D_{Tl(III)}$ values as they are constant regardless the amount of oxidizing agent added into the aqueous phase. To ensure oxidation of Tl(I) to Tl(III), 25 µL of Br_2 water or Cl_2 water were used in the chemical system for the entire Tl(III) extraction experiments.

Next, the kinetics of Tl(III) extraction was studied. This study is an important factor to determine that the chemical reaction for metal extraction has completed and ultimately to ensure the reliability of the extraction data. During the extraction process, the aqueous and organic phase were put in contact and vigorously mixed at 3000 rpm for 1 to 20 minutes intervals. Tl(III) was extracted from 1 M HCl into $[C_nmim][Tf_2N]$, where n = 2, 4, and 8, using Br_2 water as the oxidizing agent. The results are shown in Figure 23.

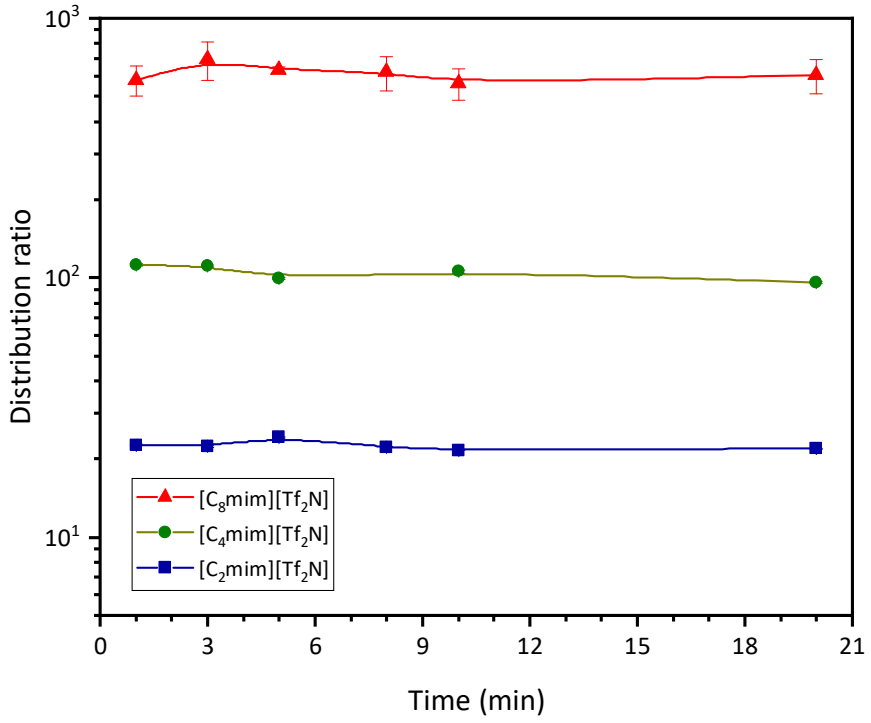

Figure 23. The study of Tl(III) extraction kinetics from 1 M HCl into $[C_nmim][Tf_2N]$, where n = 2, 4, and 8, using Br_2 water as the oxidizing agent. The lines are drawn to guide the eye.Based on the results shown in the figure above, the kinetics of Tl(III) extraction into all the ILs that were studied was sufficiently fast. Reaction equilibrium was generally reached within 1 min. However, a 5 min extraction was chosen for the entire metal extraction experiments (except for the kinetics study where time has to be varied) for experimental convenience. Figure 23 also shows that $D_{Tl(III)}$ values increase with increasing length of the cation's alkyl chain, which is consistent with the results shown in Figure 22. This finding was investigated further. In the next paragraphs, the effect of IL structure as well as the aqueous phase acidity to Tl(III) extraction will be discussed.

The distribution ratios of Tl(III) extracted into $[C_nmim][Tf_2N]$ (n = 2, 4, and 8) as the function of aqueous phase acidity are shown in Figure 24. Both Br_2 water and Cl_2 water were used to oxidize Tl(I) to Tl(III) and the $D_{Tl(III)}$ values are presented in the figure for comparison. It can be seen that $D_{Tl(III)}$ values decrease with increasing HCl concentration, regardless of the structure of the ILs and the oxiziding agent being used. The effect of oxidizing agent is more pronounced at acid concentration < 3 M; *D* values of thallium oxidized with Br_2 water are higher compared to Cl_2 water. However, above this acid concentration, $D_{Tl(III)}$ values are independent of the oxidizer. Moreover, the effect of the length of alkyl chain in the IL's cation is also observed in Figure 24. Higher $D_{Tl(III)}$ values were obtained for longer IL's cation alkyl chain.

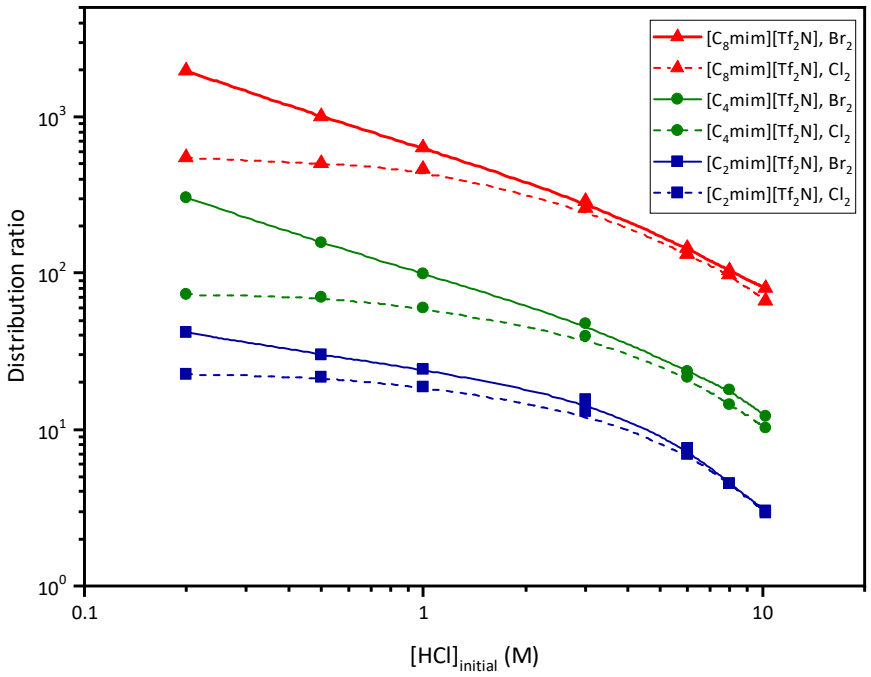

Figure 24. The effect of aqueous phase acidity and the structure of the IL's cation to the extraction of Tl(III). Both Br_2 water and Cl_2 water were used as the oxidizing agent (solid and dashed lines, respectively). The lines are drawn to guide the eye.

The influence of IL's anion structure to the extraction yield of Tl(III) was also studied. Tl(III) was extracted into [C_2mim][FSI] and [C_2mim][Tf_2N]. The results are presented in Figure 25. The extraction curves show the same trend as observed in Figure 26: $D_{Tl(III)}$ values decrease with increasing acid concentration and better extraction was found when Br_2 water was used as the oxidizing agent especially < 3 M HCl. Among these two ILs, [C_2mim][FSI] is the better organic phase media for T(III) extraction since the *D* values obtained in this system are higher compared to [C_2mim][Tf_2N].

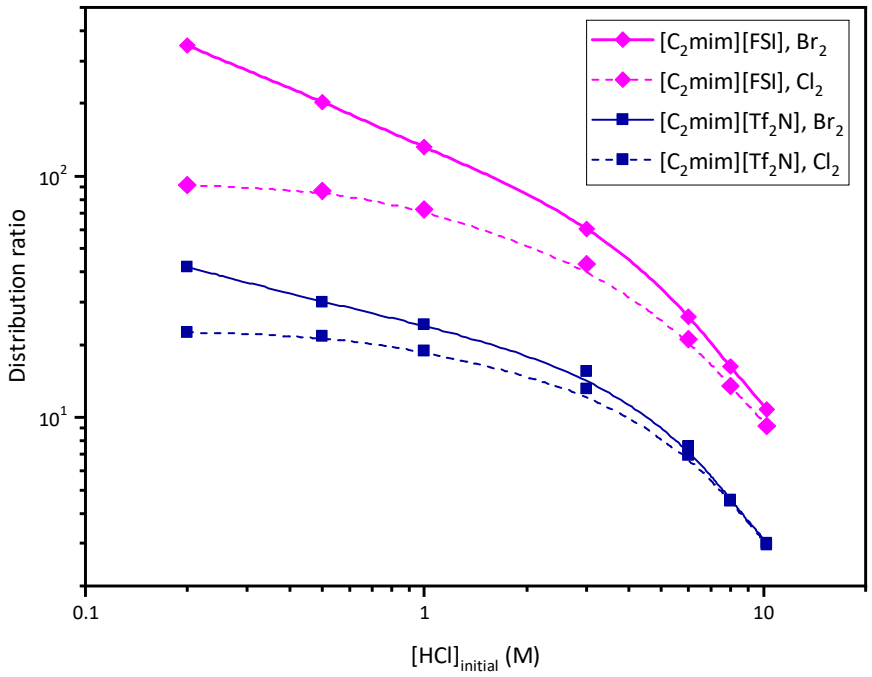

Figure 25. The effect of aqueous phase acidity and the structure of the IL's anion to the extraction of Tl(III). Both Br_2 water and Cl_2 water were used as the oxidizing agent (solid and dashed lines, respectively). The lines are drawn to guide the eye.

In order to get a comprehensive description on the influence of IL's structure on Tl(III) extraction, $D_{Tl(III)}$ values into various ILs are presented. Figure 26a and 26b show the data on Tl(III) extraction into $[C_3C_1mim][Tf_2N]$, $[C_3C_1pyrr][Tf_2N]$, $[C_4mim][Tf_2N]$ and $[C_2mim][FSI]$, with Br_2 water and Cl_2 water as the oxidizing agent, respectively. Consistent with the results in the Figure 24-25, $D_{Tl(III)}$ values with Br_2 water are higher than Cl_2 water, due to the presence of mixed thallium chloro- and bromocomplexes that have higher stability and hydrophobicity than pure chlorocomplexes [136,137].

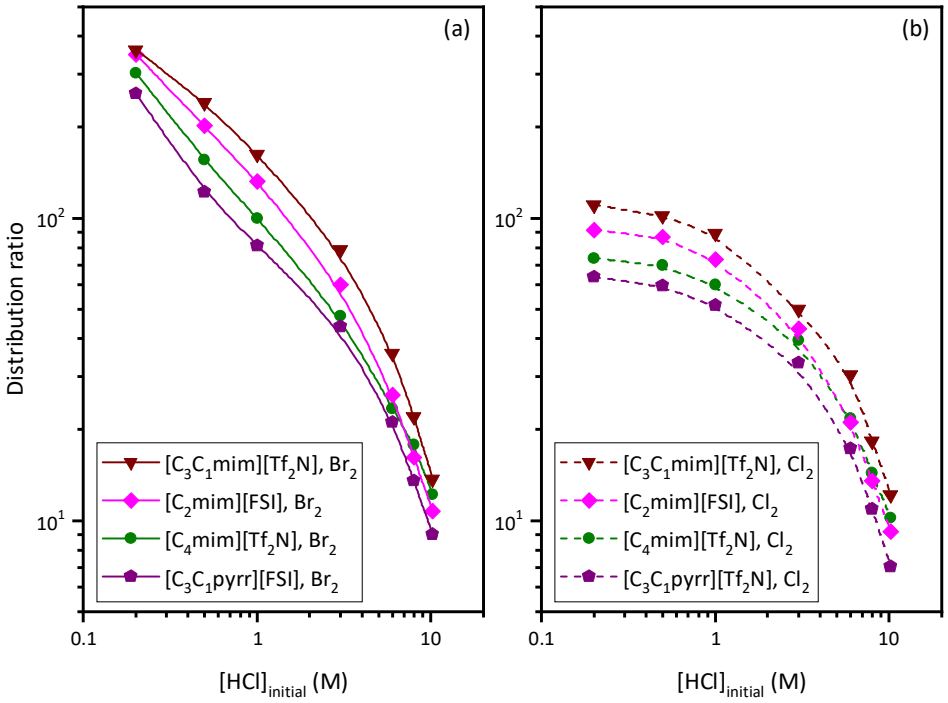

Figure 26. The effect of aqueous phase acidity and the structure of the IL's cation and anion to the extraction of Tl(III). Thallium was oxidized using Br_2 water (a) and Cl_2 water (b). The lines are drawn to guide the eye.

In both figures, it can be seen that as the acid concentration increases, $D_{Tl(III)}$ values decrease in the order $[C_3C_1mim][Tf_2N]$ > $[C_2mim][FSI]$ > $[C_4mim][Tf_2N]$ > $[C_3C_1pyrr][Tf_2N]$. It is interesting to note that, despite having identical molecular weights and anion groups, *D* values of Tl(III) extracted into $[C_3C_1mim][Tf_2N]$ are higher than $[C_4mim][Tf_2N]$. The lengthening of the alkyl chain on $[C_4mim^+]$ normally would contribute to lower the solubility of this cation in the aqueous phase compared to $[C_3C_1mim^+]$. However, the solubility values of these cations are within the error bars (6.6 ± 0.4 g/L for $[C_4mim^+]$ vs 6.8 ± 0.4 g/L for $[C_3C_1mim^+]$, see Table 4 in section 2.4.4.1).

Unfortunately, there is no data on [$C_3C_1mim^+$] hydrophobicity available in the literature. Taking into account the structure of the two cations, [$C_3C_1mim^+$] has shorter alkyl chain compared to [C_4mim^+]. Thus, the [$C_3C_1mim^+$] cation is likely to have higher charge density which might contribute to higher $D_{Tl(III)}$ values in this system. Meanwhile, D values of Tl(III) extracted into [C_2mim][FSI] are higher compared to [C_4mim][Tf_2N]. Although the solubility of [C_2mim^+] cation is higher than [C_4mim^+], it is unfair to justify the extraction results merely on this basis because the ILs have two different anion groups. The anion [FSI^-] has two fluorine atoms in its structure, while [Tf_2N^-] anion contains six fluorine atoms. Most literature data reported the IL solubility based on the cation solubility [103,135]; however, it can be expected that the presence of two fluorine atoms in [FSI^-] would increase its hydrophilicity and solubility compared to [Tf_2N^-]. Furthermore, the substitution of imidazolium ring in [C_3C_1mim][Tf_2N] with pyrrolidinium in [C_3C_1pyrr][Tf_2N] resulted in higher aqueous solubility and lower $D_{Tl(III)}$ values in the latter.

To conclude, the extraction of Tl(III) into imidazolium and pyrrolidinium-based ILs is strongly affected by the structure of the ILs. Contrary to the results obtained for Tl(I) extraction, it was found that Tl(III) is better extracted with the ILs that contain longer alkyl chains on its cation group. The efficiency of Tl(III) extraction decreases in the order [C_8mim][Tf_2N] > [C_3C_1mim][Tf_2N] > [C_4mim][Tf_2N] > [C_3C_1pyrr][Tf_2N] > [C_2mim][Tf_2N] and the cation solubility also decreases in the same order.

Overall, all the ILs used in this study were able to extract Tl(III) effectively, especially at lower acidity. The mathematical model of the extraction mechanism is discussed below.

4.1.3 Mathematical Model of the Extraction Mechanism

Metal extraction with ILs are known to occur via the transfer of charged complexes [138-140]. For Tl(III) which forms mainly negatively charged complexes, it can be extracted through anion exchange mechanism or ion pair formation with the IL cation. Equations 40 and 41 show the reaction for these two mechanisms.

$$z[\mathrm{A}^-]_{\mathrm{org}} + [\mathrm{S}^{z-}]_{\mathrm{aq}} \rightleftarrows [\mathrm{S}^{z-}]_{\mathrm{org}} + z[\mathrm{A}^-]_{\mathrm{aq}} \quad \text{Eq. 40}$$

$$z[\mathrm{C}^+]_{\mathrm{aq}} + [\mathrm{S}^{z-}]_{\mathrm{aq}} \rightleftarrows [\mathrm{S}^{z-}]_{\mathrm{org}} + z[\mathrm{C}^+]_{\mathrm{org}} \quad \text{Eq. 41}$$

Equation 40 describes an anion exchange process between the IL anion [A^-] from the organic phase and the negatively charged metal species, denoted as [S^{z-}], in the aqueous phase. The ion pair formation mechanism, shown in Eq. 41, involves the interaction between the IL cation [C^+] and the metal species [S^{z-}] in the aqueous phase followed by the transfer of this pair to the organic phase. In Eqs. 40-41, z is the number of IL's cation or anion that is required to compensate the charge of the extracted species.

The reactions above can proceed depending on the distribution of IL anion [A^-] and cation [C^+] between the organic and the aqueous phase. The IL dissolution reaction is shown in Eq. 42 below:

$$[\mathrm{C}^+]_{\mathrm{org}} + [\mathrm{A}^-]_{\mathrm{org}} \rightleftarrows [\mathrm{C}^+]_{\mathrm{aq}} + [\mathrm{A}^-]_{\mathrm{aq}} \quad \text{Eq. 42}$$

Taking into account the charge balance in the aqueous phase, the solute transfer in the form of negatively charged ions into the organic phase can be described as:

$$[\mathrm{A^-}]_{\mathrm{aq}} - [\mathrm{C^+}]_{\mathrm{aq}} = z \cdot ([\mathrm{S^{z-}}]_{\mathrm{aq,\ initial}} - [\mathrm{S^{z-}}]_{\mathrm{aq}}) = z \cdot \Delta[\mathrm{S^{z-}}]_{\mathrm{aq}} \quad \text{Eq. 43}$$

where the subscribe "initial" refers to the initial concentration of metal solutes in the aqueous phase. In Eq. 43, $\Delta[\mathrm{S^{z-}}]_{\mathrm{aq}}$ is the difference between the initial and the equilibrium concentration of the negatively charged metal species.

Since the distribution ratio of a solute is defined as the ratio of its concentration in the organic to the aqueous phase (see Eq. 5), the reactions in Eqs. 39 – 40 can be re-expressed in term of the equilibrium constants for the ion exchange (K_{IE}) and ion pair formation (K_{IP}) mechanisms:

$$K_{IE} = D_{\mathrm{S^{z-}}} \cdot [\mathrm{A^-}]_{\mathrm{aq}}^{\ z} \quad \text{Eq. 44}$$

$$K_{IP} = D_{\mathrm{S^{z-}}} \cdot [C^+]_{\mathrm{aq}}^{\ z} \quad \text{Eq. 45}$$

Meanwhile, the solubility product constant of the IL (K_{sp}) according to the reaction in Eq. 42 can be written as:

$$K_{sp} = [\mathrm{C^+}]_{\mathrm{aq}} \cdot [\mathrm{A^-}]_{\mathrm{aq}} \quad \text{Eq. 46}$$

and taking into account Eqs. 44-45, K_{sp} can also be expressed as:

$$K_{sp}^{\ z} = K_{IE} \cdot K_{IP}^{\ -1} \quad \text{Eq. 47}$$

Combining Eq. 43 and 46 results in a quadratic equation:

$$K_{sp} = \left([\mathrm{A^-}]_{\mathrm{aq}} - z \cdot \Delta[\mathrm{S^{z-}}]_{\mathrm{aq}}\right) \cdot [\mathrm{A^-}]_{\mathrm{aq}} \quad \text{Eq. 48}$$

and the solution of Eq. 48 can be substituted into Eq. 44 to obtain the following equation:

$$K_{IE} = D_{S^{z-}} \cdot \left(\frac{z \cdot \Delta[S^{z-}]_{aq} + \left(z^2 \cdot \Delta[S^{z-}]_{aq}^2 + 4 \cdot K_{sp}\right)^{1/2}}{2} \right)^z \quad \text{Eq. 49}$$

The function $D_S = f\left(\Delta[\mathrm{S}^{z\pm}]_{\mathrm{aq}}\right)$ describes the values obtained from metal extraction experiments. Varying the concentration of solute over a wide range shows that this function is not linear. In the limit of infinite $\Delta[\mathrm{S}^{z\pm}]_{\mathrm{aq}}$, Eq. 49 can be written as:

$$\log D_\infty = \log K_{IE} - z \log z - z \log \Delta[\mathrm{S}^{z\pm}]_{\mathrm{aq}} \quad \text{Eq. 50}$$

where D_∞ is the distribution ratio for the theoretical infinite $\Delta[\mathrm{S}^{z\pm}]_{\mathrm{aq}}$.

The mathematical model above only considers the chemical system in the absence of H^+ ion. In the presence of H^+, for instance in an acidic aqueous solution, the IL's anion, *i.e.,* $[Tf_2N^-]$ protonates in the aqueous phase to form $H[Tf_2N]$ acid (K_a = 0.70 ± 0.04 mol/dm^3 or pK_a = 0.16 [103]). The protonation reaction and the acid dissociation constant are shown in Eqs. 51 and 52 below:

$$[\mathrm{HA}]_{\mathrm{aq}} \rightleftarrows [\mathrm{H}^+]_{\mathrm{aq}} + [\mathrm{A}^-]_{\mathrm{aq}} \quad \text{Eq. 51}$$

$$K_a = [\mathrm{H}^+]_{\mathrm{aq}} \cdot [\mathrm{A}^-]_{\mathrm{aq}} \cdot [\mathrm{HA}]_{\mathrm{aq}}^{-1} \quad \text{Eq. 52}$$

To account for the presence of both $[\mathrm{A}^-]_{\mathrm{aq}}$ and $[\mathrm{HA}]_{\mathrm{aq}}$ in the aqueous phase, Eqs. 44 and 46 are modified. Then two new terms, conditional equilibrium constants for the ion exchange (K_{IE}') and conditional solubility product constant of the IL (K_{sp}'), are introduced:

$$K_{IE}' = D_{S^{z-}} \cdot [\mathrm{A}^-]_{\mathrm{aq}}^{\,z} \cdot \left(1 + [\mathrm{H}^+]_{\mathrm{aq}} \cdot K_a^{-1}\right)^z \quad \text{Eq. 53}$$

$$K_{sp}' = [\mathrm{C}^+]_{\mathrm{aq}} \cdot [\mathrm{A}^-]_{\mathrm{aq}} \cdot \left(1 + [\mathrm{H}^+]_{\mathrm{aq}} \cdot K_a^{-1}\right)^z \quad \text{Eq. 54}$$

where $[\mathrm{A}^-]_{\mathrm{aq}} + [\mathrm{HA}]_{\mathrm{aq}} = [\mathrm{A}^-]_{\mathrm{aq}} \cdot \left(1 + [\mathrm{H}^+]_{\mathrm{aq}} \cdot K_a^{-1}\right)$.

Addition of common ions into the aqueous phase is one of the methods to investigate metal extraction mechanisms [141,142]. For instance, Li[Tf_2N] is added to investigate the mechanism of extraction into [Tf_2N^-]-based ILs as well as to determine the charge of the extracted species. In this case, the charge balance in the acidic aqueous phase before extraction can be described as:

$$[Li^+]_{aq,\ init} + [H^+]_{aq,\ init} = [Tf_2N^-]_{aq,\ init} + [Cl^-]_{aq,\ init} + z \cdot [S^{z-}]_{aq,init} \quad \text{Eq. 55}$$

Meanwhile, the charge balance after extraction:

$$[Li^+]_{aq} + [H^+]_{aq} + [C^+]_{aq} = [Tf_2N^-]_{aq,\ total} + [Cl^-]_{aq} + z \cdot [S^{z-}]_{aq} \quad \text{Eq. 56}$$

It was confirmed that Li^+, H^+, and Cl^-, were not extracted into the organic phase from up to 5 M HCl and these results were in agreement with other reported experiments [103,114,124]. Therefore, $[Li^+]_{aq,\ init} = [Li^+]_{aq}$, $[H^+]_{aq,\ init} = [H^+]_{aq}$, and $[Cl^-]_{aq,\ init} = [Cl^-]_{aq}$. The addition of a common salt (Li[Tf_2N]) and the dissolution of IL into the aqueous phase consequently change the equilibrium amount of [Tf_2N^-] ion, where $[Tf_2N^-]_{aq,\ total} = [Tf_2N^-]_{aq,\ Li[Tf_2N]} + [A^-]_{aq,\ IL}$. The subscript "aq, Tf_2N" denotes the quantity of [Tf_2N^-] ion originated from Li[Tf_2N] in the aqueous phase. Subtracting Eq. 56 from Eq 55 gives:

$$[HA]_{aq} - [C^+]_{aq} = \Delta[Tf_2N^-]_{aq} + z \cdot \Delta[S^{z-}]_{aq} \quad \text{Eq. 57}$$

where $\Delta[Tf_2N^-]_{aq} = [Tf_2N^-]_{aq,\ init} - [Tf_2N^-]_{aq,\ total}$.

Expressing the $K_{sp}{}'$ in Eq. 54 combined with Eq. 57 consequently gives a quadratic equation:

$$K_{sp}{}' = \left([\mathrm{H^+}]_{\mathrm{aq}} \cdot [\mathrm{A^-}]_{\mathrm{aq}} \cdot \mathrm{K_a^{-1}} - \Delta[\mathrm{Tf_2N^-}]_{\mathrm{aq}} - \mathrm{z}\cdot\Delta[\mathrm{S^{z-}}]_{\mathrm{aq}}\right) \cdot [\mathrm{A^-}]_{\mathrm{aq}} \cdot \left(1 + [\mathrm{H^+}]_{\mathrm{aq}} \cdot \mathrm{K_a^{-1}}\right)$$

Eq. 58

Let $[T^-]_{aq} = \Delta[\mathrm{Tf_2N^-}]_{\mathrm{aq}} + \mathrm{z} \cdot \Delta[\mathrm{S^{z-}}]_{\mathrm{aq}}$, then solving Eq. 58 in term of $[\mathrm{A^-}]_{\mathrm{aq}}$ leads to:

$$[\mathrm{A^-}]_{\mathrm{aq}} = \frac{[\mathrm{T^-}]_{\mathrm{aq}} + \left([\mathrm{T^-}]_{\mathrm{aq}}{}^2 + 4\left(\mathrm{K_a} + [\mathrm{H^+}]_{\mathrm{aq}}\right)^{-1} \cdot [\mathrm{H^+}]_{\mathrm{aq}} \cdot K_{sp}{}'\right)^{0.5}}{2 \cdot [\mathrm{H^+}]_{\mathrm{aq}} \cdot \mathrm{K_a}^{-1}} \qquad \text{Eq. 59}$$

To confirm the theoretical mechanism described above, an experiment was performed where Tl(III) was extracted into $[C_4mim][Tf_2N]$ from 1 and 5 M HCl. $Li[Tf_2N]$ salt with varying concentrations was added into the aqueous phase. Stable Tl(III) was used as the metal source and its concentration was kept constant for the entire experiment (~ 10^{-4} M).

Figure 27 shows the distribution ratio of Tl(III) extracted into $[C_4mim][Tf_2N]$ as a function of $\Delta[\mathrm{Tf_2N^-}]_{\mathrm{aq}} + \mathrm{z} \cdot \Delta[\mathrm{TlCl_{3+z}}^{\mathrm{z-}}]_{\mathrm{aq}}$, where $\Delta[\mathrm{Tf_2N^-}]_{\mathrm{aq}}$ and $\mathrm{z} \cdot \Delta[\mathrm{TlCl_{3+z}}^{\mathrm{z-}}]_{\mathrm{aq}}$ are the difference between initial and equilibrium concentration of $[Tf_2N^-]$ and Tl(III) in the aqueous phase, respectively. Although the definition of the extracted species is $[\mathrm{T^-}]_{\mathrm{aq}} = \Delta[\mathrm{Tf_2N^-}]_{\mathrm{aq}} + \mathrm{z} \cdot \Delta[\mathrm{TlCl_{3+z}}^{\mathrm{z-}}]_{\mathrm{aq}}$, the amount of added $Li[Tf_2N]$ is twice larger than the concentration of Tl(III). Therefore, the quantity $\mathrm{z} \cdot \Delta[\mathrm{TlCl_{3+z}}^{\mathrm{z-}}]_{\mathrm{aq}}$ is considerably small compared to $\Delta[\mathrm{Tf_2N^-}]_{\mathrm{aq}}$ and can be neglected. It is shown in the figure that the distribution ratio of Tl(III) decrease with increasing $\Delta[\mathrm{Tf_2N^-}]_{\mathrm{aq}}$. Graphical analysis of the slopes of the curves at high $[\mathrm{Tf_2N^-}]_{\mathrm{aq}}$ concentration shows that the slopes at 1 and 5 M HCl are -1.1 and -1.9, respectively. The values indicate the average charge of the extracted metal complex.

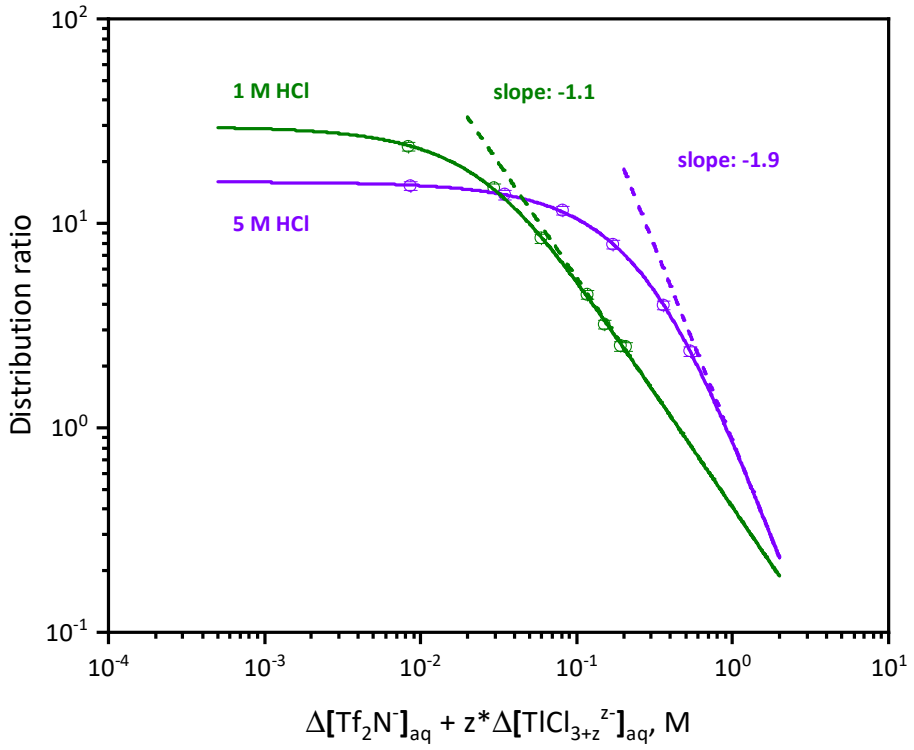

Figure 27. Extraction of stable Tl(III) into [C_4mim][Tf_2N] from 1 and 5 M HCl as the function of added Li[Tf_2N]. The solid lines are fitted data while the broken lines are slopes obtained from graphical analysis.

The experimental data in Figure 27 were fitted using the combination of Eqs. 53 and 59 with Origin 8.5 software [143]. The equilibrium concentration of protons was defined as $[H^+]_{aq} = [H^+]_{aq,init} \cdot \left(1 + [A^-]_{aq} \cdot K_a^{-1}\right)^{-1}$ and $[A^-]_{aq}$ was equal to 20 mM and independent of acid concentration in up to 5 M HCl. The solubility product constant of [C_4mim][Tf_2N] is 2.7 x 10^{-4} [135] and this value was used to set the lower limit of K_{sp}' for fitting purposes. The results of data fitting are presented in Table 7.

Table 7. Fitted parameter for Tl(III) extraction experiment into $[C_4mim][Tf_2N]$ from 1 and 5 M HCl with added $Li[Tf_2N]$.

Parameter	1 M HCl	5 M HCl
Reduced χ^2	0.703	0.069
z	1.12 ± 0.06	1.97 ± 0.16
K_{sp}'	$(8.3 \pm 2.5)\cdot10^{-4}$	0.064 ± 0.013
K_{IE}'	0.75 ± 0.06	1.22 ± 0.02
K_{IP}'	2160 ± 250	273 ± 10

The calculated parameter z in the table indicates the negative charge of the extracted complex. As can be seen, the values are in agreement with the results of the slope analysis. Thus, the extracted complex at 1 M HCl is most likely $TlCl_4^-$. Meanwhile, at 5 M HCl, the extracted complex could be $TlCl_5^{2-}$ or a mixture of $TlCl_4^-$ and $TlCl_6^{3-}$. Considering K_{IP}' value is larger than K_{IE}', the thallium species was predominantly extracted through ion pair formation with the ionic liquid anion.

4.2 In and Tl Extraction into Betanium-based IL

This section discusses the results of In(III) and Tl(I, III) extraction into water-saturated $[Hbet][Tf_2N]$ ionic liquid from HCl media. The extraction kinetics, effect of zwitterionic betaine and $Li[Tf_2N]$ addition, and effect of HCl concentration on the extraction efficiency of the metal of interest are presented in this section. Finally, the extraction mechanism for each metal is described and the possible extracted species is also proposed.

4.2.1 Extraction Kinetics

As it was mentioned previously in an earlier paragraph, the study of extraction kinetics is important to determine the time required for the chemical reaction to reach equilibrium. Thus, it helps ensure the reliability of the extraction data. The kinetics of In(III) and Tl(III) extraction into [Hbet][Tf_2N] was studied at constant HCl concentrations (0.01 M for In(III) and 0.05 M for Tl(III)). For this study, thallium was oxidized by using Cl_2 water. Meanwhile, the extraction time was varied in range of 0.5 – 15 min for In(III) and 0.5 – 10 min for Tl(III).

The results show that the metal transfer reaction into the organic phase is very fast and the equilibrium is reached within 1 min for both metals (see Figure 28). However, for all other extractions studied with this chemical system, a 5-min mixing time was chosen for convenience of handling the experiment.

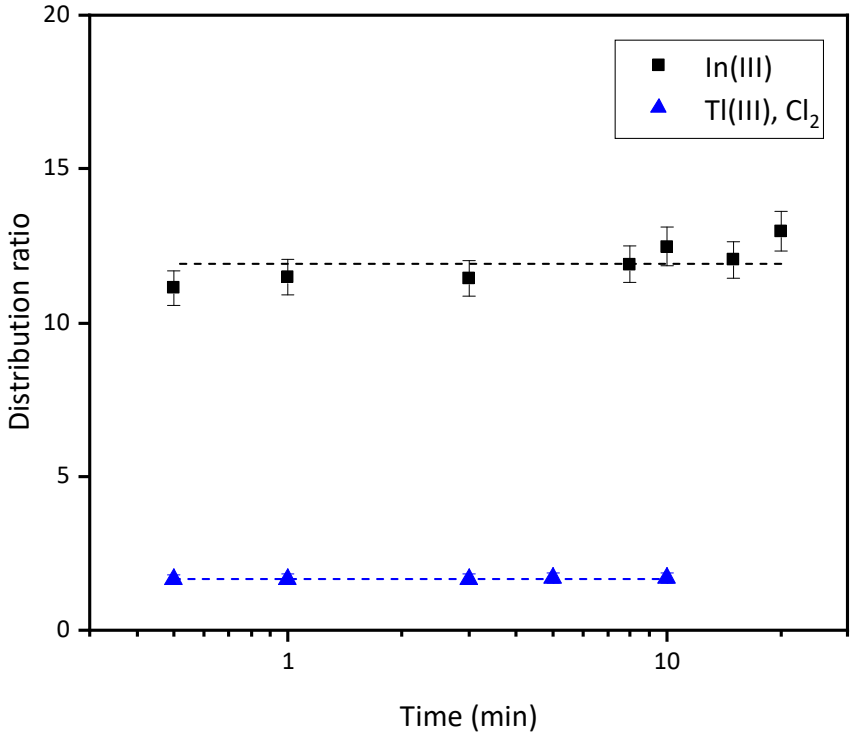

Figure 28. Extraction kinetics of In(III) and Tl(III) were studied at 0.01 M and 0.05 M HCl, respectively. Thallium was oxidized by using Cl_2 water. The broken lines show the average $D_{In(III)}$ and $D_{Tl(III)}$ as a function of mixing time. Error bars represent statistical uncertainty only; for $D_{Tl(III)}$, they are smaller than the corresponding symbols used.

4.22 Effect of Zwitterionic Betaine

Zwitterionic betaine (bet) is one of the precursors of [Hbet][Tf_2N] ionic liquid. Some studies reported that adding this compound into the aqueous phase increases the extraction efficiency of metallic species (see for example ref. [89]). The deprotonated carboxyl group in the bet structure (see Figure 6) is claimed to be responsible for coordination with the metal ions and transfer them to the organic phase [87,89]. To determine the optimum amount of bet suitable for In(III) and Tl(I, III) extraction, some

experiments were conducted where the amount of bet in the aqueous phase was varied between 5 – 20 % (w/v). The initial HCl concentration was kept constant: 0.01 M for In(III) and 0.2 M for Tl(I, III). The selection of HCl concentration for the metals was done merely based on the availability of HCl stock solution. The results are shown in Figure 29a and 29b for In(III) and Tl(I, III) extractions, respectively.

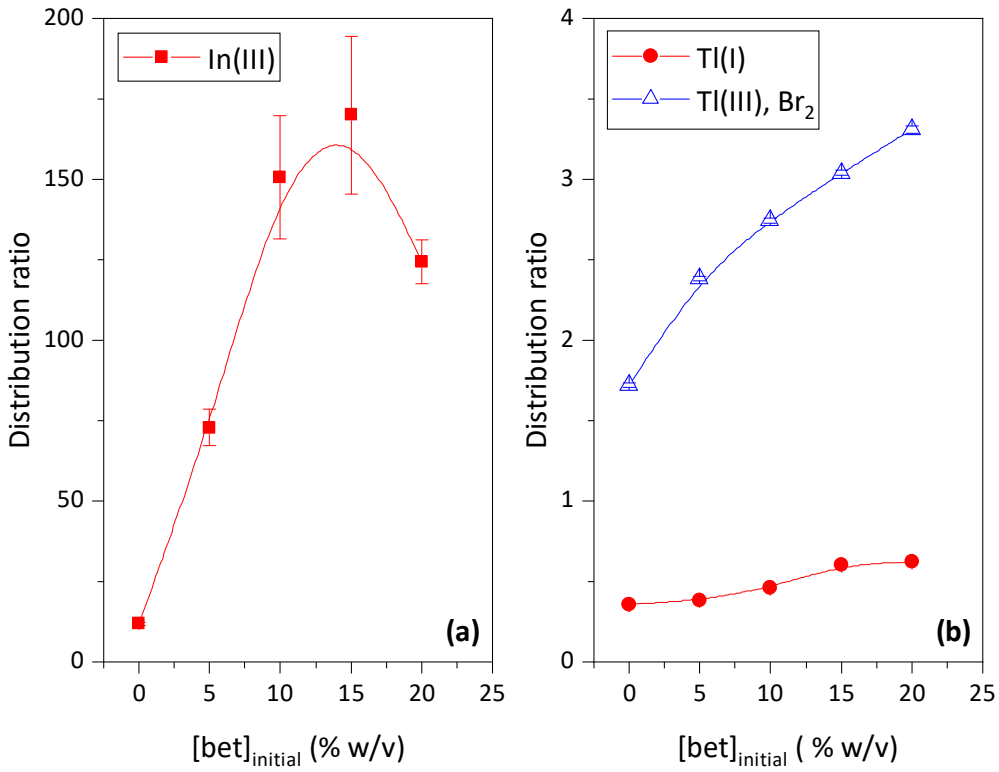

Figure 29. The variation of *D* values as a function of initial added betaine concentration. **(a)** In(III) extracted from 0.01 M HCl, **(b)** Tl(III) extracted from 0.2 M HCl. Error bars only represent statistical uncertainty and are smaller than the corresponding symbols. Thallium was oxidized using Br_2 water. The lines are drawn to guide the eye.

It can be seen in Figure 29a that adding bet up to 15 % (w/v) increases $D_{In(III)}$ values, but at 20 % bet, $D_{In(III)}$ value decreases. Some experiments were also carried out with higher bet concentration. However, it was observed that the aqueous phase became more viscous and phase miscibility increased. This is likely the effect of changes in aqueous phase equilibria according to Le Châtelier's principle (see p.82 for details). In practice, adding higher amount of betaine in the aqueous phase leads to higher deprotonation of [$Hbet^+$] according to Eq. 14 and eventually increases the aqueous

solubility of [Hbet][Tf_2N] (shown in Eq. 13). Consequently, phase separation was very poor. Adding 50% (w/v) bet into 0.01 M HCl eventually led to complete phase miscibility at room temperature. Due to inadequate amount of data, it is not possible to explicitly explain the declining trend seen at high bet concentration.

In the case of Tl(I, III), increasing *D* values were also observed with increasing amount of bet added into the aqueous phase, with more pronounced effect on *D* values of Tl(III) than Tl(I) (Figure 29b). Unlike the experiments with In(III), $D_{Tl(I, III)}$ values continuously rose even at 20% (w/v) bet. This is likely due to the presence of 0.2 M HCl compared to 0.01 M HCl in the chemical system used for In(III) extraction. Higher amount of proton available in the aqueous phase compensates betaine that present in excess. Thus, it increased the protonation of bet and reduced the solubility of the IL and the miscibility of the phases.

4.2.3 Li[Tf_2N] Dependency

In section 4.1, it was discussed how the addition of Li[Tf_2N] salt into the aqueous phase prior to extraction helps to determine the mechanism and the possible extracted species. The same method was applied for In(III) and Tl(III) extraction in this chemical system, since the IL also contains [Tf_2N^-] anion. The main objective of this study is to determine the role of [Tf_2N^-] anion in the extraction of these metals. The Li[Tf_2N] salt was added into 0.05 M HCl and its initial concentration was varied in the range of 0.004 – 0.6 M. The results are presented in Figure 30.

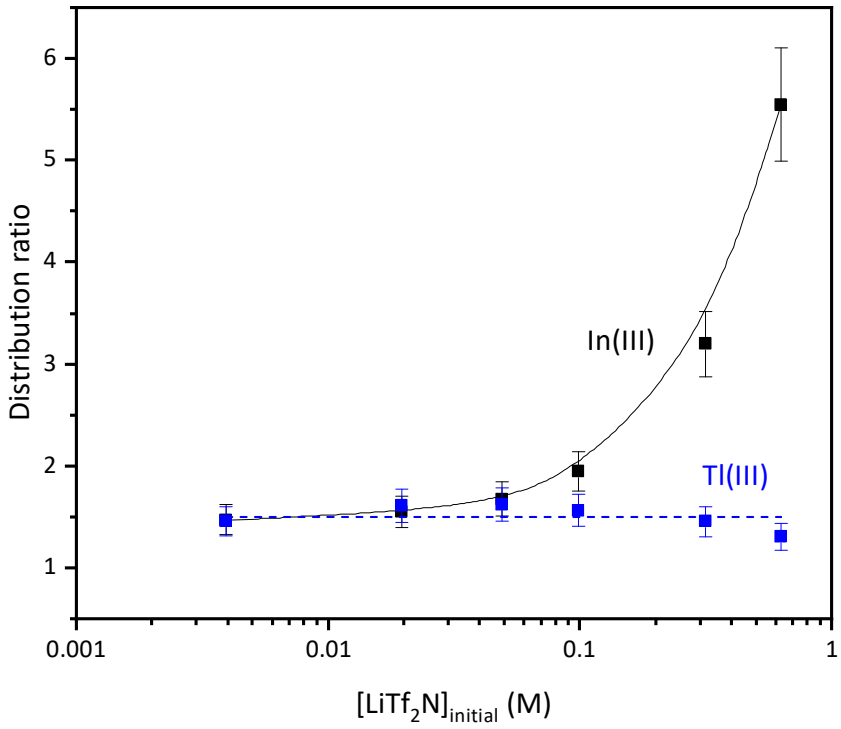

Figure 30. The dependency of In(III) and Tl(III) extraction on the Li[Tf_2N] initial concentration in the aqueous phase (0.05 M HCl). Chlorine water was used to oxidize thallium. The broken line is the average value of $D_{Tl(III)}$, while the solid line is drawn to guide the eye. Error bars only represent statistical uncertainty.An apparent increase of $D_{In(III)}$ values was observed with the addition of Li[Tf_2N] salt. It is known that at 0.05 M HCl, In(III) exists as $InCl_2^+$ and $InCl^{2+}$ species [144]. The results in Figure 30 indicate that the presence of [Tf_2N^-] anion in excess enhances the extraction efficiency of indium species in the cationic form. Meanwhile, $D_{Tl(III)}$ values are constant over the whole range of Li[Tf_2N] concentration that was studied. According to ref. [103,114,124,136], Li^+ ion is not extracted into the organic phase. In addition, Tl(III) is known to exist as neutral $TlCl_3$ and $TlCl_4^-$ at 0.05 M aqueous HCl [144]. If thallium species interacted with [Tf_2N^-] anion

i.e., through anion exchange mechanism, increasing [Tf_2N^-] anion concentration by adding Li[Tf_2N] would increase $D_{Tl(III)}$ values. However, this was not observed in Figure 30. Since there is no significant changes observed in the presence of Li[Tf_2N] salt, most likely Tl(III) was extracted as an anionic complex through ion pair formation with [$Hbet^+$]. The extraction mechanisms for these metals will be discussed in Sec. 4.2.5 below.

4.2.4 Effect of HCl Concentration

The effect of HCl concentration on the extraction of In(III) and Tl(I, III) from water-saturated [Hbet][Tf_2N] was studied. The experiments were done in the absence and presence of zwitterionic betaine (bet) in the aqueous phase. In a previous section it was shown that $D_{In(III)}$ values were the highest with the addition of 15% (w/v). Therefore, the same amount of bet was added to study the acid dependency of In(III) and Tl(I, III).

Figure 31shows $D_{In(III)}$ values as the function of initial HCl concentration. Regardless the absence or presence of 15% (w/v) bet, increasing acid concentration resulted in a decrease of $D_{In(III)}$ values. In the range of 0.01 – 1 M HCl, the presence of bet improved extraction efficiency by more than one order of magnitude. Above 1 M HCl, $D_{In(III)}$ values approach 0.01 in both of the chemical systems, which indicates metal retention in the aqueous phase.

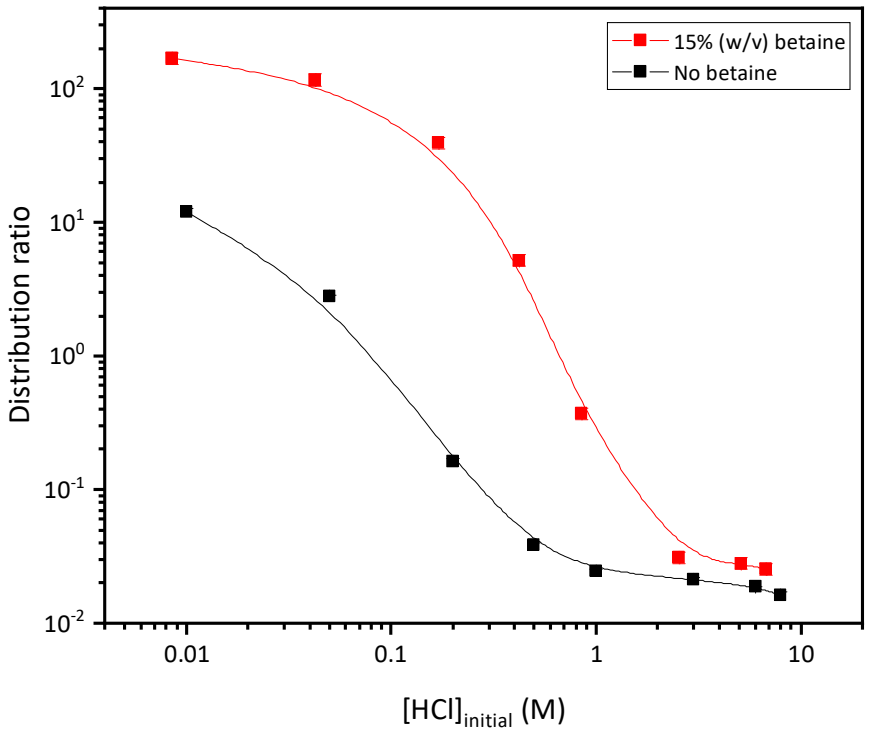

Figure 31. The acid dependency of In(III) extraction in the absence and presence of 15% (w/v) zwitterionic betaine. Error bars on D_{In} in the absence of betaine represent statistical uncertainty only. In both plots, the error bars are smaller than the corresponding symbols. The solid lines are drawn to guide the eye.

The dependency of distribution ratio on aqueous phase acidity was also observed in Tl(I, III) extraction. The experimental results are shown in Figure 32a and 32b for Tl(III) and Tl(I), respectively. Both Br_2 water and Cl_2 water were used to oxidize thallium and the results are shown in Figure 32a for comparison.

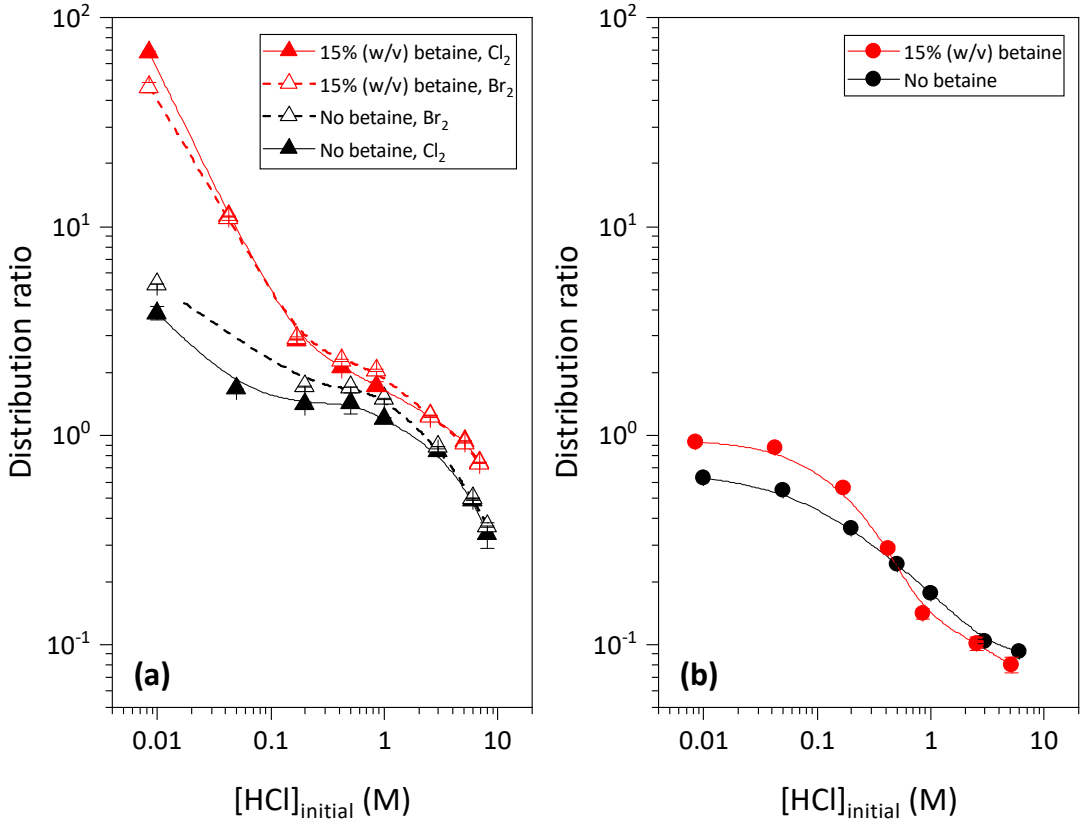

Figure 32. The acid dependency of Tl(I) and Tl(III) in the absence and presence of 15% (w/v) zwitterionic betaine. **(a)** Extraction of thallium(III) using Cl_2 water or Br_2 water as the oxidizing agent. **(b)** Extraction of thallium(I). The lines are drawn to guide the eye. Error bars only represent statistical uncertainty and are smaller than the corresponding symbols.

It can be seen in Figure 32a that, below 1 M HCl, $D_{Tl(III)}$ values are generally greater when Br_2 water was used as the oxidizer, especially in the chemical system without betaine added. This is most likely because of the presence of mixed thallium chloro- and bromocomplexes that have higher stability and hydrophobicity than pure chlorocomplexes [136,137]. Above 1 M HCl, *D* values of Tl(III) oxidized with Br_2 water and Cl_2 water are comparable as Tl(III) is most likely present as thallium

chlorocomplexes. These results are consistent with those reported in the previous section (4.1.2). It is believed that, in concentrated HCl, Cl^- anions displace Br^- in thallium complexes. Consequently, no changes were observed in $D_{Tl(III)}$ values regardless the oxidizing agent being used.

Furthermore, the presence of 15% (w/v) bet in the aqueous phase resulted in higher Tl(III) extraction yield, specifically in the range 0.01 – 0.2 M HCl (Figure 32a). At higher acid concentration, the difference of $D_{Tl(III)}$ values with and without bet added is insignificant. In addition, replacement of Cl_2 water with Br_2 water as the oxidizing agent did not improve $D_{Tl(III)}$ values in this chemical system.

The effect of aqueous phase acidity on Tl(I) extraction is similar to Tl(III). As shown in Figure 32b, $D_{Tl(I)}$ values decrease with increasing aqueous phase acidity. Addition of bet in the aqueous phase increased $D_{Tl(I)}$ values at low acidity, but the effect is less significant compared to Tl(III). At higher acid concentration (> 0.5 M), the presence of bet did not improve $D_{Tl(I)}$ values, suggesting that bet is not involved in Tl(I, III) extraction.

4.2.5 Mechanism of Extraction

Based on the results obtained on extraction behavior of In(III) and Tl(I, III) into water-saturated [Hbet][Tf_2N], the mechanism of metal extraction into this IL was investigated. There are several things that were considered. First, the influence of the presence and the concentration of hydrochloric acid was taken into account. The acid determines the speciation of metallic species in the aqueous phase. It also affects

[Hbet][Tf_2N] solubility, cation's dissociation, and anion's protonation in the aqueous phase [43,86,104,112,136,145,146]. Second, the excess of zwitterionic betaine (bet) in the aqueous phase which was found to facilitate the transfer of bet species into the organic phase and increase aqueous solubility of [Hbet][Tf_2N] [146].

Some mathematical models were developed based on the findings described in the paragraph above. There are four possible extraction pathways:

a) Ion pair formation with [Tf_2N^-];

b) Ion pair formation with [$Hbet^+$];

c) Cation exchange; and

d) Anion exchange.

The mathematical models are discussed below.

4.2.5.1 Ion Pair Formation with [Tf_2N^-]

For this mechanism, there are two consecutive processes expected to occur. First, the positively charged metal halide complexes interact with the IL's cation dissolved in the aqueous phase (Eq. 60). The products of this reaction include a betaine-containing metal complex. In the second reaction, the betaine-containing metal complex interacts with the IL anion and forms an ion pair which is then extracted into the organic phase (Eq. 61). Assuming that betaine is a monodentate ligand, the generic reactions for In(III) and Tl(III) can be written as follows:

$$ML_y^{3-y}{}_{aq} + x\,[Hbet^+]_{aq} \rightleftarrows ML_y(bet)_x^{3-y}{}_{aq} + x\,H^+{}_{aq} \qquad \text{Eq. 60}$$

$$ML_y(bet)_x^{3-y}{}_{aq} + (3-y)\,[Tf_2N^-]_{aq} \rightleftarrows \left[ML_y(bet)_x\right]\left[(Tf_2N)_{3-y}\right]_{org} \quad \text{Eq. 61}$$

where M represents the trivalent indium or thallium metal, L represents the inorganic ligand (*i.e.*, Cl^-). For the extraction of positively charged halide complexes, the values of y are limited to $0 \leq y \leq 2$. Since the coordination number of In(III) and Tl(III) is 6, the number of ligands cannot exceed this value. Therefore, the values of x are limited to $0 \leq x \leq 6$ [41,43,147,148].

From Eq. 59, the equilibrium constant of the reaction can be written as:

$$K_{M(III)} = \frac{\left[ML_y(bet)_x^{3-y}\right]_{aq} \cdot (a_{H^+})^x{}_{aq}}{\left[ML_y^{3-y}\right]_{aq} \cdot [Hbet^+]^x{}_{aq}} \quad \text{Eq. 62}$$

where M(III) represents In(III) or Tl(III). Meanwhile, the activity of proton, a_{H^+}, in Eq. 61 is defined as:

$$a_{H^+} = \gamma_{HCl\pm} \cdot [H^+] \quad \text{Eq. 63}$$

where $\gamma_{HCl\pm}$ has the same definition as before.

Due to limitation of data available on the activity coefficient of the protons [149,150], the mean activity coefficient of HCl, $\gamma_{HCl\pm}$, in Eq. 63 is used as an approximation. This quantity was obtained using a lookup table based on literature data combined with linear interpolation [126,146]. However, the mathematical models presented in this manuscript do not take into account the activity coefficients of the ionic liquid species ($[Hbet^+]$ and $[Tf_2N^-]$) as these values are unknown.

The extraction constant of ion pair formation with $[Tf_2N^-]$, $K_{ext\_IP^-}$, is obtained from combination of Eqs. 60 and 61, and is defined as:

$$K_{ext\_IP^-\ M(III)} = \frac{[ML_y(bet)_x][(Tf_2N)_{3-y}]_{org} \cdot (a_{H^+})^x{}_{aq}}{K_{M(III)} \cdot [ML_y{}^{3-y}]_{aq} \cdot [Hbet^+]^x{}_{aq} \cdot [Tf_2N^-]^{3-y}{}_{aq}} \quad \text{Eq. 64}$$

Using the same approach, the ion pair formation mechanism for extraction of positively charged Tl(I) can be written as follows:

$$Tl^+{}_{aq} + x\,[Hbet^+]_{aq} \rightleftarrows Tl(bet)_x{}^+{}_{aq} + xH^+{}_{aq} \quad \text{Eq. 65}$$

$$Tl(bet)_x{}^+{}_{aq} + [Tf_2N^-]_{aq} \rightleftarrows [Tl(bet)_x][Tf_2N]_{org} \quad \text{Eq. 66.}$$

Since the coordination number of Tl(I) is 4 [45], the number of ligands cannot exceed this value. Therefore, x is limited to $0 \leq x \leq 4$.

The equilibrium constant of the reaction in Eq. 65 can be written as:

$$K_{Tl(I)} = \frac{[Tl(bet)_x{}^+]_{aq} \cdot (a_{H^+})^x{}_{aq}}{[Tl^+]_{aq} \cdot [Hbet^+]^x{}_{aq}} \quad \text{Eq. 67.}$$

Meanwhile, the extraction constant of ion pair formation with $[Tf_2N^-]$, $K_{ext\_IP^-}$, based on the reactions in Eqs. 65-66, is:

$$K_{ext\_IP^-\ Tl(I)} = \frac{[Tl(bet)_x][Tf_2N]_{org} \cdot (a_{H^+})^x{}_{aq}}{K_{Tl(I)} \cdot [Tl^+]_{aq} \cdot [Hbet^+]^x{}_{aq} \cdot [Tf_2N^-]_{aq}} \quad \text{Eq. 68}$$

Expressing Eqs. 64 and 68 in terms of the logarithm of the distribution ratio leads to:

$$\log D = \log C_{ext\_IP^-} - x \log\ (a_{H^+}) \quad \text{Eq. 69}$$

where D is the metallic species ratio in both phases according to Eq. 5. The value $C_{ext\_IP^-}$, which is equal to $K_{ext\_IP^-\ M(III)} \cdot K_{M(III)} \cdot [Hbet^+]^x{}_{aq} \cdot [Tf_2N^-]^{3-y}$ for In(III) and Tl(III) or $K_{ext\_IP^-\ Tl(I)} \cdot K_{Tl(I)} \cdot [Hbet^+]^x{}_{aq} \cdot [Tf_2N^-]_{aq}$ for Tl(I), is a constant. The

value *x* obtained from Eq. 69 is the number of protonated betaine molecules that formed a complex with the metallic species (Eq. 60 or 65).

4.2.5.2 Ion Pair Formation with [$Hbet^+$]

The generic chemical reaction for In(III) and Tl(III) extraction through ion pair formation between negatively charged halide complexes and the IL cation is written below. The extraction based on the following equation occurs after the reaction in Eq. 60 is completed.

$$ML_y(bet)_x{}^{3-y}{}_{aq} + (y-3)[Hbet^+]_{aq} \rightleftarrows [Hbet]_{y-3}\left[ML_y(bet)_x\right]_{org} \quad \text{Eq. 70.}$$

Since the halide complexes in the reaction above must be negatively charged, the value of y is limited to $4 \leq y \leq 6$. Meanwhile, the value of x, which represents number of betaine molecule that can potentially coordinate with the metal, is limited to $0 \leq x \leq 2$ due to the extraction of anionic complexes with the number of ligands between 4 – 6 (the coordination numbers of In(III) and Tl(III) are 6) [41,43,147,148].

The extraction reaction for Tl(I) is written below:

$$TlL_y(bet)_x{}^{1-y}{}_{aq} + (y-1)\,[Hbet^+]_{aq} \rightleftarrows [Hbet]_{y-1}[TlL_y(bet)_x]_{org} \quad \text{Eq. 71.}$$

where $2 \leq y \leq 4$ since the halide complexes must be negatively charged. Due to the extraction of anionic complexes with the number of ligands between 2 – 4 (the coordination number of Tl(I) is 4 [45]) the number of betaine than can potentially

coordinate with the metal ion is limited to 0 – 2. Therefore, the value of x is limited to $0 \leq x \leq 2$.

Based on the reactions above, the corresponding extraction constants for In(III)/Tl(III) and Tl(I) after taking into account the equilibrium constant of the reactions in Eq. 62 and 67, may be expressed as:

$$K_{ext\_IP^+\ M(III)} = \frac{[Hbet^+]_{y-3}[ML_y(bet)_x]_{org} \cdot (a_{H^+})^x_{aq}}{K_{M(III)} \cdot [ML_y{}^{3-y}]_{aq} \cdot [Hbet^+]^{y-3+x}_{aq}} \quad \text{Eq. 72}$$

$$K_{ext\_IP^+\ Tl(I)} = \frac{[Hbet^+]_{y-1}[TlL_y(bet)_x]_{org} \cdot (a_{H^+})^x_{aq}}{K_{Tl(I)} \cdot [TlL_y{}^{1-y}]_{aq} \cdot [Hbet^+]^{y-1+x}_{aq}} \quad \text{Eq. 73.}$$

The logarithmic form of these equations is identical to Eq. 69, but the value $C_{ext\_IP^+}$ is now equal to $K_{ext\_IP^+\ Tl(III)} \cdot K_{M(III)} \cdot [Hbet^+]^{y-3+x}$ for In(III) and Tl(III) and $K_{ext\_IP^+\ Tl(I)} \cdot K_{Tl(I)} \cdot [Hbet^+]^{y-1+x}_{aq}$ for Tl(I).

4.2.5.3 Cation Exchange

The mathematical model for metal extraction through the cation exchange mechanism is shown below. It was assumed that the extraction occurs after the reaction in Eq. 60 is completed, and the positively charged trivalent indium or thallium cations or halo complexes are exchanged with the betainium cation from the ionic liquid.

$$ML_y(bet)_x{}^{3-y}_{aq} + (3-y)[Hbet^+]_{org} \rightleftarrows ML_y(bet)_x{}^{3-y}_{org} + (3-y)[Hbet^+]_{aq} \quad \text{Eq. 74}$$

The value of y is limited to $0 \leq y \leq 2$ since the halide complexes must be positively charged and x is limited to $0 \leq x \leq 6$ (see section 4.2.5.1 for details). The corresponding

extraction constants for In(III) and Tl(III), after taking into account the equilibrium constant of the reactions in Eq. 61, are:

$$K_{ext\_CE\ M(III)} = \frac{[ML_y(bet)_x{}^{3-y}]_{org} \cdot [Hbet^+]^{3-y-x}{}_{aq} \cdot (a_{H^+})^x{}_{aq}}{K_{M(III)} \cdot [ML_y{}^{3-y}]_{aq}} \quad \text{Eq. 75}$$

Assuming the complex formation reaction in Eq. 65 is completed, the extraction of monovalent thallium through cation exchange mechanism can be expressed as:

$$Tl(bet)_x{}^+{}_{aq} + [Hbet^+]_{org} \rightleftarrows Tl(bet)_x{}^+{}_{org} + [Hbet^+]_{aq} \quad \text{Eq. 76}$$

where $0 \leq x \leq 4$ (see section 4.2.5.1 for details). The corresponding equilibrium constant of extraction is written as follows:

$$K_{ext\_CE\ Tl(I)} = \frac{[Tl(bet)_x{}^+]_{org} \cdot [Hbet^+]^{1-x}{}_{aq} \cdot (a_{H^+})^x{}_{aq}}{K_{Tl(I)} \cdot [Tl^+]_{aq}} \quad \text{Eq. 77.}$$

The logarithmic forms of the equations for In(III) and Tl(III) (Eq. 74) and for Tl(I) (Eq. 77) are identical to Eq. 69, but the value C_{ext_CE} for In(III) and Tl(III) in this model is equal to $K_{ext\_CE\ M(III)} \cdot K_{Tl(III)} / [Hbet^+]^{3-y-x}{}_{aq}$ and for Tl(I) is equal to $K_{ext\_CE\ Tl(I)} \cdot K_{Tl(I)} / [Hbet^+]^{1-x}{}_{aq}$.

4.2.5.4 Anion Exchange

The anion exchange mechanism can possibly occur between anionic metal complexes and the IL's anion. The following equation shows the extraction of In(III) and Tl(III) through anion exchange, after the reaction in Eq. 60 is complete:

$$ML_y(bet)_x{}^{3-y}{}_{aq} + (y-3)[Tf_2N^-]_{org} \rightleftarrows ML_y(bet)_x{}^{3-y}{}_{org} + (y-3)[Tf_2N^-]_{aq} \quad \text{Eq. 78}$$

Since the halide complexes must be negatively charged, the value of y is limited to $4 \leq y \leq 6$ and $0 \leq x \leq 2$ (see Sec. 4.2.5.2 for details). Taking into account the equilibrium reaction in Eq. 62, the extraction constant for anion exchange in the reaction above can be written:

$$K_{ext\_AE\ M(III)} = \frac{\left[ML_y(bet)_x{}^{3-y}\right]_{org} \cdot [Tf_2N^-]^{y-3}{}_{aq} \cdot (a_{H^+})^x{}_{aq}}{K_{M(III)} \cdot \left[ML_y{}^{3-y}\right]_{aq} \cdot [Hbet^+]^x{}_{aq}} \quad \text{Eq. 79}$$

For monovalent thallium, the following equation describes the extraction through the anion exchange mechanism, after completion of the reaction in Eq. 65:

$$TlL_y(bet)_x{}^{1-y}{}_{aq} + (y-1)[Tf_2N^-]_{org} \rightleftarrows TlL_y(bet)_x{}^{1-y}{}_{org} + (y-1)[Tf_2N^-]_{aq} \quad \text{Eq. 80}$$

where $2 \leq y \leq 4$ since the halide complexes must be negatively charged and $0 \leq x \leq 2$ (see Sec. 4.2.5.1 for details).

The equilibrium constant of extraction can be written as:

$$K_{ext\_AE\ Tl(I)} = \frac{\left[TlL_y(bet)_x{}^{1-y}\right]_{org} \cdot [Tf_2N^-]^{y-1}{}_{aq} \cdot (a_{H^+})^x{}_{aq}}{K_{Tl(I)} \cdot [Tl^+]_{aq} \cdot [Hbet^+]^x{}_{aq}} \quad \text{Eq. 81.}$$

The logarithmic forms of Eq. 79 and 81 are identical to Eq. 68, but the value of C_{ext_AE} for In(III) and Tl(III) is equal to $K_{ext\_AE\ M(III)} \cdot K_{Tl(III)} \cdot [Hbet^+]^x{}_{aq} / [Tf_2N^-]^{y-3}{}_{aq}$ and for Tl(I) is equal to $K_{ext\_CE\ [Tl(I)]} \cdot K_{Tl(I)} \cdot [Hbet^+]^x{}_{aq} / [Tf_2N^-]^{y-1}{}_{aq}$.

4.2.5.5 Comparison of the Proposed Mechanisms

The plots of *D* values as a function of aqueous phase acidity (see section 4.2.4) were reconstructed to satisfy the linear equation for all mechanisms based on Eq. 69. The logarithmic values of the distribution ratio were plotted as a function of logarithmic

proton activity. The slopes of these plots, denoted as *x* in the linear equation for all four proposed mechanisms based on Eq. 69, indicate the number of betaine molecules coordinated in the extracted complex. This information was used to determine the most likely extraction pathways for In(III) and Tl(I, III) among all possible mechanisms. All of the data were analyzed in $\lim_{[H^+]\to 0} \log D$, namely $[H^+] = 10^{-10}$ M, which practically represents the absence of acid in the aqueous phase.

The intercepts of the linear functions (for example, Eq. 69) must be analyzed because they are considered as functions of the equilibrium constants of extraction: $K_{ext\_IP^-}$, $K_{ext\_IP^+}$, K_{ext_CE}, and K_{ext_AE}. The equilibrium constants of complex formation $K_{[In(III),\ Tl(III)]}$ and $K_{Tl(I)}$ are also part of the same function and are unknown. Therefore, these models mostly can estimate only the value of $K_{ext} \cdot K$, except in some cases when the values of the slopes are negligible. In these cases, the extracted metal complex does not contain betaine and the reactions shown in Eqs. 60 and 65 do not occur. As a result, the constants $K_{[In(III),\ Tl(III)]}$ and $K_{Tl(I)}$ are no longer relevant and the value of K_{ext} can be obtained.

The concentrations of $[Hbet^+]_{eq}$ and $[Tf_2N^-]_{eq}$ are required to calculate the intercept *C* ($[H^+]_{eq} = 10^{-10}$ M). These values were estimated based on the results of solubility of [Hbet][Tf_2N] in the aqueous phase (see Appendix A for the values) reported in Chapter 3.

All the analysis for the dominant extraction mechanism was done through several steps. First, the known metal speciation in the acid region of interest was evaluated. Then,

according to the calculations of $K_{ext} \cdot K$ (where K_{ext} represents the extraction constant of a particular mechanism and K is the formation constant of the extractable metal complex), the largest possible value of the product was chosen. To determine the extraction pathway, these two factors were taken into account, provided that the result is consistent with the known chemistry of In(III) and Tl(I, III).

The plot of the logarithm values of $D_{In(III)}$ as a linear function of the logarithm of the hydrogen ion activity (a_{H^+}) is shown in Figure 33. The slopes at low proton activities ($\log a_{H^+} < -1$) in the absence and presence of betaine are –5.8 ± 1.2 and –3.04 ± 0.14, respectively. At higher proton activities, the slopes in both chemical systems are negligible and should be considered equal to zero.

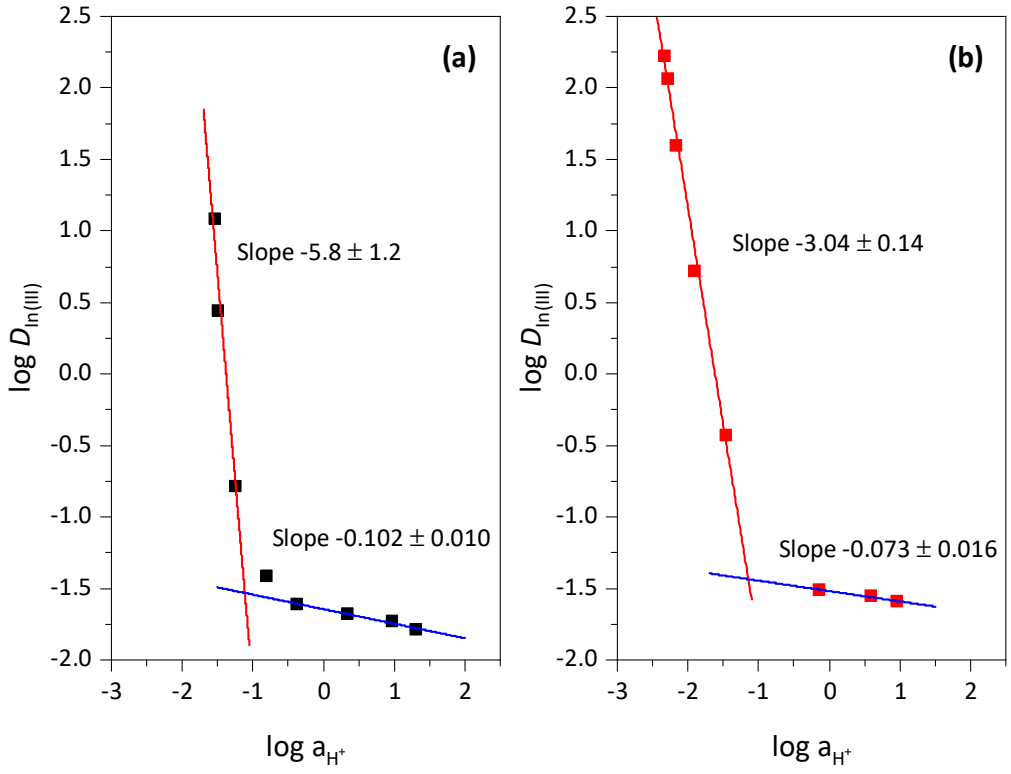

Figure 33. The plot of log $D_{In(III)}$ values as a function of log a_{H^+}. **(a)** The chemical system does not contain additional bet. **(b)** The chemical system contains 15% (w/v) bet. For simplicity, the uncertainties are not shown on the plots. The lines are the results of linear fitting according to Eq. 69.

Having obtained the slopes, the values of $K_{ext\ In(III)} \cdot K_{In(III)}$ were calculated for all four mechanisms. Unfortunately, these values at lower acidity (the region where $\log a_{H^+} < -1$) have relative uncertainties greater than 100%. Due to this reason, it was not possible to make any inference about the mechanism based on these results.

At higher acidity where the slopes approach zero, betaine does not participate in the formation of the metal complexes. Therefore, $K_{In(III)}$ values were irrelevant and the equilibrium constant of extraction, $K_{ext\ In}$, were calculated for all four mechanisms. The

$K_{ext\ In(III)}$ values for ion pair formation mechanism with [Tf_2N^-] and [$Hbet^+$] are shown in Table 8 and for cation and anion exchange mechanisms are shown in Table 9.

Table 8. The estimated values of $K_{ext\ In(III)}$ for ion pair formation mechanisms. The slopes in the absence and presence of 15% (w/v) bet are –0.102 ± 0.010 and –0.073 ± 0.016, respectively.

$K_{ext\_IP^-}$ In			$K_{ext\_IP^+}$ In		
Species	**Absence of betaine**	**15% (w/v) betaine**	**Species**	**Absence of betaine**	**15% (w/v) betaine**
$InCl_2^+$	1.05 ± 0.24	0.68 ± 0.26	$InCl_4^-$	1.08 ± 0.27	0.61 ± 0.24

Table 9. The estimated values of $K_{ext\ In(III)}$ for ion exchange mechanisms. The slopes in the absence and presence of 15% (w/v) bet are –0.102 ± 0.010 and –0.073 ± 0.016, respectively.

$K_{ext\_CE\ In(III)}$			$K_{ext\_AE\ In(III)}$		
Species	**Absence of betaine**	**15% (w/v) betaine**	**Species**	**Absence of betaine**	**15% (w/v) betaine**
$InCl_2^+$	$(6.8 \pm 1.7) \cdot 10^{-2}$	$(5.1 \pm 2.0) \cdot 10^{-2}$	$InCl_4^-$	$(7.0 \pm 1.6) \cdot 10^{-2}$	$(4.6 \pm 1.7) \cdot 10^{-2}$

In the acid region where the $K_{ext\ In(III)}$ values above are calculated, the dominant charged indium species are reported to be $InCl_2^+$ and $InCl_4^-$ [42,43,144]. Based on the $K_{ext\ In(III)}$ values in Table 9, the likelihood of the extraction of $InCl_2^+$ through cation exchange mechanism and $InCl_4^-$ species through anion exchange mechanism is

approximately equal. However, compared to the $K_{ext\ In(III)}$ values for ion pair extraction in Table 8, the values in Table 9 are two orders of magnitude lower. Therefore, ion pair formation is considered as a more likely extraction mechanism for In(III) than exchange reactions.

The data in Table 8 for the ion pair formation mechanism shows that the $K_{ext\_IP^-\ In(III)}$ values are almost the same as $K_{ext\_IP^+\ In(III)}$. However, taking into account the predominant indium species at low acidity (< 0.2 M HCl) is $InCl_2^+$ [43,144], this species is most likely to be extracted through the ion pair mechanism with [Tf_2N^-] anion in this acid region. It was shown previously that the addition of Li[Tf_2N] salt into 0.05 M HCl was able to increase $D_{In(III)}$ values (see section 4.2.3). Since Li^+ ion was not extracted into the organic phase [103,114,124], this can be possible if In(III) was extracted as positively charged complex through the interaction with [Tf_2N^-] anion. Considering that the indium coordination number is 6 [43], the possible extracted complex is [$InCl_2(bet)_4$][Tf_2N]. Meanwhile, $InCl_4^-$ is predominant at higher acidity [43,144]. This leads to the conclusion that this indium species is extracted through ion pair mechanism with [$Hbet^+$] cation at acid concentration above 0.2 M. Although the neutral species $InCl_3$ also exists in the aqueous phase [43], this species is unlikely to be extracted since this chemical system favors the extraction of charged species.

Figure 33b shows that the presence of 15% (w/v) bet at lower proton activities (the region where $\log a_{H^+} < -1$) resulted in the slope being 3.04 ± 0.14. This indicates a lower number of bet molecules in the extracted metal complex compared to the system

without bet added. In all the proposed mathematical models, bet is assumed to be a monodentate ligand. Based on the value of the slope, it is possible that bet binds with indium as a bidentate ligand. For carboxylate compounds, this type of binding mode is not uncommon. It was reported that these compounds can serve as ionic, monodentate, and bidentate ligand with metal ions [151]. For instance, in a study on crystal structures of uranyl-betaine complexes, it was shown that bet is coordinated to uranyl as bidentate ligand [152]. This possibility is not ruled out in this case, but further study would be needed to clarify this hypothesis. Alternatively, lower amounts of bet could also indicate increasing amount of water molecules in the metal coordination sphere which is known to occur [43,153]. However, the proposed mathematical models do not take the presence of water into account.

The plot of the logarithm values of the distribution ratio as a function of the logarithm of the hydrogen ion activity (a_{H^+}) for Tl(III) is shown in Figure 34. The two-panel figure shows the system without and with betaine added (Figure 34a and 34b, respectively). In each corresponding acid region in both systems, the values of the slope are comparable. This means that the extracted complexes are the same regardless of the addition of bet.

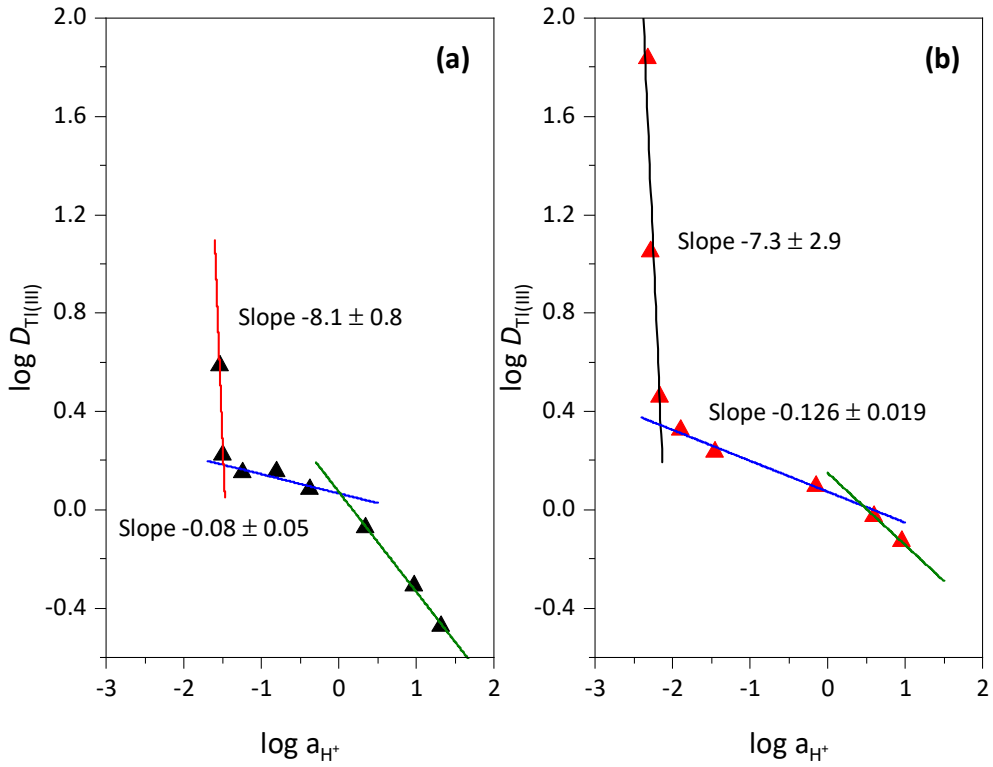

Figure 34**.** The plot of log $D_{Tl(III)}$ values as a function of log a_{H^+}. **(a)** The chemical system does not contain additional bet. **(b)** The chemical system contains 15% (w/v) bet. Thallium was oxidized using Cl_2 water. For clarity, the uncertainties are not shown on the plots. The lines are the results of linear fitting according to Eq. 69.

The calculated $K_{ext\ Tl(III)} \cdot K_{Tl(III)}$ values in the acid ranges where the slopes are -8.1 ± 0.8 and -7.3 ± 2.9 have relative uncertainties close to, and in some cases greater than, 100%. Therefore, these data were not considered in defining the extraction mechanism. Meanwhile, at higher acidity the slopes are -0.08 ± 0.05 and -0.126 ± 0.019 and should be considered zero. Consequently, the parameter $K_{Tl(III)}$ is no longer relevant and $K_{ext\ Tl(III)}$ can be estimated.

Table 10 shows the calculated $K_{ext\ Tl(III)}$ values for ion pair formation with $[Tf_2N^-]$ and $[Hbet^+]$. The results show the values are not significantly different; however, $TlCl_4^-$ is known to be the predominant Tl(III) species in this acid region [144]. Therefore, ion pair formation with $[Hbet^+]$ is a possible extraction mechanism for Tl(III).

Table 10. The estimated values of $K_{ext\ Tl(III)}$ for ion pair formation mechanisms. The slopes in the absence and presence of 15% (w/v) bet are –0.08 ± 0.05 and –0.126 ± 0.019, respectively.

$K_{ext\_IP^-\ Tl(III)}$			$K_{ext\_IP^+Tl(III)}$		
Species	**Absence of betaine**	**15% (w/v) betaine**	**Species**	**Absence of betaine**	**15% (w/v) betaine**
$TlCl_2^+$	30 ± 5	97 ± 40	$TlCl_4^-$	30 ± 6	90 ± 40

In Table 11, the $K_{ext\ Tl(III)}$ values according to ion exchange mechanisms for $TlCl_2^+$ and $TlCl_4^-$ species are reported. Although the $K_{ext\ Tl(III)}$ values for both mechanisms are comparable, the studies on Tl(III) speciation in aqueous HCl show that the formation of positively charged thallium(III) complexes in 0.2 – 1 M HCl is unlikely [144,154]. This rules out the possibility of extraction of $TlCl_2^+$ through the cation exchange mechanism.

Table 11. The estimated values of $K_{ext\ Tl(III)}$ for ion exchange mechanisms. The slopes in the absence and presence of 15% (w/v) bet are –0.08 ± 0.05 and –0.126 ± 0.019, respectively.

$K_{ext\_CE\ Tl(III)}$			$K_{ext\_AE\ Tl(III)}$		
Species	**Absence of betaine**	**15% (w/v) betaine**	**Species**	**Absence of betaine**	**15% (w/v) betaine**
$TlCl_2^+$	2.0 ± 0.4	7 ± 3	$TlCl_4^-$	2.0 ± 0.3	6.4 ± 2.9

Based on the analysis above, there are two possible extraction pathways for $TlCl_4^-$ species: ion pair formation with [$Hbet^+$] cation and anion exchange with [Tf_2N^-]. However, it can be seen that the $K_{ext\_IP^+\ Tl(III)}$ for $TlCl_4^-$ in Table 10 is higher than the $K_{ext\_AE\ Tl(III)}$ value shown in Table 11. In addition, according to Eq. 77 in the mathematical model for the anion exchange mechanism, higher amounts of [Tf_2N^-] in the aqueous phase would lead to a more efficient extraction of Tl(III). On the other hand, addition of Li[Tf_2N] did not affect Tl(III) extraction yield (see Figure 30 in section 4.2.3). This suggests that [Tf_2N^-] anion does not participate in the extraction in the acid range that was considered. Therefore, it is believed that ion pair formation with [$Hbet^+$] cation is the predominant extraction mechanism for $TlCl_4^-$ species.

The change in the slope at 1 M HCl in Figure 34 must be attributed to formation of a non-extractable $TlCl_5^{2-}$ complex [154]. Meanwhile, at lower acidity range where the slopes are –8.1 ± 0.8 and –7.3 ± 2.9, the predominant Tl(III) species is $TlCl_2^+$ [144]. The value of the slopes indicates that the extracted thallium complex contains betaine

molecules. Unfortunately, no conclusion on the speciation of the extracted complex can be made due to insufficient data and the large uncertainty on the slope.

Figure 35 shows the plot of the logarithm value of $D_{Tl(I)}$ as a function of hydrogen ion activity. The slope analysis shows the values are –0.78 ± 0.07 and –1.20 ± 0.06 at low acidity for the system without and with betaine added, respectively. Meanwhile, at higher acidity, the corresponding slopes in the absence and presence of betaine are –0.274 ± 0.019 and –0.130 ± 0.012.

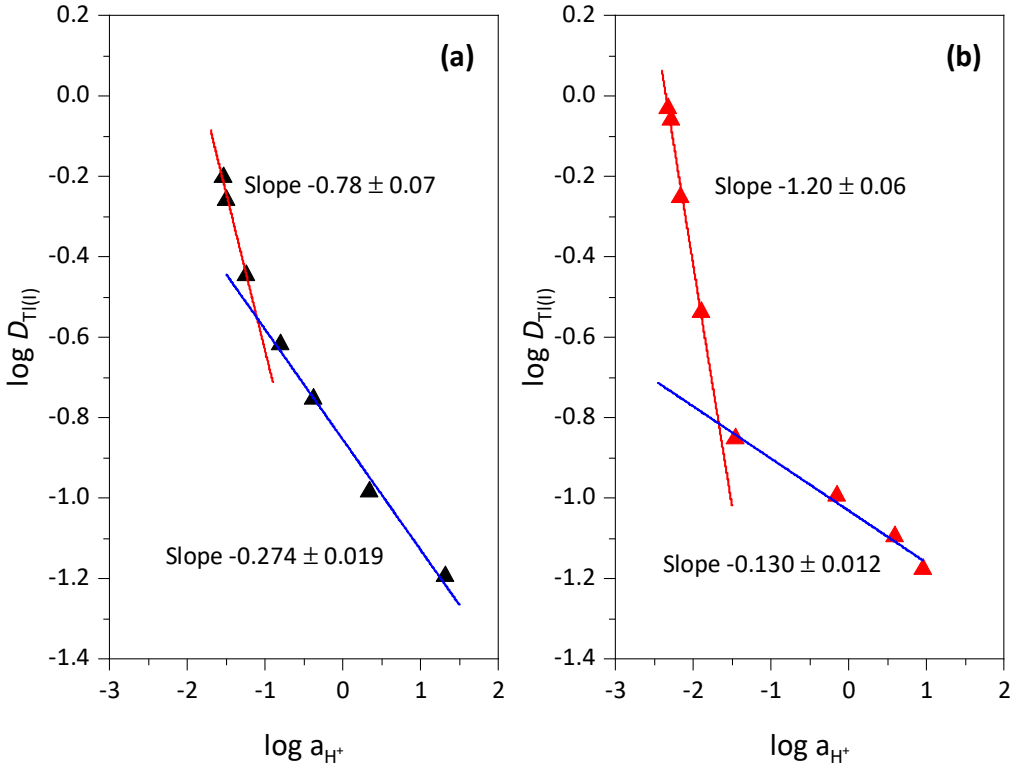

Figure 35. The plot of log $D_{Tl(I)}$ values as a function of log a_{H^+}. (a) The chemical system does not contain additional bet. (b) The chemical system contains 15% (w/v) bet. For clarity, the uncertainties are not shown on the plots. The lines are the results of linear fitting according to Eq. 69.

An attempt to analyze the mechanism of Tl(I) based on the $K_{ext\ Tl(I)} \cdot K_{Tl(I)}$ values was made. Unfortunately, the estimated values for all mechanisms have relative uncertainties more than 100%, except for the cation exchange mechanism at high acidity. The $K_{ext\ Tl(I)}$ values for this mechanism are presented in Table 12.

Table 12. The estimated values of $K_{ext\ Tl(I)}$ for ion exchange mechanism. The corresponding slopes at high acid range are –0.274 ± 0.019 and –0.130 ± 0.012, respectively.

$K_{ext\_CE\ Tl(I)}$		
Species	**Absence of betaine**	**15% (w/v) betaine**
Tl^+	28 ± 13	$(6.2 \pm 1.9) \cdot 10^{-1}$

In the acid range where the slopes are –0.274 ± 0.019 and –0.130 ± 0.012 (high acidity), it was reported that both Tl^+ and $TlCl_2^-$ species are likely to exist [46]. The values in Table 12 show that the extraction of Tl^+ species through the cation exchange mechanism with [$Hbet^+$] is possible. Furthermore, although the $K_{ext\ Tl(I)}$ values for anion exchange mechanism with [Tf_2N^-] cannot be presented, a logical reasoning can be made based on the obtained data. For this mechanism to occur, there must be an exchange reaction between $TlCl_2^-$ species in the aqueous phase with [Tf_2N^-] anion in the organic phase. If this negatively charged Tl(I) species would have been extracted through an anion exchange mechanism, $D_{Tl(I)}$ values would have been increased with increasing HCl concentration (conditions that favor the formation of anionic Tl(I) complexes). However,

the data on Tl(I) extraction as a function of aqueous phase acidity show the opposite trend (see Figure 32b in section 4.2.4). Therefore, based on this result, anion exchange with [Tf_2N^-] anion is not a possible extraction mechanism for Tl(I).

A similar analysis was also be made for ion pair formation mechanism. In this case, Tl^+ and $TlCl_2^-$ can be extracted though ion pair formation with [Tf_2N^-] and [$Hbet^+$], respectively. A previous study showed that Li[Tf_2N] was not extracted into the organic phase [136]. Considering the chemistry of Li^+ and Tl^+ is similar [44], the extraction of Tl[Tf_2N] should not be expected either and ion pair formation with [Tf_2N^-] anion is unlikely. Nevertheless, the possibility of extraction of [$TlCl_2^-$] species through ion pair formation with [$Hbet^+$] cannot be ruled out.

At lower acidity where the slopes are -0.78 ± 0.07 and -1.20 ± 0.06 in Figure 35, Tl^+ is the predominant species in the aqueous phase [46]. Due to this reason, the extraction of $TlCl_2^-$ through anion exchange and ion pair formation with [$Hbet^+$] is not applicable. The extraction of Tl^+ species through cation exchange with [$Hbet^+$] is considered more likely and the extracted complex should be [$Tl(bet)^+$].

4.3 In and Tl Extraction into DL-menthol-based Eutectic Solvent

Eutectic solvents (ESs) have not been studied extensively for metal extraction. Although the preparation of this type of solvent is simple, most of the ESs are water-soluble and therefore, are not suitable for metal partition as it requires two phases that are not miscible. An ES composed of DL-menthol and lauric acid with molar ratio 2:1 is

among the few hydrophobic ESs that are available. As a proof of principle, in this section, the ability of this DL-menthol-based ES to extract In(III) and Tl(I, III) from HCl media is discussed. First, the results of In(III) and Tl(I, III) extraction into DL-menthol-based ES in the absence and presence of an extracting agent called HDEHP are presented. Then, these results are also compared with a classical solvent extraction system composed of kerosene as the organic solvent. To demonstrate the ability of DL-menthol based ES to extract the metal in a sufficient amount of time, the kinetics of Tl(III) extraction was studied. Hereinafter, the DL-menthol and lauric acid ES is simply addressed as "ES-MLA".

4.3.1 In(III) Extraction into DL-menthol and Lauric Acid ES

In this experiment, In(III) was extracted from 0.2 – 10.2 M HCl into ES-MLA in the absence and presence of HDEHP as an extracting agent. The effect of HDEHP on In(III) extraction yield was studied by adding 30 % (v/v) of this compound into the organic phase. The extraction results are shown in Figure 36.

In the whole HCl range that was studied, In(III) was only poorly extracted into pure ES-MLA (Figure 36). Although $D_{In(III)}$ values tend to increase with increasing acid concentration, the values are all below 0.1. Meanwhile, in the presence of HDEHP, an obvious increase in In(III) extraction yield was observed at lower acid concentrations. Below 3 M HCl, $D_{In(III)}$ values increase with decreasing acidity, reaching maximum at 0.2 M HCl with $D_{In(III)} \sim 28$. At higher acid concentrations (above 3 M), In(III) extraction

into ES-MLA containing HDEHP shows a similar trend to the system without HDEHP added and the difference in $D_{In(III)}$ values between the two systems are not significant.

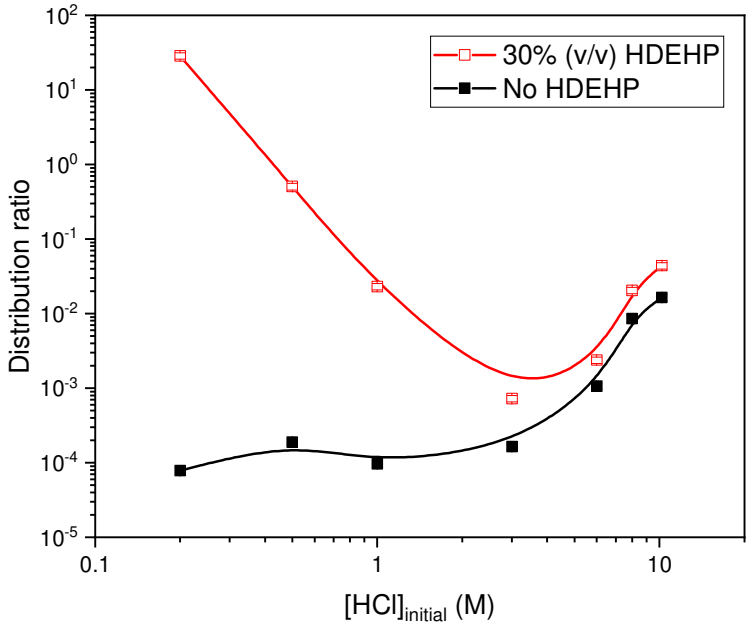

Figure 36. In(III) extraction into ES DL-menthol and lauric acid (2:1 M) in the absence and presence of HDEHP as the extracting agent. The lines are drawn to guide eye. Error bars are smaller than the corresponding symbols.

This finding is evidence that ES-MLA is not an effective extracting solvent for In(III) by itself, particularly in the range of HCl concentrations that was studied. Tereshatov et al. investigated the extraction of this metal into pure ES-MLA also in HCl range 0.1 – 0.001 M [106]. They found that $D_{In(III)}$ values increased with decreasing acidity, with the highest D value approximately 20 at 0.001 M HCl. The authors claimed the carboxylic acid group in the lauric acid component of the ES to be responsible for the extraction of In(III). The extraction mechanism that they proposed requires the

deprotonation of the carboxyl group. Considering the acid dissociation constant (pK_a) of lauric acid is 5.3 [155], it is not surprising that the increase of $D_{In(III)}$ values was observed at very low acid concentration (pH 1 – 3 according to their data). The same explanation applies to In(III) extraction into ES-MLA containing HDEHP. Metal extraction with this compound proceeds through a cation exchange reaction that requires the deprotonation of the acid [107]. The role of HDEHP in the extraction was evident at lower acidity (or higher pH); the pK_a of this compound is 3.24 [96], which means that the degree of acid dissociation is larger as the pH increases and approaches the pK_a value.

Taking into account the speciation of In(III) in aqueous HCl solution [43,107,144], in both chemical systems with and without HDEHP added, most likely In(III) was extracted as a $InCl^{2+}$ or $InCl_2^+$ complex at low acid concentration. The predominant species at higher acid concentration is $InCl_4^-$; however, it is unlikely that this species is extracted as both HDEHP and lauric acid are strongly protonated. Therefore, the extraction of neutral $InCl_3$ species through solvating reactions with HDEHP and/or lauric acid is considered more likely to occur at higher acid concentration.

4.3.2 Tl(I) Extraction into DL-menthol and Lauric Acid ES

The extraction of Tl(I) into ES-MLA is discussed in this section. Shown in Figure 37, the shapes of Tl(I) extraction curves in the system with and without HDEHP added are similar to that of In(III). The results show that, in general, Tl(I) is also poorly extracted into ES-MLA but the extraction yields are better than In(III). For example, the

highest $D_{Tl(I)}$ value extracted into pure ES-MLA is obtained at the most concentrated HCl, and the value is one order of magnitude larger than the $D_{In(III)}$ value (0.36 as opposed to 0.01). In the system with HDEHP added, the increase of $D_{Tl(I)}$ values at lower acidity was also observed but the effect of HDEHP was not significant compared to In(III) extraction. The highest $D_{Tl(I)}$ value in this system is at a level of 0.3 which is obtained at 0.01 M and 10.2 M HCl.

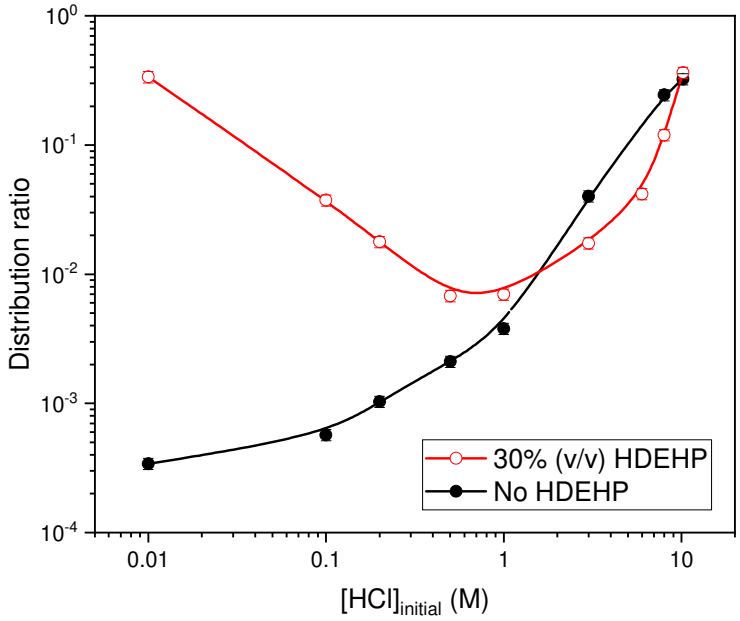

Figure 37. Tl(I) extraction into ES-MLA (2:1 M) in the absence and presence of HDEHP as the extracting agent. The lines are drawn to guide eye.

The similar extraction curves between In(III) and Tl(I) shows that the metal partition between the two immiscible phases occur through the same mechanism. In the case of Tl(I), this means a cation exchange reaction takes place between the predominant

Tl^+ species with the protons from HDEHP and lauric acid at low acid concentrations. Metal extraction with HDEDP through solvation reaction with neutral species at high acidity has been reported [107]. It is likely that the neutral TlCl species is also extracted with HDEHP and lauric acid molecules under the same condition.

4.3.3 Tl(III) Extraction into DL-menthol and Lauric Acid ES

Figure 38 shows the extraction of Tl(III) into ES-MLA in the absence and presence of HDEHP as the extracting agent. The comparison between $D_{Tl(III)}$ values oxidized with Cl_2 water and Br_2 water are shown in panels (a) and (b), respectively. In the system without HDEHP added, indicated by the black color curves in both panels, the $D_{Tl(III)}$ values extracted from 3 M HCl and above are comparable regardless of the oxidizing agent used. Below 3 M HCl, $D_{Tl(III)}$ values with Br_2 water are generally higher compared to the results with Cl_2 water. Overall, it can be seen from the figure that Tl(III) extraction into pure ES-MLA is the best among the three metals of interest, particularly when Br_2 water was used as the oxidizing agent (Figure 38b). Addition of HDEHP was able to improve Tl(III) extraction yields especially when it was oxidized by using Br_2 water. The $D_{Tl(III)}$ values with Cl_2 water in this system at high acid region (3 M HCl and above) are not significantly different compared to the system without HDEHP added.

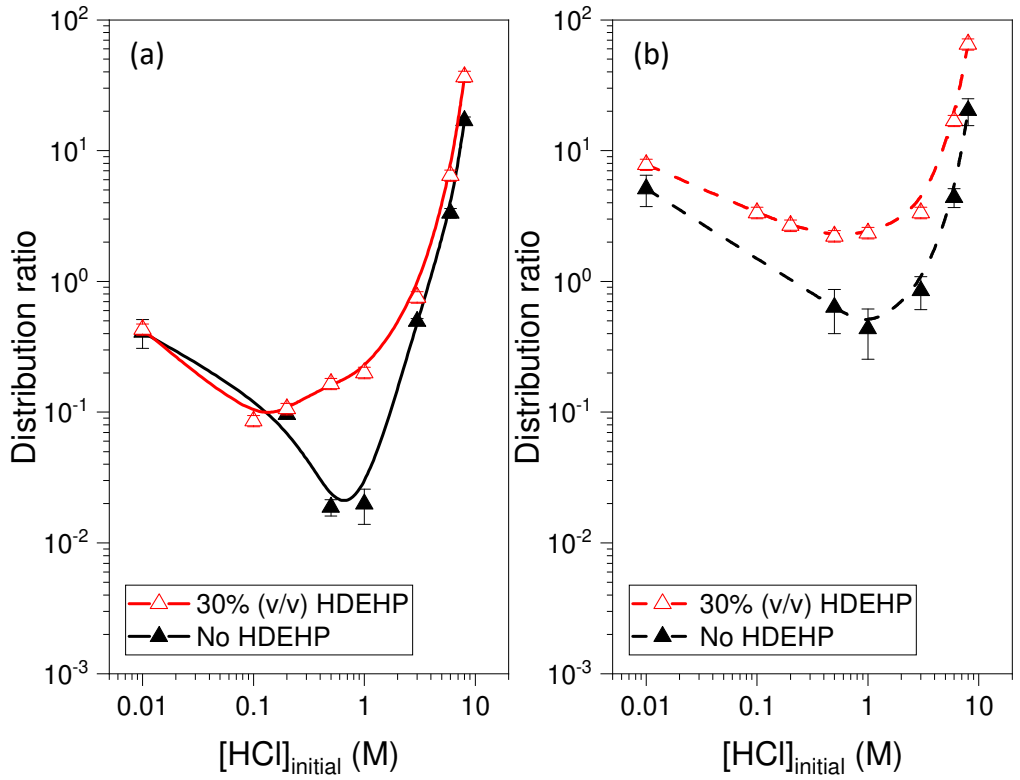

Figure 38. Tl(III) extraction into ES-MLA (2:1 M) in the absence and presence of HDEHP as the extracting agent. Panel (a) shows the results with Cl_2 water as the oxidizing agent and panel (b) shows the results with Br_2 water. The lines are drawn to guide eye.

The higher extraction yield of thallium oxidized with Br_2 water at acid concentrations below 3 M that is seen in Figure 38 may be attributed to the presence of mixed thallium chloro- and bromocomplexes. These complexes are found to have higher stability and hydrophobicity than pure chlorocomplexes that are dominant at high acid concentrations [136,137]. Considering the similarity between Tl(III) extraction curves in Figure 38 with In(III) and Tl(I) in Figure 36 and 37, respectively, it is believed that Tl(III) is also extracted into pure ES-MLA or ES-MLA containing HDEHP through the

same mechanisms. Based on the Tl(III) speciation study, the cationic $TlCl^{2+}$ and $TlCl_2^+$ species are predominant at lower chloride concentrations [144]. These species may be extracted through cation exchange processes with liberated protons from HDEHP and lauric acid at low HCl concentration. Meanwhile, the neutral $TlCl_3$ species is likely to be extracted through a solvation reaction at high acidity.

4.3.4 The Solvent Effect

In a conventional liquid-liquid extraction process, the organic solvent is also commonly called diluent. This is a liquid substance used to dissolve the metal extracting agent. However, it can also interact with the extractant molecules and/or with the extracted metal complex [156]. This interaction can affect the activity of the extracting agent and lower its performance as well as changing the composition of the extracted complex due to coordination and/or substitution of the diluent molecules [156,157]. Among other factors, the polarity or dielectric constant of the diluent plays an important role in the solvent-extractant and solvent-solute interactions [157].

Kerosene is a non-polar organic solvent that is widely used as a diluent for HDEHP in a solvent extraction process. To determine the solvent effect on the extraction of In(III) and Tl(III), the performance of HDEHP as an extractant in ES-MLA is compared with the system consisting of kerosene as a diluent for this extractant. The results are presented in Figure 39.

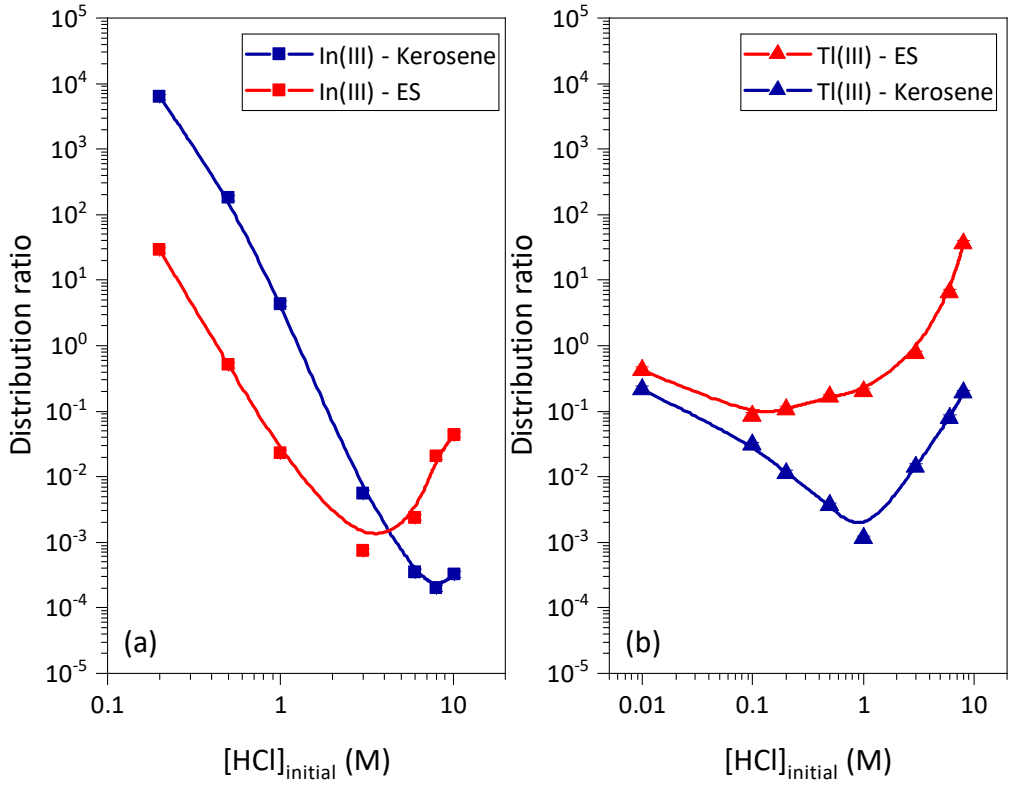

Figure 39. Comparison of $D_{In(III)}$ values and $D_{Tl(III)}$ values extracted into ES-MLA (2:1 M) and into kerosene in the presence of 30% (v/v) HDEHP as the extracting agent. Panel (a) shows the results for In(III) and panel (b) for Tl(III). Thallium was oxidized using Cl_2 water. The lines are drawn to guide eye.

The extraction of In(III) into kerosene containing HDEHP is more effective compared to the system with ES-MLA, especially at 0.2 – 3 M HCl (Figure 39a). In that acidity range, the increase in $D_{In(III)}$ values are almost always two orders of magnitude larger. Interestingly, above 3 M HCl, the trend is the opposite. Meanwhile, for the extraction of Tl(III) where Cl_2 water was used as the oxidizing agent, replacing ES-MLA with kerosene resulted in lower $D_{Tl(III)}$ values in the whole acid range that was studied (from 0.01 – 10.2 M HCl).

The phenomena described in the paragraph above indicate the correlation with the solvent-extractant and solvent-solute interactions mentioned in the literature. In a non-polar solvent such as kerosene, HDEHP is known to exist primarily as a dimer (see for example refs. [156,158,159]). It has the tendency to undergo self-aggregation which results in the formation of reverse micelles with the polar group in the center and non-polar alkyl group in the outer part of the micelle [96]. The aqueous solubility of HDEHP in a non-polar diluent is also known to be extremely low [158], which is an advantage as it prevents the loss of the extractant in the aqueous phase and thus, avoids the reduction of metal extraction efficiency [160]. On the other hand, ES-MLA is comprised of DL-menthol as the hydrogen bond acceptor (HBA) and lauric acid as the hydrogen bond donor (HBD). Both DL-menthol and lauric acid have higher dielectric constants compared to kerosene (4 and 6, respectively as opposed to 1.8 for kerosene) and therefore, are more polar. In addition, the presence of a HBD in a solvent system was found to lower the metal extraction efficiency due to intermolecular interactions with a polar diluent molecule [161]. This may explain the different behavior of In(III) extraction into kerosene and ES-MLA. The extractability of HDEHP in kerosene is higher due to weak interactions between these two compounds; meanwhile the presence of lauric acid as HBD increases an intermolecular interaction which in turn lowers the extraction efficiency of In(III) in the system.

The opposite extraction trend that is observed in Tl(III) extraction into kerosene containing HDEHP is rather unexpected. One possible explanation is the synergistic effect due to the presence of ES-MLA that improves the extractability of HDEHP

compared to in kerosene. In addition, the stability of Tl(III) complexes with HDEHP may be enhanced in the presence of ES-MLA. It is known that higher stability complexation of metal with extractant resulted in higher metal-extractant complex in the aqueous phase [160]. This eventually increases the transfer of metal-extractant complex into the organic phase and results in increasing *D* values of the metal.

4.3.5 Extraction Kinetics

The kinetics of In(III) extraction into ES-MLA has been reported in ref. [106]. It was shown that the extraction equilibrium was reached within 3 min. The results of the kinetics study of Tl(III) extraction into ES-MLA in the absence and presence of HDEHP is shown in Figure 40. Thallium was oxidized by using Cl_2 water and it was extracted from 6 M HCl. The mixing time was varied between 5 s – 20 min. In both systems, with and without HDEHP added, it can be seen that the equilibrium of extraction was achieved within 1 min. Therefore, the 5-min extraction time for this chemical system is adequate to ensure that the reaction for metal partition has completed.

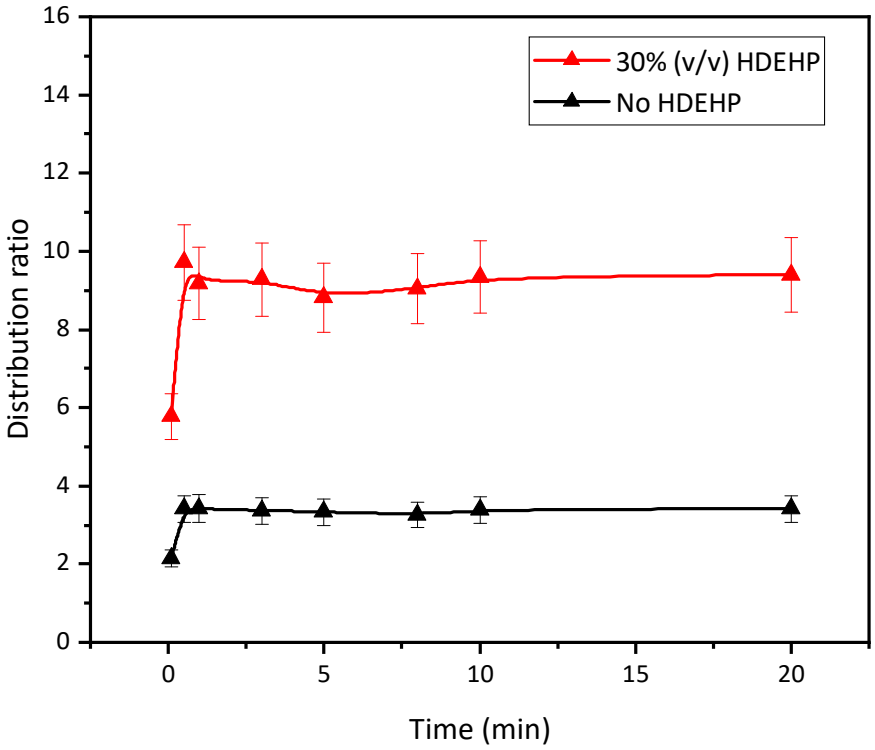

Figure 40. Distribution ratio of Tl(III) as a function of mixing time. Thallium(III) was extracted into ES-MLA (2:1 M) from 6 M HCl in the absence and the presence of HDEHP as an extracting agent. Chlorine water was used as the oxidizing agent. The lines are drawn to guide eye.

5. CONCLUSIONS AND FUTURE WORK

5.1 Conclusions

The partition behaviors of In(III) and Tl(I, III) in several chemical systems have been studied. The metals were extracted from aqueous hydrochloric acid into imidazolium-, pyrrolidinium, and betanium-based ILs, as well as into DL-menthol and lauric acid ES. Several parameters that influence the distribution ratio of the metals have been investigated, including the effect of aqueous phase acidity, extraction kinetics, and concentration of extractants, when applicable. In addition, a study on mutual solubility between betainium-based IL ([Hbet][Tf_2N]) and water was carried out. This study was necessary to understand the chemical interactions between the molecules in the system and to explain In(III) and Tl(I, III) extraction mechanisms into this IL.

The study on mutual solubility between betainium-based IL ([Hbet][Tf_2N]) and water was performed in the presence of acid and zwitterionic betaine (bet) in the aqueous phase. The range of acid concentrations was consistent with that used for metal extraction experiments involving [Hbet][Tf_2N], and 15% (w/v) of bet was added according to the results from the same experiments. It was found that the aqueous solubility of the IL cation increased in the acidic aqueous phase, but the opposite effect was observed on the IL anion. It is believed that cation exchange between the protons from the aqueous phase and [$Hbet^+$] species from the organic phase occurred and caused the increasing of the IL cation solubility. Meanwhile, the lower aqueous [Tf_2N^-] anion concentration in the presence of acid is attributed to the transfer of this anion into the organic phase in the

form of [HTf_2N] acid. Additionally, the transfer of [$Hbet^+$] species into the aqueous phase is likely to be accompanied by the transfer of water molecules. In the presence of both acid and 15% (w/v) bet, the amount of water transferred into the aqueous phase was generally higher compared to the systems containing only acid. It was also interesting to find that bet species were partially distributed between the aqueous and the organic phases. When 15% (w/v) of bet was added into the aqueous phase, the solubility of [Hbet][Tf_2N] notably increased. The value of the conditional solubility product constants (K_{sp}') obtained in this study show that the K_{sp}' in the presence of 15% (w/v) of bet is twice larger than in the system without betaine added.

For metal extraction experiments, the distribution ratio (*D* value) of the metals between the organic and the aqueous phases was used as the main indicator to determine the chemical systems that extract Tl(I) and/or Tl(III) effectively. It was found that Tl(I) was not extracted into imidazolium- and/or pyrrolidinium-based IL ($D_{Tl(I)}$ values were below 1). In the case of Tl(I), the extraction was carried out with several imidazolium-based ILs with different alkyl chain lengths ([$C_n$mim][Tf_2N], n = 2, 4, 8). The results show that, at lower acidities, $D_{Tl(I)}$ values decreased in the order [C_2mim^+]>[C_4mim^+]>[C_8mim^+]. While at higher acidities, $D_{Tl(I)}$ values were approximately the same, regardless of the ILs being used. The opposite trend was observed on Tl(III) extraction; $D_{Tl(III)}$ values increased with increasing alkyl chain length on the IL's cation structure. The IL's anion structure also affected the Tl(III) extractability. Overall, Tl(III) extraction efficiency increased in the order of [C_2mim][Tf_2N] < [C_3C_1pyrr][Tf_2N] < [C_4mim][Tf_2N] < [C_2mim][FSI] <

$[C_3C_1mim][Tf_2N]$ < $[C_8mim][Tf_2N]$. Consistently, the solubility of $[Tf_2N^-]$-based IL in water decreases in the same order. This indicates that IL solubility is one of the determining factors for Tl(III) extraction efficiency into this type of solvent.

The extraction mechanism of the metallic species is strongly influenced by the aqueous phase acidity. For instance, Tl(I) extraction into $[C_nmim][Tf_2N]$ (n = 2, 4, 8) at lower acidity is likely to proceed via cation exchange mechanism between the IL cation and Tl^+ species. Meanwhile, at higher acidity, Tl(I) predominantly exists as $TlCl_2^-$, and this species was most likely extracted through an anion exchange mechanism with an IL anion. Ion pair formation between $TlCl_2^-$ with the IL cation could also occur at higher acidity. In the case of Tl(III), ion pair formation between $TlCl_4^-$ species and the IL cation is found to be the most possible extraction mechanism at low acid concentration. The same extraction mechanism is likely to take place at high acid concentrations, but the extracted species is either $TlCl_5^{2-}$ or the mixture of $TlCl_4^-$ and $TlCl_6^{3-}$.

The results of In(III) and Tl(I, III) extraction into water-saturated $[Hbet][Tf_2N]$ showed that In(III) and Tl(III) were better extracted at low HCl concentrations and in the presence of 15% (w/v) bet. Addition of bet increased the solubility of $[Hbet][Tf_2N]$; consequently, the metal extraction yield (III) increased. The highest $D_{In(III)}$ and $D_{Tl(III)}$ obtained in these experiments were 200 and 70, respectively.

To understand the role of $[Tf_2N^-]$ anions in the In(III) and Tl(III) extraction process into $[Hbet][Tf_2N]$, $Li[Tf_2N]$ salt with different concentrations was added into the aqueous phase. The increased amount of $[Tf_2N^-]$ anion led to higher In(III) extraction

yield, but its effect on Tl(III) was insignificant. These findings suggest that In(III) exists in the aqueous phase as a positively charged complex, while Tl(III) is in negatively charged form. Then, several mathematical models were developed to explain the extraction mechanisms. Considering that In(III) and Tl(I, III) can exist in the form of positively or negatively charged complexes, it is believed that metal extraction can occur through either ion pair formation with [$Hbet^+$] or [Tf_2N^-] in the aqueous phase, or cation exchange with [$Hbet^+$] and anion exchange with [Tf_2N^-] in the organic phase.

All of the mathematical models mentioned above are based on the initial interaction between metal-halide complexes with [$Hbet^+$], which leads to the formation of metal-betaine complexes in the aqueous phase. The number of betaine ligands in the extracted metal complex, as well as the complex structure, was determined using a slope analysis method. Ideally, these mathematical models can also estimate the product of extraction constant and complex formation constant ($K_{ext\_M(III),Tl(I)} \cdot K_{M(III),Tl(I)}$). These values are useful in deciding the predominant extraction mechanism for each metal among all possible options. However, in many cases their values have large uncertainties and thus, were not used as the main determining factor. Therefore, the most possible extraction pathway was chosen based on the combination of three factors: the results from the slope analysis, the value of the extracted constant, and the expected chemical behavior of the metal. On this basis, at low HCl concentrations, In(III) was shown to be extracted mostly as $InCl_2^+$ species through an ion pair formation with [Tf_2N^-], and the extracted complex is [$InCl_2(bet)_4$][Tf_2N]. In the presence of 15% (w/v) bet, the extracted In(III) complex contains approximately three bet molecules. It is likely that, when it is

present in excess, bet binds with In(III) as a bidentate ligand. At high HCl concentrations, In(III) is predominantly extracted as $[InCl_2][Tf_2N]$. Meanwhile, Tl(III) is most likely extracted through ion pair formation with $[Hbet^+]$ as $TlCl_4^-$ species in the entire HCl concentration. It is possible that the extracted complex contains some bet species at low acidity, but the number of betaine ligands cannot be estimated due to insufficient data and the large uncertainty on the slope. In the case of Tl(I), a cation exchange mechanism with $[Hbet^+]$ is shown to be the predominant extraction pathway. The extracted species are $[Tl(bet)^+]$ at acid concentrations below 0.5 M, Tl^+ in the acid range of 0.5 – 5 M, and $TlCl_2^-$ above 5 M HCl. The extraction of $[Hbet][TlCl_2]$ through ion pair formation at high acidity is also possible.

Extraction of In(III) and Tl(I, III) into DL-menthol and lauric acid ES was generally poor. Addition of HDEHP as the extracting agent was able to increase $D_{In(III)}$ values up to five orders of magnitude larger at acid concentrations below 1 M HCl, but it did not have a significant effect at higher acid concentrations. The highest $D_{In(III)}$ value obtained in this chemical system was approximately 28 at 0.2 M HCl. Similarly, increasing of $D_{Tl(I)}$ values in the presence of HDEHP was also observed at lower acidity. The overall $D_{Tl(I)}$ value is considerably low; the maximum value of 0.3 was reached in the presence of HDEHP at 0.01 and 10.2 M HCl. In the case of Tl(III) extraction, both Cl_2 water and Br_2 water were used as an oxidizing agent and the resultant $D_{Tl(III)}$ values were compared. It was found that below 3 M HCl, $D_{Tl(III)}$ values with Br_2 water were better than Cl_2 water. Above this acid concentration, the $D_{Tl(III)}$ values are comparable. Furthermore, the effect of HDEHP addition into the system was not very significant

although improvement of $D_{Tl(III)}$ values was also observed. Interestingly, HDEHP was found to be more effective as an extracting agent for In(III) when it was diluted with kerosene, which is a non-polar solvent, compared to in ES-MLA. However, the solvent effect on Tl(III) was the opposite. Better Tl(III) extraction was obtained when HDEHP was diluted with the ES-MLA.

Based on the known metal speciation in aqueous HCl media and the HDEHP-based extraction mechanism, In(III) and Tl(I, III) are likely to be extracted through a cation exchange mechanism as positively charged $InCl^{2+}$ or $InCl_2^+$, Tl^+, and $TlCl^{2+}$ or $TlCl_2^+$ species at low acid concentrations. Meanwhile, at high acid concentrations, a solvation reaction is likely to occur and the extracted species are $InCl_3$, TlCl, and $TlCl_3$.

From these results, it can be concluded that, among all the chemical systems that have been studied, the extraction systems containing imidazolium-based ionic liquids with a relatively long alkyl chain such as $[C_4mim][Tf_2N]$ are the most promising ones. This imidazolium-based ionic liquid was shown to extract Tl(III) effectively and had a distinct distribution ratio between In(III) and Tl(I, III).

In principle, the results of this study are valuable not only for future nihonium chemistry but also for many other fields. As an example, In-111 and Tl-201 used in this research are both medical radionuclides. The same chemical systems that were studied could potentially be used for separation or purification of these nuclides from unwanted reaction products. Furthermore, indium is one of the key metals listed in critical material reports in Europe and the USA [162,163]. Due to high demand of indium, and the fact that only certain countries produce this metal (China being the largest producer [162]),

there is a high incentive to recover it from secondary raw material [109]. Solvent extraction is one of the techniques used for that purpose [164] and the chemical systems used in this work, in particular betainium-based IL extraction, could be an option for a greener extraction process for indium recovery. Additionally, the knowledge of the mutual solubility of [Hbet][Tf_2N] and water obtained from this study could be implemented in the forward osmosis for seawater desalination where [Hbet][Tf_2N] was used as the "draw" solution in the process [165].

5.2 Future Work

The results from this research have provided valuable information about the chemistry of In(III) and Tl(I, III) in the ionic liquid-based solvent extraction process. However, even though the study of the reaction kinetics in all chemical systems showed that In and Tl extraction was accomplished in less than 1 min, which is potentially fast enough to study Nh chemistry, determining the feasibility of these chemical systems for Nh chemistry study requires more research. For instance, the current chemical system should be modified to be applicable in an online chemistry setup, where the production of the elements and the chemical experiments are carried out together.

Thus, there are several possibilities to extend the current study. One option is to investigate the applicability of the ionic liquid-based chemical system for the online chemical experiment in the liquid phase. The online study of In and Tl extraction into an imidazolium-based ionic liquid has been reported [30], but it does not include the automation of the extraction process. It would be beneficial to repeat the experiment and

automatize the extraction system, for instance by using the well-known fast chemical-separation system for liquid-liquid extraction called SISAK [166], and compare the results between the offline and online experiments. Similar online experiments can also be done with the betainium-based ionic liquid, [Hbet][Tf_2N]. This protic ionic liquid has a different extraction mechanism compared to that of an imidazolium-based ionic liquid, where betaine in the cationic part of the ionic liquid is involved in extracting the metal ion by forming a coordination bond with the metal. In this current study, it was shown that In(III) was extracted into [Hbet][Tf_2N], and the presence of betaine in excess improves the extraction efficiency. Thallium(III) was also extracted, but its extraction yields were lower than In(III). It would be interesting to compare the results of In(III) and Tl(III) extraction and separation in an online chemical experiment with the offline one. In addition, the online chemical system with [Hbet][Tf_2N] can also be extended to studying other SHEs and their homologs, such as the well-studied SHE Rf and its homologs, Zr and Hf, and other SHEs that have been produced in a rather high rate, such as group 5 and group 6 elements.

Some other potential studies could be aimed toward using the ionic liquid for detection of a radionuclide of interest. Recently, a new prototype for alpha spectrometry was developed. The method would allow for direct and selective measurement of the nuclide of interest by grafting a sulfonyl group as an ion exchanger onto the surface of a silicon detector [167]. The cation moieties of [Hbet][Tf_2N] might be a candidate for the grafted functional group. It is a cation exchanger and shows selectivity towards In(III) and Tl(I, III) in a liquid-liquid extraction process. It would be interesting to investigate

whether the same result can be obtained when the cation [Hbet$^+$] is used as the functional group on a detector. The ionic liquid [Hbet][Tf_2N] can also be potentially used in the detection as a cation exchanger by physically attaching the molecules onto the detector surface. A proof-of-principle experiment using polymerized ionic liquid to coat an inner surface of a plastic tube and a tube filled with beads has been reported by Tereshatov et al. [168]. To the extent of the author's knowledge, polymerized [Hbet][Tf_2N] is not available commercially. However, this ionic liquid crystallized after hours or weeks [88] and crystal formation can be prevented by saturating the ionic liquid with water. Tereshatov et al.'s method might be adopted to coat the inner surface of a plastic tube with [Hbet][Tf_2N], then remove the water from the ionic liquid to promote the crystal formation and form a solid layer. However, it might be hard to control the thickness of the layer with this method and there is no guarantee that the crystal properties do not change over time. Then, polymerizing [Hbet][Tf_2N] would be an alternative route in the attempt to solidify the material. Should these experiments work, there are possibilities to use the coated detector for online chemical experiments in both liquid and gas phase chemistry system.

REFERENCES

[1] J. Karol Paul, C. Barber Robert, M. Sherrill Bradley, E. Vardaci, and T. Yamazaki, Discovery of the Element with Atomic Number Z = 118 Completing the 7th Row of the Periodic Table (IUPAC Technical Report), Pure Appl Chem **88**, 155, (2016). DOI:10.1515/pac-2015-0501.

[2] L. Öhrström and J. Reedijk, Names and Symbols of the Elements with Atomic Numbers 113, 115, 117 and 118 (IUPAC Recommendations 2016), Pure Appl Chem **88**, 1225, (2016). DOI:10.1515/pac-2016-0501.

[3] A. A. Andriiko and H.-J. Lunk, The Short Form of Mendeleev's Periodic Table of Chemical Elements: Toolbox for Learning the Basics of Inorganic Chemistry. A Contribution to Celebrate 150 years of the Periodic Table in 2019, ChemTexts **4**, 4, (2018). DOI:10.1007/s40828-018-0059-y.

[4] M. Schadel, Chemistry of the Superheavy Elements, Philos T R Soc A **373**, (2015). DOI:10.1098/rsta.2014.0191.

[5] R.-D. Herzberg, in *The Chemistry of Superheavy Elements*, edited by D. S. Matthias Schädel (Springer, Berlin, Germany, 2014), pp. 83.

[6] C. E. Düllmann, Studying Chemical Properties of the Heaviest Elements: One Atom at a Time, Nuclear Physics News **27**, 14, (2017). DOI:10.1080/10619127.2017.1280333.

[7] Periodic Tables of Elements, (IUPAC) https://iupac.org/what-we-do/periodic-table-of-elements/ (Accessed 20 January 2019).

[8] A. Nasirov, A. Muminov, G. Giardina, and G. Mandaglio, Basic Distinctions between Cold- and Hot-Fusion Reactions in the Synthesis of Superheavy Elements, Physics of Atomic Nuclei **77**, 881, (2014). DOI:10.1134/S1063778814070126.

[9] A. Turler and V. Pershina, Advances in the Production and Chemistry of the Heaviest Elements, Chem Rev **113**, 1237, (2013). DOI:10.1021/cr3002438.

[10] K. J. Moody, in *The Chemistry of Superheavy Elements*, edited by D. S. Matthias Schädel (Springer, Berlin, Germany, 2014), pp. 1.

[11] A. Ghiorso, J. M. Nitschke, J. R. Alonso, C. T. Alonso, M. Nurmia, G. T. Seaborg, E. K. Hulet, and R. W. Lougheed, Element 106, Phys Rev Lett **33**, 1490, (1974). DOI:10.1103/PhysRevLett.33.1490.

[12] Y. T. Oganessian and V. K. Utyonkov, Superheavy Nuclei from Ca-48-Induced Reactions, Nucl Phys A **944**, 62, (2015). DOI:10.1016/j.nuclphysa.2015.07.003.

[13] Y. T. Oganessian, A. G. Demin, A. S. Iljinov, S. P. Tretyakova, A. A. Pleve, Y. E. Penionzhkevich, M. P. Ivanov, and Y. P. Tretyakov, Experiments on the Synthesis of Neutron-Deficient Kurchatovium Isotopes in Reactions Induced by ^{50}Ti Ions, Nucl Phys A **239**, 157, (1975). DOI:10.1016/0375-9474(75)91140-9.

[14] M. G. Itkis, E. Vardaci, I. M. Itkis, G. N. Knyazheva, and E. M. Kozulin, Fusion and Fission of Heavy and Superheavy Nuclei (Experiment), Nucl Phys A **944**, 204, (2015). DOI:10.1016/j.nuclphysa.2015.09.007.

[15] J. S. Thayer, in *Relativistic Methods for Chemists* (Springer, Dordrecht, Netherlands, 2010), pp. 63.

[16] P. Pyykko and J. P. Desclaux, Relativity and the Periodic System of Elements, Accounts Chem Res **12**, 276, (1979). DOI:10.1021/ar50140a002.

[17] D. C. Hoffman and D. M. Lee, Chemistry of the Heaviest Elements - One Atom at a Time, J Chem Educ **76**, 331, (1999). DOI:10.1021/ed076p331.

[18] E. Eliav, S. Fritzsche, and U. Kaldor, Electronic Structure Theory of the Superheavy Elements, Nucl Phys A **944**, 518, (2015). DOI:10.1016/j.nuclphysa.2015.06.017.

[19] Y. T. Oganessian, V. K. Utyonkoy, Y. V. Lobanov, F. S. Abdullin, A. N. Polyakov, I. V. Shirokovsky, Y. S. Tsyganov, G. G. Gulbekian, S. L. Bogomolov, A. N. Mezentsev, S. Iliev, V. G. Subbotin, A. M. Sukhov, A. A. Voinov, G. V. Buklanov, K. Subotic, V. I. Zagrebaev, M. G. Itkis, J. B. Patin, K. J. Moody, J. F. Wild, M. A. Stoyer, N. J. Stoyer, D. A. Shaughnessy, J. M. Kenneally, and R. W. Lougheed, Experiments on the Synthesis of Element 115 in the Reaction ^{243}Am(^{48}Ca,*xn*)$^{291-X}$115, Phys Rev C **69**, 02601, (2004). DOI:10.1103/PhysRevC.69.021601.

[20] K. Morita, K. Morimoto, D. Kaji, T. Akiyama, S. Goto, H. Haba, E. Ideguchi, R. Kanungo, K. Katori, H. Koura, H. Kudo, T. Ohnishi, A. Ozawa, T. Suda, K. Sueki, H. S. Xu, T. Yamaguchi, A. Yoneda, A. Yoshida, and Y. L. Zhao, Experiment on the Synthesis of Element 113 in the Reaction ^{209}Bi(^{70}Zn,n)^{278}113, J Phys Soc Jpn **73**, 2593, (2004). DOI:10.1143/Jpsj.73.2593.

[21] Y. T. Oganessian, V. K. Utyonkov, Y. V. Lobanov, F. S. Abdullin, A. N. Polyakov, R. N. Sagaidak, I. V. Shirokovsky, Y. S. Tsyganov, A. A. Voinov, G. G. Gulbekian, S. L. Bogomolov, B. N. Gikal, A. N. Mezentsev, V. G. Subbotin, A. M. Sukhov, K. Subotic, V. I. Zagrebaev, G. K. Vostokin, M. G. Itkis, R. A. Henderson, J. M. Kenneally, J. H. Landrum, K. J. Moody, D. A. Shaughnessy, M. A. Stoyer, N. J. Stoyer, and P. A. Wilk, Synthesis of the Isotope ^{282}113 in the ^{237}Np+^{48}Ca Fusion Reaction, Phys Rev C **76**, 011601(1, (2007). DOI:10.1103/PhysRevC.76.011601.

[22] Y. T. Oganessian, F. S. Abdullin, P. D. Bailey, D. E. Benker, M. E. Bennett, S. N. Dmitriev, J. G. Ezold, J. H. Hamilton, R. A. Henderson, M. G. Itkis, Y. V. Lobanov, A. N. Mezentsev, K. J. Moody, S. L. Nelson, A. N. Polyakov, C. E. Porter, A. V. Ramayya, F. D. Riley, J. B. Roberto, M. A. Ryabinin, K. P. Rykaczewski, R. N. Sagaidak, D. A. Shaughnessy, I. V. Shirokovsky, M. A. Stoyer, V. G. Subbotin, R. Sudowe, A. M. Sukhov, Y. S. Tsyganov, V. K. Utyonkov, A. A. Voinov, G. K. Vostokin, and P. A. Wilk, Synthesis of a New Element with Atomic Number Z=117, Phys Rev Lett **104**, (2010). DOI:10.1103/PhysRevLett.104.142502.

[23] S. N. Dmitriev, N. V. Aksenov, Y. V. Albin, G. A. Bozhikov, M. L. Chelnokov, V. I. Chepygin, R. Eichler, A. V. Isaev, D. E. Katrasev, V. Y. Lebedev, O. N. Malyshev, O. V. Petrushkin, L. S. Porobanuk, M. A. Ryabinin, A. V. Sabel'nikov, E. A. Sokol, A. V. Svirikhin, G. Y. Starodub, I. Usoltsev, G. K. Vostokin, and A. V. Yeremin, Pioneering Experiments on the Chemical Properties of Element 113, Mendeleev Commun **24**, 253, (2014). DOI:10.1016/j.mencom.2014.09.001.

[24] B. Fricke and J. T. Waber, Theoretical Predictons of Chemistry of Superheavy Elements - Continuation of Periodic Table up to Z = 184, Actin Rev **1**, 433, (1971).

[25] V. Pershina, A Theoretical Study on the Adsorption Behavior of Element 113 and Its Homologue Tl on a Quartz Surface: Relativistic Periodic DFT Calculations, J Phys Chem C **120**, 20232, (2016). DOI:10.1021/acs.jpcc.6b07834.

[26] V. Pershina, J. Anton, and T. Jacob, Electronic Structures and Properties of MAu and MOh, Where M=Tl and Element 113, Chem Phys Lett **480**, 157, (2009). DOI:10.1016/j.cplett.2009.08.069.

[27] V. Pershina, A. Borschevsky, J. Anton, and T. Jacob, Theoretical Predictions of Trends in Spectroscopic Properties of Homonuclear Dimers and Volatility of the 7p Elements, J Chem Phys **132**, 194314, (2010). DOI:10.1063/1.3425996.

[28] N. V. Aksenov, P. Steinegger, F. S. Abdullin, Y. V. Albin, G. A. Bozhikov, V. I. Chepigin, R. Eichler, V. Y. Lebedev, A. S. Madumarov, O. N. Malyshev, O. V.

Petrushkin, A. N. Polyakov, Y. A. Popov, A. V. Sabel'nikov, R. N. Sagaidak, I. V. Shirokovsky, M. V. Shumeiko, G. Y. Starodub, Y. S. Tsyganov, V. K. Utyonkov, A. A. Voinov, G. K. Vostokin, A. V. Yeremin, and S. N. Dmitriev, On the Volatility of Nihonium (Nh, Z = 113), Eur Phys J A **53**, 158, (2017). DOI:10.1140/epja/i2017-12348-8.

[29] L. Lens, A. Yakushev, C. E. Düllmann, M. Asai, J. Ballof, M. Block, M. David Helena, J. Despotopulos, A. Di Nitto, K. Eberhardt, J. Even, M. Götz, S. Götz, H. Haba, L. Harkness-Brennan, P. Heßberger Fritz, D. Herzberg Rodi, J. Hoffmann, A. Hübner, E. Jäger, D. Judson, J. Khuyagbaatar, B. Kindler, Y. Komori, J. Konki, V. Kratz Jens, J. Krier, N. Kurz, M. Laatiaoui, S. Lahiri, B. Lommel, M. Maiti, K. Mistry Andrew, C. Mokry, K. Moody, Y. Nagame, P. Omtvedt Jon, P. Papadakis, V. Pershina, J. Runke, M. Schädel, P. Scharrer, T. Sato, D. Shaughnessy, B. Schausten, P. Thörle-Pospiech, N. Trautmann, K. Tsukada, J. Uusitalo, A. Ward, M. Wegrzecki, N. Wiehl, and V. Yakusheva, Online Chemical Adsorption Studies of Hg, Tl, and Pb on SiO_2 and Au Surfaces in Preparation for Chemical Investigations on Cn, Nh, and Fl at Tasca, Radiochim Acta **106**, 949, (2018). DOI:10.1515/ract-2017-2914.

[30] K. Cubova, M. Semelova, M. Nemec, J. John, J. Milacic, J. P. Omtvedt, and J. Stursa, Extraction of Thallium and Indium Isotopes as the Homologues of Nihonium into the Ionic Liquids, J Radioanal Nucl Ch **318**, 2455, (2018). DOI:10.1007/s10967-018-6270-x.

[31] M. Schädel, Chemistry of Superheavy Elements, Radiochim Acta **100**, 579, (2012). DOI:10.1524/ract.2012.1965.

[32] R. Sudowe, M. G. Calvert, C. E. Dullmann, L. M. Farina, C. M. Folden III, K. E. Gregorich, S. E. H. Gallaher, D. C. Hoffman, S. L. Nelson, D. C. Phillips, J. M. Schwantes, R. E. Wilson, P. M. Zielinski, and H. Nitsche, Extraction of Short-Lived Zirconium and Hafnium Isotopes Using Crown Ethers: A Model System for the Study of Rutherfordium, Radiochim Acta **94**, 123, (2006). DOI:10.1524/ract.2006.94.3.123.

[33] C. Le Naour, D. C. Hoffman, and D. Trubert, in *The Chemistry of Superheavy Elements*, edited by M. Schädel, and D. A. Shaughnessy (Springer, Berlin, Heidelberg, Germany, 2014), pp. 241.

[34] I. Zvára, *The Inorganic Radiochemistry of Heavy Elements* (Springer, Dordrecht, Netherlands, 2008).

[35] Y. Nagame, J. V. Kratz, and M. Schadel, Chemical Studies of Elements with Z >= 104 in Liquid Phase, Nucl Phys A **944**, 614, (2015). DOI:10.1016/j.nuclphysa.2015.07.013.

[36] J. V. Kratz and Y. Nagame, (Springer, Berlin, Heidelberg, Germany, 2013).

[37] M. Schädel, Aqueous Chemistry of Transactinides, Radiochim Acta **89**, 721, (2001). DOI:10.1524/ract.2001.89.11-12.721.

[38] A. Turler and K. E. Gregorich, in *The Chemistry of Superheavy Elements*, edited by M. Schädel, and D. A. Shaughnessy (Springer, Berlin, Heidelberg, Germany, 2014), pp. 261.

[39] A. Türler, R. Eichler, and A. Yakushev, Chemical Studies of Elements with $Z \geqslant 104$ in Gas Phase, Nucl Phys A **944**, 640, (2015). DOI:10.1016/j.nuclphysa.2015.09.012.

[40] *The Group 13 Metals Aluminium, Gallium, Indium and Thallium: Chemical Patterns and Peculiarities* (John Wiley & Sons, Ltd, Chichester, West Sussex, United Kingdom, 2011).

[41] A. E. Martell and R. D. Hancock, *Metal Complexes in Aqueous Solutions* (Springer US, 1996), 1st edn., Modern Inorganic Chemistry.

[42] T. Jarv, J. T. Bulmer, and D. E. Irish, An Investigation of the Digitized Raman Band Profiles of Aqueous Indium(III) Chloride Solutions, J Phys Chem-US **81**, 649, (1977). DOI:10.1021/j100522a012.

[43] C. Deferm, B. Onghena, T. V. Hoogerstraete, D. Banerjee, J. Luyten, H. Oosterhof, J. Fransaer, and K. Binnemans, Speciation of Indium(III) Chloro Complexes in the Solvent Extraction Process from Chloride Aqueous Solutions to Ionic Liquids, Dalton T **46**, 4412, (2017).

[44] N. N. Greenwood and A. Earnshaw, in *Chemistry of the Elements* (Butterworth-Heinemann, Burlington, MA, 1997), pp. 216.

[45] A. G. Lee, The Coordination Chemistry of Thallium(I), Coordin Chem Rev **8**, 289, (1972). DOI:10.1016/S0010-8545(00)80001-6.

[46] A. J. Read and L. P. Aldridge, Thallous Chloride Complexes in 0 to 6 Molal Sodium Chloride at 25 ^{O}C, J Solution Chem **21**, 1231, (1992). DOI:10.1007/Bf00667219.

[47] Y. Marcus, in *Solvent Extraction Principles and Practice, Revised and Expanded*, edited by J. Rydberg (CRC Press, New York, 2004), pp. 27

[48] J. Rydberg, G. R. Choppin, C. Musikas, and T. Sekine, in *Solvent Extraction Principles and Practice, Revised and Expanded*, edited by J. Rydberg (CRC Press, New York, 2004), pp. 109.

[49] Y. Marcus, *The Properties of Solvents* (Wiley, Chichester ; New York, 1998), Wiley Series in Solution Chemistry: V. 4.

[50] J. A. Riddick, W. B. Bunger, T. Sakano, and A. Weissberger, *Organic Solvents : Physical Properties and Methods of Purification.* (Wiley, New York, 1986), 4th edn., Techniques of Chemistry: V. 2.

[51] M. Cox and J. Rydberg, in *Solvent Extraction Principles and Practice, Revised and Expanded*, edited by J. Rydberg (CRC Press, New York, 2004), pp. 1.

[52] P. Anastas and N. Eghbali, Green Chemistry: Principles and Practice, Chem Soc Rev **39**, 301, (2010). DOI:10.1039/b918763b.

[53] P. T. Anastas and J. C. Warner, *Green Chemistry : Theory and Practice* (Oxford University Press, Oxford, 1998).

[54] M. L. Dietz, Ionic Liquids as Extraction Solvents: Where Do We Stand?, Sep Sci Technol **41**, 2047, (2006). DOI:10.1080/01496390600743144.

[55] S. Aparicio, M. Atilhan, and F. Karadas, Thermophysical Properties of Pure Ionic Liquids: Review of Present Situation, Ind Eng Chem Res **49**, 9580, (2010). DOI:10.1021/ie101441s.

[56] H. L. Ngo, K. LeCompte, L. Hargens, and A. B. McEwen, Thermal Properties of Imidazolium Ionic Liquids, Thermochim Acta **357**, 97, (2000). DOI:10.1016/S0040-6031(00)00373-7.

[57] S. L. I. Toh, J. McFarlane, C. Tsouris, D. W. DePaoli, H. Luo, and S. Dai, Room-Temperature Ionic Liquids in Liquid-Liquid Extraction: Effects of Solubility in Aqueous Solutions on Surface Properties, Solvent Extr Ion Exc **24**, 33, (2006). DOI:10.1080/07366290500388400.

[58] M. G. Freire, L. M. N. B. F. Santos, A. M. Fernandes, J. A. P. Coutinho, and I. M. Marrucho, An Overview of the Mutual Solubilities of Water-Imidazolium-Based Ionic Liquids Systems, Fluid Phase Equilibr **261**, 449, (2007). DOI:10.1016/j.fluid.2007.07.033.

[59] W. Kunz and K. Häckl, The Hype with Ionic Liquids as Solvents, Chem Phys Lett **661**, 6, (2016). DOI:10.1016/j.cplett.2016.07.044.

[60] T. Welton, Room-Temperature Ionic Liquids. Solvents for Synthesis and Catalysis, Chem Rev **99**, 2071, (1999). DOI:10.1021/cr980032t.

[61] C. Chiappe and D. Pieraccini, Ionic Liquids: Solvent Properties and Organic Reactivity, J Phys Org Chem **18**, 275, (2005). DOI:10.1002/poc.863.

[62] M. E. Bluhm, M. G. Bradley, R. Butterick, U. Kusari, and L. G. Sneddon, Amineborane-Based Chemical Hydrogen Storage: Enhanced Ammonia Borane Dehydrogenation in Ionic Liquids, J Am Chem Soc **128**, 7748, (2006). DOI:10.1021/ja062085v.

[63] J. Rani and S. Anju Sablok, Preparation and Applications of Room Temperature Ionic Liquids in Organic Synthesis: A Review on Recent Efforts, Curr Green Chem **2**, 135, (2015). DOI:10.2174/2213346101666140915212515.

[64] C. M. Gordon, New Developments in Catalysis Using Ionic Liquids, Appl Catal A-Gen **222**, 101, (2001). DOI:10.1016/S0926-860X(01)00834-1.

[65] P. Wasserscheid and W. Keim, Ionic Liquids—New "Solutions" for Transition Metal Catalysis, Angew Chem Int Edit **39**, 3772, (2000). DOI:10.1002/1521-3773(20001103)39:21<3772::AID-ANIE3772>3.0.CO;2-5.

[66] R. Ratti, Ionic Liquids: Synthesis and Applications in Catalysis, Adv Chem **2014**, 16, 729842 (2014). DOI:10.1155/2014/729842.

[67] M. R. Ganjali, H. Khoshsafar, A. Shirzadmehi, M. Javanbakht, and F. Faridbod, Improvement of Carbon Paste Ion Selective Electrode Response by Using Room Temperature Ionic Liquids (RTILs) and Multi-Walled Carbon Nanotubes (MWCNTs), Int J Electrochem Sc **4**, 435, (2009). DOI:10.1002/elan.200904642.

[68] C. Lagrost, D. Carrié, M. Vaultier, and P. Hapiot, Reactivities of Some Electrogenerated Organic Cation Radicals in Room-Temperature Ionic Liquids: Toward an Alternative to Volatile Organic Solvents?, J Phys Chem A **107**, 745, (2003). DOI:10.1021/jp026907w.

[69] O. Brummel, F. Faisal, T. Bauer, K. Pohako-Esko, P. Wasserscheid, and J. Libuda, Ionic Liquid-Modified Electrocatalysts: The Interaction of $[C_1C_2im][Otf]$ with Pt(111) and Its Influence on Methanol Oxidation Studied by Electrochemical Ir Spectroscopy, Electrochim Acta **188**, 825, (2016). DOI:10.1016/j.electacta.2015.12.006.

[70] J.-P. T. Mikkola, P. P. Virtanen, K. Kordás, H. Karhu, and T. O. Salmi, SILCA—Supported Ionic Liquid Catalysts for Fine Chemicals, Appl Catal A-Gen **328**, 68, (2007). DOI:10.1016/j.apcata.2007.05.030.

[71] S. Mehl, A. Toghan, T. Bauer, O. Brummel, N. Taccardi, P. Wasserscheid, and J. Libuda, Pd Nanoparticle Formation in Ionic Liquid Thin Films Monitored by in Situ Vibrational Spectroscopy, Langmuir **31**, 12126, (2015). DOI:10.1021/acs.langmuir.5b03386.

[72] K. D. Clark, M. N. Emaus, M. Varona, A. N. Bowers, and J. L. Anderson, Ionic Liquids: Solvents and Sorbents in Sample Preparation, J Sep Sci **41**, 209, (2018). DOI:10.1002/jssc.201700864.

[73] S. P. M. Ventura, F. A. e Silva, M. V. Quental, D. Mondal, M. G. Freire, and J. A. P. Coutinho, Ionic-Liquid-Mediated Extraction and Separation Processes for Bioactive Compounds: Past, Present, and Future Trends, Chem Rev **117**, 6984, (2017). DOI:10.1021/acs.chemrev.6b00550.

[74] P. K. Mohapatra, Actinide Ion Extraction Using Room Temperature Ionic Liquids: Opportunities and Challenges for Nuclear Fuel Cycle Applications, Dalton T **46**, 1730, (2017). DOI:10.1039/C6DT04898F.

[75] V. N. Emel'yanenko, G. Boeck, S. P. Verevkin, and R. Ludwig, Volatile Times for the Very First Ionic Liquid: Understanding the Vapor Pressures and Enthalpies of Vaporization of Ethylammonium Nitrate, Chem-Eur J **20**, 11640, (2014). DOI:10.1002/chem.201403508.

[76] R. Hayes, G. G. Warr, and R. Atkin, Structure and Nanostructure in Ionic Liquids, Chem Rev **115**, 6357, (2015). DOI:10.1021/cr500411q.

[77] B. Wang, L. Qin, T. Mu, Z. Xue, and G. Gao, Are Ionic Liquids Chemically Stable?, Chem Rev **117**, 7113, (2017). DOI:10.1021/acs.chemrev.6b00594.

[78] F. H. Hurley and T. P. W. Jr., The Electrodeposition of Aluminum from Nonaqueous Solutions at Room Temperature, J Electrochem Soc **98**, 207, (1952). DOI:10.1149/1.2778133.

[79] M. V. Fedorov and A. A. Kornyshev, Ionic Liquids at Electrified Interfaces, Chem Rev **114**, 2978, (2014). DOI:10.1021/cr400374x.

[80] J. S. Wilkes and M. J. Zaworotko, Air and Water Stable 1-Ethyl-3-Methylimidazolium Based Ionic Liquids, J Chem Soc Chem Comm, 965, (1992). DOI:10.1039/C39920000965.

[81] C. P. Fredlake, J. M. Crosthwaite, D. G. Hert, S. N. V. K. Aki, and J. F. Brennecke, Thermophysical Properties of Imidazolium-Based Ionic Liquids, J Chem Eng Data **49**, 954, (2004). DOI:10.1021/je034261a.

[82] H. Tokuda, K. Hayamizu, K. Ishii, M. A. B. H. Susan, and M. Watanabe, Physicochemical Properties and Structures of Room Temperature Ionic Liquids. 2. Variation of Alkyl Chain Length in Imidazolium Cation, J Phys Chem B **109**, 6103, (2005). DOI:10.1021/jp044626d.

[83] A. V. Blokhin, Y. U. Paulechka, A. A. Strechan, and G. J. Kabo, Physicochemical Properties, Structure, and Conformations of 1-Butyl-3-Methylimidazolium Bis(trifluoromethanesulfonyl)imide [C_4mim]Ntf_2 Ionic Liquid, J Phys Chem B **112**, 4357, (2008). DOI:10.1021/jp710872s.

[84] M. Geppert-Rybczyńska, J. K. Lehmann, and A. Heintz, Physicochemical Properties of Two 1-Alkyl-1-Methylpyrrolidinium Bis[(Trifluoromethyl)Sulfonyl]Imide Ionic Liquids and of Binary Mixtures of 1-Butyl-1-Methylpyrrolidinium Bis[(trifluoromethyl)sulfonyl]imide with Methanol or Acetonitrile, J Chem Thermodyn **71**, 171, (2014). DOI:10.1016/j.jct.2013.12.009.

[85] T. Li, Y. Cui, J. Mathaga, R. Kumar, and D. G. Kuroda, Hydration and Vibrational Dynamics of Betaine (N,N,N-Trimethylglycine), J Chem Phys **142**, (2015). DOI:10.1063/1.4919795.

[86] B. Onghena and K. Binnemans, Recovery of Scandium(Iii) from Aqueous Solutions by Solvent Extraction with the Functionalized Ionic Liquid Betainium Bis(trifluoromethylsulfonyl)imide, Ind Eng Chem Res **54**, 1887, (2015). DOI:10.1021/ie504765v.

[87] T. V. Hoogerstraete, B. Onghena, and K. Binnemans, Homogeneous Liquid-Liquid Extraction of Metal Ions with a Functionalized Ionic Liquid, J Phys Chem Lett **4**, 1659, (2013). DOI:10.1021/jz4005366.

[88] P. Nockemann, B. Thijs, S. Pittois, J. Thoen, C. Glorieux, K. Van Hecke, L. Van Meervelt, B. Kirchner, and K. Binnemans, Task-Specific Ionic Liquid for Solubilizing Metal Oxides, J Phys Chem B **110**, 20978, (2006). DOI:10.1021/jp0642995.

[89] T. V. Hoogerstraete, B. Onghena, and K. Binnemans, Homogeneous Liquid–Liquid Extraction of Rare Earths with the Betaine—Betainium Bis(trifluoromethylsulfonyl)imide Ionic Liquid System, Int J Mol Sci **14**, 21353, (2013). DOI:10.3390/ijms141121353.

[90] S. Ikeda, T. Mori, Y. Ikeda, and K. Takao, Microwave-Assisted Solvent Extraction of Inert Platinum Group Metals from HNO_3(Aq) to Betainium-Based Thermomorphic Ionic Liquid, Acs Sustain Chem Eng **4**, 2459, (2016). DOI:10.1021/acssuschemeng.6b00186.

[91] T. Mori, Y. Ikeda, and K. Takao, Extraction Behavior of U(VI) Using Novel Betainium-Type Ionic Liquids: More Hydrophobic Cations Enhance Extractability, Selectivity, and Recyclability, B Chem Soc Jpn **89**, 1354, (2016). DOI:10.1246/bcsj.20160210.

[92] A. P. Abbott, G. Capper, D. L. Davies, R. K. Rasheed, and V. Tambyrajah, Novel Solvent Properties of Choline Chloride/Urea Mixtures, Chem Commun, 70, (2003). DOI:10.1039/B210714G.

[93] E. L. Smith, A. P. Abbott, and K. S. Ryder, Deep Eutectic Solvents (DESs) and Their Applications, Chem Rev **114**, 11060, (2014). DOI:10.1021/cr300162p.

[94] M. A. R. Martins, S. P. Pinho, and J. A. P. Coutinho, Insights into the Nature of Eutectic and Deep Eutectic Mixtures, J Solution Chem, (2018). DOI:10.1007/s10953-018-0793-1.

[95] B. D. Ribeiro, C. Florindo, L. C. Iff, M. A. Z. Coelho, and I. M. Marrucho, Menthol-Based Eutectic Mixtures: Hydrophobic Low Viscosity Solvents, ACS Sustain Chem Eng **3**, 2469, (2015). DOI:10.1021/acssuschemeng.5b00532.

[96] K. R. Swami, R. Kumaresan, K. A. Venkatesan, and M. P. Antony, Minimizing the Aggregation of Diglycolamide Reverse Micelles in the N-Dodecane Phase with Bis-(2-Ethylhexyl)Phosphoric Acid "Reactive" Phase Modifier, New J Chem **42**, 8891, (2018). DOI:10.1039/C8NJ01074A.

[97] D. F. Peppard, S. W. Moline, and G. W. Mason, Isolation of Berkelium by Solvent Extraction of the Tetravalent Species, J Inorg Nucl Chem **4**, 344, (1957). DOI:10.1016/0022-1902(57)80017-7.

[98] M. Nilsson and K. L. Nash, Review Article: A Review of the Development and Operational Characteristics of the TALSPEAK Process, Solvent Extr Ion Exc **25**, 665, (2007). DOI:10.1080/07366290701634636.

[99] K. L. Nash, The Chemistry of TALSPEAK: A Review of the Science, Solvent Extr Ion Exc **33**, 1, (2015). DOI:10.1080/07366299.2014.985912.

[100] E. Krahn, C. Marie, and K. Nash, Probing Organic Phase Ligand Exchange Kinetics of 4f/5f Solvent Extraction Systems with NMR Spectroscopy, Coordin Chem Rev **316**, 21, (2016). DOI:10.1016/j.ccr.2016.01.008.

[101] C. Scharf and A. Ditze, Solvent Extraction: Fundamental Equilibrium Studies of Neodymium and DEHPA, Metall Res Technol **114**, (2017). DOI:10.1051/metal/2017017.

[102] F. Kubota, Y. Shimobori, Y. Koyanagi, K. Nakashima, K. Shimojo, N. Kamiya, and M. Goto, Extraction Behavior of Indium with TOPO into Ionic Liquids, Solvent Extr Res Dev **16**, 151, (2009).

[103] S. Katsuta, Y. Watanabe, Y. Araki, and Y. Kudo, Extraction of Gold(III) from Hydrochloric Acid into Various Ionic Liquids: Relationship between Extraction

Efficiency and Aqueous Solubility of Ionic Liquids, ACS Sustain Chem Eng **4**, 564, (2016). DOI:10.1021/acssuschemeng.5b00976.

[104] E. E. Tereshatov, M. Y. Boltoeva, and C. M. Folden III, Resin Ion Exchange and Liquid-Liquid Extraction of Indium and Thallium from Chloride Media, Solvent Extr Ion Exc **33**, 607, (2015). DOI:10.1080/07366299.2015.1080529.

[105] M. Matsumiya, M. Sumi, Y. Uchino, and I. Yanagi, Recovery of Indium Based on the Combined Methods of Ionic Liquid Extraction and Electrodeposition, Sep Purif Technol **201**, 25, (2018). DOI:10.1016/j.seppur.2018.02.027.

[106] E. E. Tereshatov, M. Y. Boltoeva, and C. M. Folden III, First Evidence of Metal Transfer into Hydrophobic Deep Eutectic and Low-Transition-Temperature Mixtures: Indium Extraction from Hydrochloric and Oxalic Acids, Green Chem **18**, 4616, (2016). DOI:10.1039/c5gc03080c.

[107] T. Sato and K. Sato, Liquid-Liquid-Extraction of Indium (III) from Aqueous Acid-Solutions by Acid Organophosphorus Compounds, Hydrometallurgy **30**, 367, (1992). DOI:10.1016/0304-386x(92)90094-G.

[108] T. Nakamura, A. Sakai, S. Nishihama, and K. Yoshizuka, Solvent Extraction of Indium, Gallium, and Zinc Ions with Acidic Organophosphates Having Bulky Alkyl Groups, Solvent Extr Ion Exc **27**, 501, (2009). DOI:10.1080/07366290902967017.

[109] S. Virolainen, D. Ibana, and E. Paatero, Recovery of Indium from Indium Tin Oxide by Solvent Extraction, Hydrometallurgy **107**, 56, (2011). DOI:10.1016/j.hydromet.2011.01.005.

[110] J. X. Yang, T. Retegan, and C. Ekberg, Indium Recovery from Discarded LCD Panel Glass by Solvent Extraction, Hydrometallurgy **137**, 68, (2013). DOI:10.1016/j.hydromet.2013.05.008.

[111] K. Ghosh, M. Maiti, and S. Lahiri, Separation of No-Carrier-Added ^{113,117m}Sn and ^{113m,114m}In from Alpha Particle Irradiated Natural Cadmium Target, J Radioanal Nucl Ch **295**, 865, (2013). DOI:10.1007/s10967-012-2115-1.

[112] D. Dupont, D. Depuydt, and K. Binnemans, Overview of the Effect of Salts on Biphasic Ionic Liquid/Water Solvent Extraction Systems: Anion Exchange, Mutual Solubility, and Thermomorphic Properties, J Phys Chem B **119**, 6747, (2015). DOI:10.1021/acs.jpcb.5b02980.

[113] S. K. Bharti and R. Roy, Quantitative ^{1}H NMR Spectroscopy, TrAC Trends in Analytical Chemistry **35**, 5, (2012). DOI:10.1016/j.trac.2012.02.007.

[114] V. Mazan, I. Billard, and N. Papaiconomou, Experimental Connections between Aqueous-Aqueous and Aqueous-Ionic Liquid Biphasic Systems, RSC Adv **4**, 13371, (2014). DOI:10.1039/C4RA00645C.

[115] R. Belcher, A. M. G. Macdonald, and E. Parry, On Mohr's Method for the Determination of Chlorides, Anal Chim Acta **16**, 524, (1957). DOI:10.1016/S0003-2670(00)89979-1.

[116] 2480 Wizard^{2}™ Gamma Counter, http://www.perkinelmer.com/product/wizard2-gamma-counter-1-detw-3-1k-sampl-2480-0010 (Accessed 20 February 2019).

[117] E. E. Tereshatov and C. M. Folden III, A Labview Solution for Coupling an Automated Gamma-Ray Counter and Software for Spectra Analysis, 2015.

[118] G. F. Knoll, *Radiation Detection and Measurement* (John Wiley, Hoboken, N.J, 2010), 4th edn.

[119] R. L. Heath and C. Phillips Petroleum, *Scintillation Spectrometry: Gamma-Ray Catalogue* (U.S. Atomic Energy Commission, Idaho Operations Office, Idaho Falls, Idaho, 1964), AEC Research and Development Report., 2 v. p.

[120] B. Meermann and V. Nischwitz, ICP-MS for the Analysis at the Nanoscale – a Tutorial Review, J Anal Atom Spectrom **33**, 1432, (2018). DOI:10.1039/C8JA00037A.

[121] R. S. Khandpur, *Handbook of Analytical Instruments* (McGraw-Hill Education LLC, New York, N.Y, 2006), 2nd edn.

[122] K. E. Jarvis, A. L. Gray, and R. S. Houk, *Handbook of Inductively Coupled Plasma Mass Spectrometry* (Chapman and Hall, Glasgow : Blackie ; New York, 1992).

[123] T. Mori, K. Takao, and Y. Ikeda, Syntheses and Physical Properties of Novel Betainium-Type Ionic Liquids Derived from Amino Acids, Chem Lett **45**, 164, (2016). DOI:10.1246/cl.151044.

[124] C. Gaillard, V. Mazan, S. Georg, O. Klimchuk, M. Sypula, I. Billard, R. Schurhammer, and G. Wipff, Acid Extraction to a Hydrophobic Ionic Liquid: The Role of Added Tributylphosphate Investigated by Experiments and Simulations, Phys Chem Chem Phys **14**, 5187, (2012). DOI:10.1039/c2cp40129k.

[125] J. Ranke, A. Othman, P. Fan, and A. Muller, Explaining Ionic Liquid Water Solubility in Terms of Cation and Anion Hydrophobicity, Int J Mol Sci **10**, 1271, (2009). DOI:10.3390/ijms10031271.

[126] B. P. Nikolsky, in *Chemical Equilibrium and Kinetic, Property of Solutions, Electrode Processes* (Chemistry, Leningrad, 1965), p. 1008. In Russian.

[127] G. Åkerlöf and J. Teare, A Note on the Density of Aqueous Solutions of Hydrochloric Acid, J Am Chem Soc **60**, 1226, (1938). DOI:10.1021/ja01272a063.

[128] Thermo Scientific, *Measuring pH of Concentrated Samples* (Thermo Scientific, Waltham, MA, 2014), Rev. A edn., Application Note, 009.

[129] I. A. Shkrob, T. W. Marin, and M. P. Jensen, Ionic Liquid Based Separations of Trivalent Lanthanide and Actinide Ions, Ind Eng Chem Res **53**, 3641, (2014). DOI:10.1021/ie4036719.

[130] M. Civera, A. Fornili, M. Sironi, and S. L. Fornili, Molecular Dynamics Simulation of Aqueous Solutions of Glycine Betaine, Chem Phys Lett **367**, 238, (2003). DOI:10.1016/S0009-2614(02)01707-4.

[131] K. W. Whitten, R. E. Davis, M. L. Peck, and G. G. Stanley, *Chemistry* (Thomson Brooks/Cole, Belmont, CA, 2010), 9th edn.

[132] M. V. Fedotova and S. E. Kruchinin, Hydration and Ion-Binding of Glycine Betaine: How They May Be Involved into Protection of Proteins under Abiotic Stresses, J Mol Liq **244**, 489, (2017). DOI:10.1016/j.molliq.2017.08.117.

[133] W. Li, C. Qi, X. Wu, H. Rong, and L. Gong, Theoretical Investigation of Interactions between Glycine Cation Based Ionic Liquids and Water Molecules, J Mol Struc: Theochem **855**, 34, (2008). DOI:10.1016/j.theochem.2008.01.011.

[134] S. Venkatesan and S. L. Lee, Computational Investigation on Microsolvation of the Osmolyte Glycine Betaine [Gb(H_2)O($_{1-7}$)], J Mol Model **18**, 5017, (2012). DOI:10.1007/s00894-012-1501-5.

[135] S. Katsuta, K.-i. Nakamura, Y. Kudo, and Y. Takeda, Mechanisms and Rules of Anion Partition into Ionic Liquids: Phenolate Ions in Ionic Liquid/Water Biphasic Systems, J Phys Chem B **116**, 852, (2012). DOI:10.1021/jp210444n.

[136] E. E. Tereshatov, M. Y. Boltoeva, V. Mazan, M. F. Volia, and C. M. Folden III, Thallium Transfer from Hydrochloric Acid Media into Pure Ionic Liquids, J Phys Chem B **120**, 2311, (2016). DOI:10.1021/acs.jpcb.5b08924.

[137] I. G. Sten Ahrland, Lars Johansson, and Bertil Noren, The Stability of Metal Halide Complexes in Aqueous Solution. V. The Chloride and Bromide Complexes of Thallium (III), Acta Chem Scand **17**, 1567, (1963). DOI:10.3891/acta.chem.scand.17-1567.

[138] X. Sun, H. Luo, and S. Dai, Ionic Liquids-Based Extraction: A Promising Strategy for the Advanced Nuclear Fuel Cycle, Chem Rev **112**, 2100, (2012). DOI:10.1021/cr200193x.

[139] M. P. Jensen, J. Neuefeind, J. V. Beitz, S. Skanthakumar, and L. Soderholm, Mechanisms of Metal Ion Transfer into Room-Temperature Ionic Liquids: The Role of Anion Exchange, J Am Chem Soc **125**, 15466, (2003). DOI:10.1021/ja037577b.

[140] C. H. C. Janssen, N. A. Macías-Ruvalcaba, M. Aguilar-Martínez, and M. N. Kobrak, Metal Extraction to Ionic Liquids: The Relationship between Structure, Mechanism and Application, Int Rev Phys Chem **34**, 591, (2015). DOI:10.1080/0144235X.2015.1088217.

[141] S. A. Ansari, P. K. Mohapatra, V. Mazan, and I. Billard, Extraction of Actinides by Tertiary Amines in Room Temperature Ionic Liquids: Evidence for Anion Exchange as a Major Process at High Acidity and Impact of Acid Nature, RSC Adv **5**, 35821, (2015). DOI:10.1039/c5ra04882f.

[142] T. X. Sun, X. H. Shen, and Q. D. Chen, A Further Understanding of the Cation Exchange Mechanism for the Extraction of Sr^{2+} and Cs^{+} by Ionic Liquid, Sci China Chem **56**, 782, (2013). DOI:10.1007/s11426-013-4859-z.

[143] P. Lopez-Arce, J. Garcia-Guinea, and F. Garrido, Chemistry and Phase Evolution During Roasting of Toxic Thallium-Bearing Pyrite, Chemosphere **181**, 447, (2017). DOI:10.1016/j.chemosphere.2017.04.109.

[144] T. Sato, Liquid-Liquid Extraction of Trivalent Gallium, Indium and Thallium from Hydrochloric Acid Solutions by Trioctyl Phosphine Oxide, Shigen-to-Sozai **112**, 123, (1996). DOI:10.2473/shigentosozai.112.123.

[145] K. Inoue and S. Alam, Hydrometallurgical Recovery of Indium from Flat-Panel Displays of Spent Liquid Crystal Televisions, Jom-Us **67**, 400, (2015). DOI:10.1007/s11837-014-1287-2.

[146] M. F. Volia, E. E. Tereshatov, V. Mazan, C. M. Folden III, and M. Boltoeva, Effect of Aqueous Hydrochloric Acid and Zwitterionic Betaine on the Mutual Solubility between a Protic Betainium-Based Ionic Liquid and Water, J Mol Liq **276**, 296, (2019). DOI:10.1016/j.molliq.2018.11.136.

[147] I. Banyai and J. Glaser, Equilibrium Dynamics in the Thallium(III)-Chloride System in Acidic Aqueous Solution, J Am Chem Soc **111**, 3186, (1989). DOI:10.1021/ja00191a013.

[148] J. Blixt, J. Glaser, J. Mink, I. Persson, P. Persson, and M. Sandstroem, Structure of Thallium(III) Chloride, Bromide, and Cyanide Complexes in Aqueous Solution, J Am Chem Soc **117**, 5089, (1995). DOI:10.1021/ja00123a011.

[149] A. C. Schneider, C. Pasel, M. Luckas, K. G. Schmidt, and J.-D. Herbell, Determination of Hydrogen Single Ion Activity Coefficients in Aqueous HCl Solutions at 25°C, J Solution Chem **33**, 257, (2004). DOI:10.1023/B:JOSL.0000035359.00943.14.

[150] H. Sakaida and T. Kakiuchi, Determination of Single-Ion Activities of H^+ and Cl^- in Aqueous Hydrochloric Acid Solutions by Use of an Ionic Liquid Salt Bridge, J Phys Chem B **115**, 13222, (2011). DOI:10.1021/jp2052079.

[151] M.-Y. Chow, The Chinese University of Hong Kong, 1992.

[152] A. Smith Philip, L. Spano Tyler, and C. Burns Peter, in *Zeitschrift für Kristallographie - Crystalline Materials*2018), p. 507.

[153] H. Narita, M. Tanaka, H. Shiwaku, Y. Okamoto, S. Suzuki, A. Ikeda-Ohno, and T. Yaita, Structural Properties of the Inner Coordination Sphere of Indium Chloride Complexes in Organic and Aqueous Solutions, Dalton T **43**, 1630, (2014). DOI:10.1039/C3DT52474D.

[154] T. G. Spiro, A Raman Study of Thallium(III) Chloride Complexes in Aqueous Solution, Inorg Chem **4**, 731, (1965). DOI:10.1021/ic50027a029.

[155] E. P. Serjeant and B. Dempsey, *Ionisation Constants of Organic Acid in Aqueous Solution* (Pergamon Press, Oxford, 1979), 1st edn., IUPAC Chemical Data Series, 23.

[156] I. Komasawa, T. Otake, and Y. Ogawa, The Effect of Diluent in the Liquid-Liquid Extraction of Cobalt and Nickel Using Acidic Organophosporus Compounds, J Chem Eng Jpn **17**, 410, (1984). DOI:10.1252/jcej.17.410.

[157] F. Ghebghoub and D. Barkat, The Effect of Diluents on Extraction of Copper(II) with Di(2-Ethylhexyl)Phosphoric Acid, J Coord Chem **62**, 1449, (2009). DOI:10.1080/00958970802588265.

[158] I. Komasawa, T. Otake, and Y. Higaki, Equilibrium Studies of the Extraction of Divalent Metals from Nitrate Media with Di-(2ethylhexyl)Phosphoric-Acid, J Inorg Nucl Chem **43**, 3351, (1981). DOI:10.1016/0022-1902(81)80114-5.

[159] T. C. Huang and T. H. Tsai, Extraction Equilibrium of Cobalt(II) from Sulfate-Solutions by Di(2-Ethylhexyl)Phosphoric-Acid Dissolved in Kerosene, Polyhedron **9**, 1147, (1990). DOI:10.1016/S0277-5387(00)86889-8.

[160] P.-C. Lee, C.-W. Li, J.-Y. Chen, Y.-S. Li, and S.-S. Chen, Dissolution of D_2EHPA in Liquid–Liquid Extraction Process: Implication on Metal Removal and Organic Content of the Treated Water, Water Research **45**, 5953, (2011). DOI:10.1016/j.watres.2011.08.054.

[161] I. Komasawa and T. Otake, The Effects of Diluent in the Liquid-Liquid-Extraction of Copper and Nickel Using 2-Hydroxy-5-Nonylbenzophenone Oxime, J Chem Eng Jpn **16**, 377, (1983). DOI:10.1252/jcej.16.377.

[162] Report on Critical Raw Materials for the Eu, https://ec.europa.eu/growth/sectors/raw-materials/specific-interest/critical_en (2019).

[163] Critical Materials Strategy, https://www.energy.gov/sites/prod/files/DOE_CMS2011_FINAL_Full.pdf (2019).

[164] A. M. Alfantazi and R. R. Moskalyk, Processing of Indium: A Review, Minerals Engineering **16**, 687, (2003). DOI:https://doi.org/10.1016/S0892-6875(03)00168-7.

[165] Y. Zhong, X. Feng, W. Chen, X. Wang, K.-W. Huang, Y. Gnanou, and Z. Lai, Using UCST Ionic Liquid as a Draw Solute in Forward Osmosis to Treat High-Salinity Water, Environ Sci Technol **50**, 1039, (2016). DOI:10.1021/acs.est.5b03747.

[166] J. P. Omtvedt, J. Alstad, H. Breivik, J. E. Dyve, K. Eberhardt, C. M. F. III, T. Ginter, K. E. Gregorich, E. A. Hult, M. Johansson, U. W. Kirbach, D. M. Lee, M. Mendel, A. Nahler, V. Ninov, L. A. Omtvedt, J. B. Patin, G. Skarnemark, L. Stavsetra, R. Sudowe, N. Wiehl, B. Wierczinski, P. A. Wilk, P. M. Zielinski, J. V. Kratz, N. Trautmann, H. Nitsche, and D. C. Hoffman, SISAK Liquid-Liquid Extraction Experiments with Preseparated ^{257}rf, J Nucl Radiochem Sc **3**, 121, (2002).

[167] D. Krupp and U. W. Scherer, Prototype Development of Ion Exchanging Alpha Detectors, Nucl Instrum Meth A **897**, 120, (2018). DOI:10.1016/j.nima.2018.04.038.

[168] E. E. Tereshatov, M. Boltoeva, V. Mazan, C. Baley, and C. M. Folden III, Hydrophobic Polymerized Ionic Liquids for Trace Metal Solid Phase Extraction: Thallium Transfer from Hydrochloric Acid Media, New J Chem **43**, 8958, (2019). DOI:10.1039/C9NJ00689C.

APPENDIX A

SUPPLEMENTARY INFORMATION

The mutual solubility study of [Hbet][Tf_2N] ionic liquid and water is described in Chapter 3. Some additional data and information obtained from the mutual solubility experiments are presented below.

The concentrations of individual species were evaluated by using the system of equations (Eqs. 16 – 21) and presented in Figs. 10 – 12 in the main text. The numerical values of the data points on the figures are shown in Tables A1 and A2.

Table A1 The concentration of individual species evaluated by the system of equations (Eqs. 16 -21 in the main text). The chemical system consists of water or DCl (aqueous phase) and pre-equilibrated [Hbet][Tf_2N] (organic phase).

DCl_{init} (M)	**$[H^+]$ (M)**	**$[HTf_2N]$ (M)**	**$[Tf_2N^-]$ (M)**	**$[Hbet^+]$ (M)**	**[bet] (M)**	**$\gamma_{HCl\pm}$**
0	0.048 ± 0.005	0.0147 ± 0.0007	0.259 ± 0.013	0.251 ± 0.025	0.093 ± 0.009	0.834
0.012	0.0314 ± 0.0006	0.0103 ± 0.0005	0.269 ± 0.013	0.236 ± 0.024	0.130 ± 0.013	0.858
0.051	0.0378 ± 0.0008	0.0117 ± 0.0006	0.256 ± 0.013	0.248 ± 0.025	0.115 ± 0.011	0.848
0.226	0.0770 ± 0.0015	0.0189 ± 0.0009	0.211 ± 0.011	0.329 ± 0.033	0.078 ± 0.008	0.812
0.497	0.202 ± 0.004	0.0407 ± 0.0020	0.184 ± 0.009	0.410 ± 0.040	0.0394 ± 0.0039	0.767
1.132	0.658 ± 0.013	0.091 ± 0.005	0.126 ± 0.006	0.430 ± 0.040	0.0126 ± 0.0013	0.769
3.191	2.220 ± 0.040	0.152 ± 0.008	$(4.37 \pm 0.22) \cdot 10^{-2}$	0.510 ± 0.050	$(3.10 \pm 0.31) \cdot 10^{-3}$	1.100
5.976	4.300 ± 0.090	0.168 ± 0.008	$(1.26 \pm 0.06) \cdot 10^{-2}$	0.620 ± 0.060	$(9.7 \pm 1.0) \cdot 10^{-4}$	2.186
8.036	5.659 ± 0.113	0.185 ± 0.009	$(6.19 \pm 0.31) \cdot 10^{-3}$	0.710 ± 0.070	$(5.1 \pm 0.5) \cdot 10^{-4}$	3.696

Table A2. The concentration of individual species evaluated by the system of equations (Eqs. 16 -21 in the main text). The chemical system consists of water or DCl and 15 % (w/v) betaine (aqueous phase) and pre-equilibrated [Hbet][Tf_2N] (organic phase).

DCl_{init} (M)	$[H^+]$ (M)	$[HTf_2N]$ (M)	$[Tf_2N^-]$ (M)	$[Hbet^+]$ (M)	[bet] (M)	$\gamma_{HCl\pm}$
0	$(6.3 \pm 0.6) \cdot 10^{-3}$	$(2.11 \pm 0.11) \cdot 10^{-3}$	0.258 ± 0.013	0.288 ± 0.029	0.750 ± 0.080	0.923
0.009	$(5.07 \pm 0.10) \cdot 10^{-3}$	$(1.77 \pm 0.09) \cdot 10^{-3}$	0.263 ± 0.013	0.251 ± 0.025	0.790 ± 0.080	0.928
0.041	$(5.48 \pm 0.11) \cdot 10^{-3}$	$(1.74 \pm 0.09) \cdot 10^{-3}$	0.240 ± 0.012	0.261 ± 0.026	0.760 ± 0.080	0.926
0.198	$(8.02 \pm 0.16) \cdot 10^{-3}$	$(1.83 \pm 0.09) \cdot 10^{-3}$	0.175 ± 0.009	0.341 ± 0.034	0.690 ± 0.070	0.914
0.436	0.0146 ± 0.0003	$(2.40 \pm 0.12) \cdot 10^{-3}$	0.130 ± 0.006	0.490 ± 0.050	0.560 ± 0.060	0.891
0.998	0.0515 ± 0.0010	$(6.10 \pm 0.31) \cdot 10^{-3}$	0.100 ± 0.005	0.930 ± 0.090	0.323 ± 0.032	0.829
2.786	1.033 ± 0.021	$(5.41 \pm 0.27) \cdot 10^{-2}$	$(4.49 \pm 0.22) \cdot 10^{-2}$	1.420 ± 0.140	$(2.49 \pm 0.25) \cdot 10^{-2}$	0.818
5.150	2.960 ± 0.060	$(8.2 \pm 0.4) \cdot 10\text{-}^{2}$	$(1.400 \pm 0.070) \cdot 10^{-2}$	1.460 ± 0.150	$(5.3 \pm 0.5) \cdot 10^{-3}$	1.380
6.883	4.290 ± 0.090	$(1.06 \pm 0.05) \cdot 10^{-1}$	$(7.9 \pm 0.4) \cdot 10^{-3}$	1.490 ± 0.150	$(2.35 \pm 0.24) \cdot 10^{-3}$	2.182

The dependency of the mean ionic activity coefficient of HCl ($\gamma_{HCl\pm}$) on the H^+ concentration in molal quantity is available in ref. [126]. Meanwhile, the system of equations (Eqs. 16 – 21 in the main text) includes $\gamma_{HCl\pm}$ as a function of [H^+] in molar. Therefore, the literature values were converted into the appropriate unit by taking into account the density of HCl based on the data available in ref. [127]. The results are shown in Figure A1 and the numerical values are listed in Table A3.

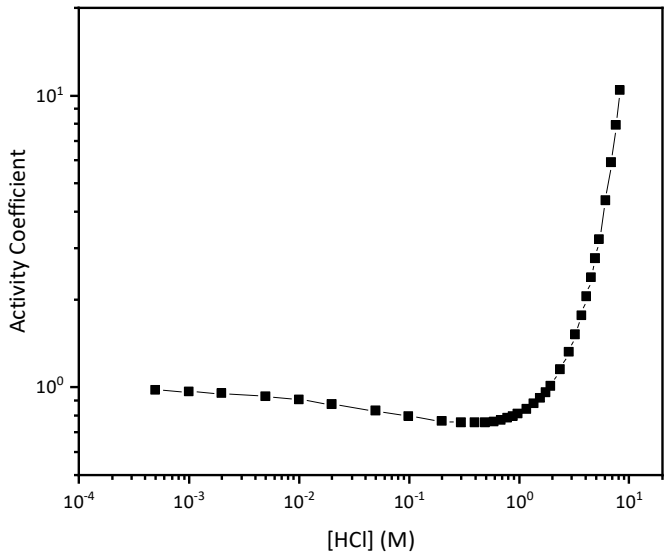

Figure A1. Mean ionic activity coefficient of HCl as the function of HCl concentration.

Table A3. Mean ionic activity coefficient of HCl.

HCl (M)	γ±	HCl (M)	γ±	HCl (M)	γ±
0.000498	0.9752	0.591377	0.763	2.825111	1.316
0.000997	0.9656	0.6886294	0.772	3.264648	1.518
0.001993	0.9521	0.7855178	0.783	3.695738	1.762
0.004983	0.9285	0.8820464	0.795	4.118617	2.04
0.009966	0.9048	0.9782187	0.809	4.533048	2.38
0.019928	0.8755	1.1694586	0.84	4.939543	2.77
0.049791	0.8304	1.3591544	0.876	5.338412	3.22
0.099488	0.796	1.5474427	0.916	6.112676	4.37
0.198602	0.767	1.7342964	0.96	6.857565	5.9
0.297345	0.756	1.9196011	1.009	7.574278	7.94
0.395722	0.755	2.3767715	1.147	8.263997	10.44
0.493737	0.757				

Chloride ion concentrations measured by the Mohr method are plotted as a function of initial DCl concentration (Figure A2). Based on this figure, there was no transfer of chloride ions into the organic phase.

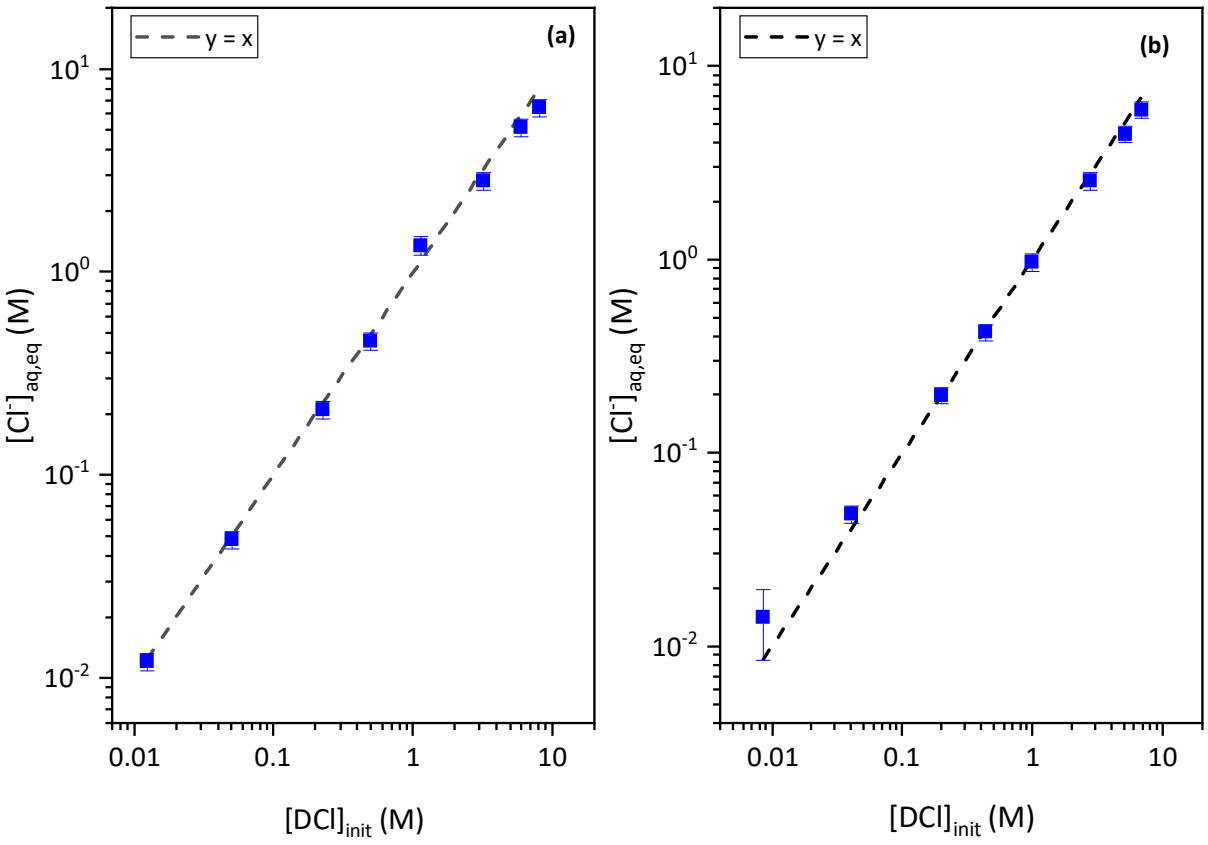

Figure A2. The equilibrium concentrations of [Cl^-] after contacted with [Hbet][Tf_2N] without the presence of bet (pure DCl) **(a)** and in the presence of 15 % (w/v) bet **(b)**. The dashed line shows the trend expected for perfect agreement between the initial and final concentrations.

The equilibrium concentrations of $[H^+]$ and $[Cl^{-}]$ ions in 3 – 8 M DCl were plotted as functions of the initial acid concentrations. The results show that the equilibrium concentrations of these ions are lower than the initial ones (Figure A3).

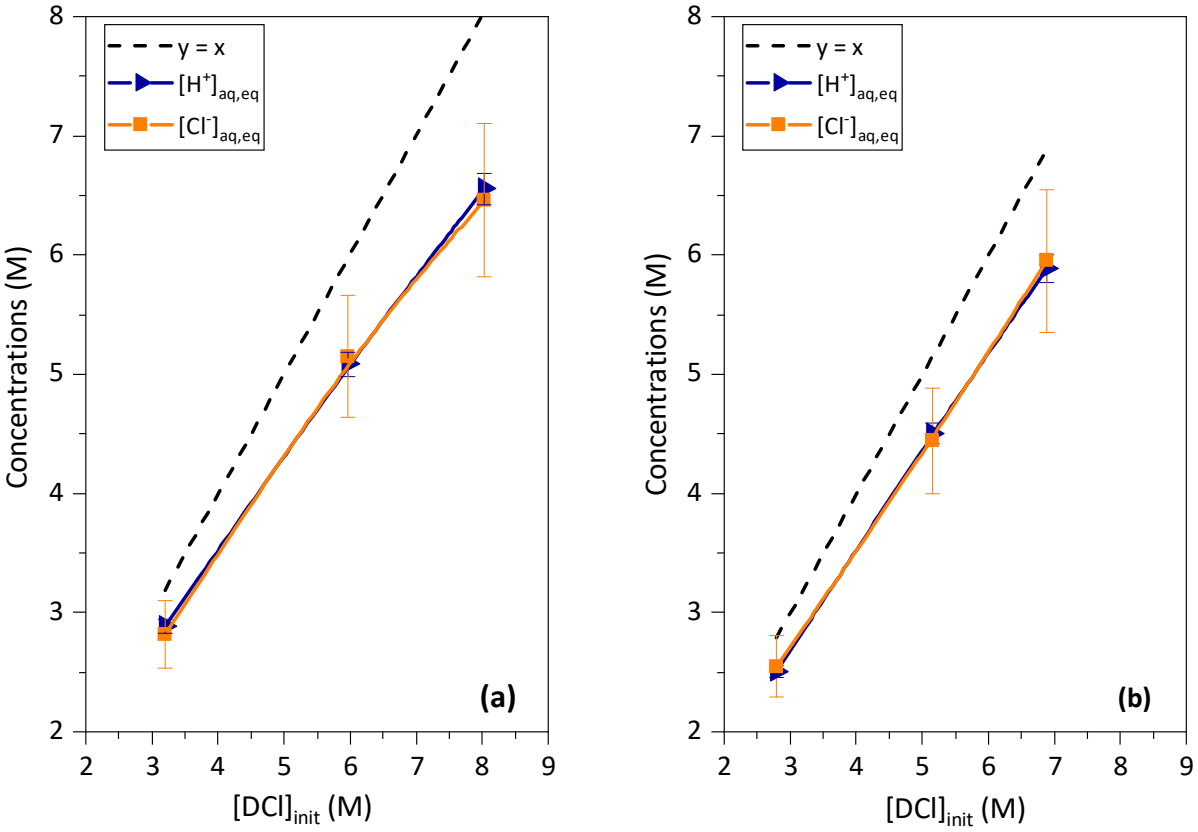

Figure A3. Plots of $[H^+]$ and $[Cl^-]$ equilibrium concentrations after contact with [Hbet][Tf_2N] without the presence of bet (pure DCl) **(a)** and in the presence of 15 % (w/v) bet **(b)**. The dashed line (y = x) indicates the reference value when the initial and equilibrium $[H^+]$ and $[Cl^-]$ are equal. The solid lines are drawn to guide the eye.

To verify this observation, in a separate experiments, [Hbet][Tf_2N] and [C_4mim][Tf_2N] ionic liquids (the latter was chosen for comparison) were washed with

deionized water after being in contact with > 3 M HCl. The corresponding aqueous phases (after rinsing) were qualitatively tested for chloride content. In all cases, an addition of $AgNO_3$ led to a precipitate formation. Table A4 shows the measurement of the equilibrium pH of the aqueous phases. The results show that the ILs were acidified after contact with concentrated acid (the uncertainty of the measurement is 0.05 pH units). Thus, HCl was shown to be transferred into the organic phase (neglecting anion exchange between $[Cl^-]_{aq}$ and $[Tf_2N^-]_{org}$, which is in agreement with the literature) [112]. It is likely that this acid is dissolved in water contained in the organic phase.

Table A4. The measurement of the equilibrium pH of the aqueous phases after the ionic liquid is washed with water. The ionic liquids were previously contacted with either water or 3 – 8 M HCl. The uncertainty of the pH measurements is 0.05 pH units.

$[HCl]_{initial}$ (M)	**[Hbet][Tf_2N]**	**[C_4mim][Tf_2N]**
	pH_{eq}	pH_{eq}
0	1.42	7.04
3	0.70	1.67
6	0.44	1.05
8	0.20	0.92

The extraction of species into [Hbet][Tf_2N] was described in Chapter 3. The concentrations of the extracted species are depicted in Fig. 15 in the main text and their numerical values are shown in Tables A5.1 and A5.2 below.

Table A5 The concentrations of proton, bet, and HTf_2N species that were extracted into the organic phase from pure water and DCl.

DCl_{init} (M)	$[H^+]_{org,eq}$ (M)	$[HTf_2N]_{org,eq}$ (M)	$[bet]_{org,eq}$ (M)
0.000	0	0	$(1.9 \pm 1.0) \cdot 10^{-2}$
0.012	0.022 ± 0.039	-0.005 ± 0.020	$(2.5 \pm 1.3) \cdot 10^{-2}$
0.051	0.019 ± 0.039	0.006 ± 0.019	$(2.2 \pm 1.2) \cdot 10^{-2}$
0.226	0.060 ± 0.040	0.044 ± 0.018	$(1.3 \pm 0.7) \cdot 10^{-2}$
0.497	0.110 ± 0.050	0.049 ± 0.018	$(6.1 \pm 3.2) \cdot 10^{-3}$
1.132	0.100 ± 0.050	0.057 ± 0.017	$(2.0 \pm 1.1) \cdot 10^{-3}$
3.191	0.170 ± 0.050	0.078 ± 0.017	$(4.2 \pm 2.2) \cdot 10^{-4}$
5.976	0.280 ± 0.060	0.093 ± 0.016	$(1.1 \pm 0.6) \cdot 10^{-4}$
8.036	0.370 ± 0.070	0.083 ± 0.017	$(4.9 \pm 2.6) \cdot 10^{-5}$

Table A6. The concentrations of proton, bet, and HTf_2N species that were extracted into the organic phase from water and DCl containing 15 % (w/v) bet.

DCl_{init} (M)	$[H^+]_{org,eq}$ (M)	$[HTf_2N]_{org,eq}$ (M)	$[bet]_{org,eq}$ (M)
0	0	0	0.560 ± 0.080
0.009	0.000 ± 0.150	-0.005 ± 0.019	0.590 ± 0.080
0.041	-0.010 ± 0.150	0.018 ± 0.018	0.580 ± 0.080
0.198	0.000 ± 0.150	0.083 ± 0.016	0.520 ± 0.070
0.436	0.020 ± 0.150	0.128 ± 0.015	0.410 ± 0.060
0.998	0.220 ± 0.160	0.154 ± 0.014	0.200 ± 0.030
2.786	0.410 ± 0.180	0.161 ± 0.014	$(1.3 \pm 0.2) \cdot 10^{-2}$
5.150	0.430 ± 0.180	0.164 ± 0.014	$(2.8 \pm 0.4) \cdot 10^{-3}$
6.883	0.460 ± 0.180	0.146 ± 0.014	$(1.2 \pm 0.2) \cdot 10^{-3}$